

Improving nerve guidance conduits with biodegradable aligned microfibres

¹C Murray-Dunning, ²SL McArthur, ³AJ Ryan & ¹JW Haycock

¹Department of Engineering Materials (Kroto Research Institute), University of Sheffield, UK.

²Faculty of Engineering and Industrial Sciences, Swinburne University of Technology, Victoria 3122, Australia.

³Department of Chemistry, University of Sheffield, UK.

INTRODUCTION: The ability of the peripheral nervous system to regenerate following injury is limited. Autografting is the gold standard treatment but there are a number of drawbacks to this procedure including donor site morbidity and lack of donor material. High cell death and a lack of accurate axonal orientation following injury has lead to an increased interest in the use of nerve guidance conduits (NGC). NGCs can be surgically implanted to bridge the gap left by injury to provide mechanical strength and physical guidance cues but these devices do not encourage re-innervation beyond a few millimeters. NGCs can incorporate a number of features to improve the basic design. The aim of the present study was to place electrospun degradable microfibres within the lumen of the device to improve physical guidance.

METHODS: Electrospun aligned poly L-lactide (PLLA) fibres were fabricated with an average diameter of 5µm (figure 1). A pin-hole free acrylic acid coating (10nm) was deposited on the fibres using plasma deposition. Cellular attachment and growth were investigated on coated surfaces versus uncoated. RN22 Schwann cells were deposited on the surfaces and cell number and viability examined. This was repeated using NG108-15 neuronal cells. Primary rat Schwann cells were isolated from the sciatic nerve and cultured on each surface either alone or as co-cultures with NG108-15 neuronal cells. Cell behaviour was investigated in 2D on different substrates including laminin versus acrylic acid. Contact angle and XPS analysis was used to confirm changes in surface chemistry.

RESULTS: Initial work showed that PLLA fibres could support RN22 Schwann cell growth, but viability was only about 60% after 96hr culture. This increased significantly to over 90% when fibre surfaces were functionalized with acrylic acid. Cell attachment and number also increased. NG108-15 cell number and neurite outgrowth was increased, with maximum neurite extension found for acrylic acid surfaces, compared to glass or PLLA alone (figure 2).

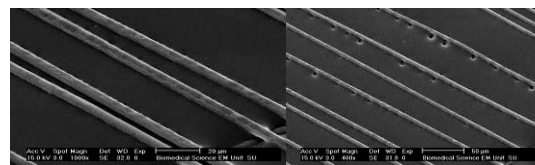


Figure 1: SEM of aligned electrospun PLLA fibres

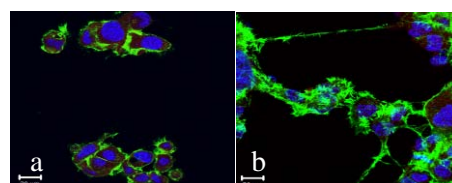


Figure 2: NG108-15 cells after 72hr culture on: a) glass and b) acrylic acid coated glass (labeled with phalloidin-FITC and DAPI)

A high level ($98\% \pm 1\%$) of primary Schwann cell purity was seen on all surfaces. An acrylic acid coating was found to provide a substrate that sustained primary Schwann cell growth (figure 3b) with a higher number of cells attached compared to glass (figure 3a) and comparable to the number of cells found on a laminin surface (figure 3c).

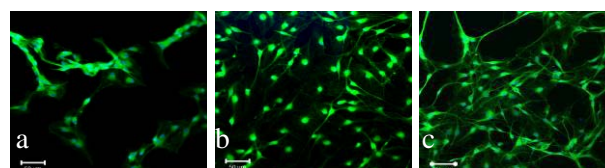


Figure 3: Primary Schwann cells cultured on: a) glass, b) acrylic acid and c) laminin for 20 days (labelled with S100).

DISCUSSION & CONCLUSIONS: There was a significantly higher viability and adherence of RN22 Schwann cells when cultured on fibres coated with acrylic acid. This was also observed for culture of NG108-15 neuronal cells, with increased neurite outgrowth, of which lengths were significantly longer. Primary Schwann cells cultured on an acrylic acid surface resulted in high cell purity, with cell number being comparable to that of laminin coated surfaces.

ACKNOWLEDGEMENTS: We are grateful to the EPSRC for funding.

REFERENCES:

1. C Murray-Dunning & JW Haycock (2010). Methods in Molecular Biology (In press).

Regenerating Tendons using Scaffolds of Appropriate Biomimicry

L. Bosworth¹ & S. Downes¹

¹*School of Materials, The University of Manchester, Grosvenor Street, Manchester, M1 7HS, UK*

INTRODUCTION: Tendons are highly organised structures, which are principally composed of aligned collagen type I fibres (extracellular matrix (ECM)) that lie parallel to the tendon axis [1]. Their hierarchical configuration is established on the grouping of these fibres into bundles of increasing size to form the overall tendon structure. The main cell type is tenocytes; these are located amongst the collagen fibres in a columnar array and are responsible for ECM production and regulation [2]. Tendons are commonly affected by injury and degenerative diseases, leading to chronic pain and spontaneous rupture. The rate of these tendinopathies is increasing, mostly due to population aging and an increased participation in sporting and recreational activities [3]. With a poor healing response, tendons are prone to further morbidity and risk of rupture. Current interventions often have a poor outcome, resulting in loss of function, further degeneration and rupture [4,5]. There is no commercially approved synthetic, biodegradable repair device available for clinical use. Using electrospinning, we have developed a technique that enables fabrication of bioresorbable nanofibres, which can be purposefully oriented and manipulated to create 3D scaffolds that mimic the tendon hierarchical structure.

METHODS: Polycaprolactone (Mn 80,000; Sigma) dissolved in Acetone (Fisher Scientific) (concentration 10%w/v) was electrospun using pre-determined parameters: voltage - 20kV, flow rate - 0.05ml/min, distance to collector - 15cm. Fibres were collected on a fine edged rotating mandrel. Mandrel rotation speeds; random fibres - 50RPM, aligned fibres - 500RPM. 3D bundles were developed by manipulation of the assembled aligned fibres. Cellular interactions with fibrous scaffolds were investigated by SEM over a two-week period to determine the effects of material contact guidance on cell morphology. The tensile properties of the fibrous scaffolds were also investigated by loading the scaffolds to failure using an Instron with 5N load cell and 5mm/min crosshead speed.

RESULTS: Figure 1 shows the entire surface of the 3D bundle structure to be covered with cells (and suspected matrix) after two weeks culture;

and that these cells are oriented in the same direction as the main bundle axis.

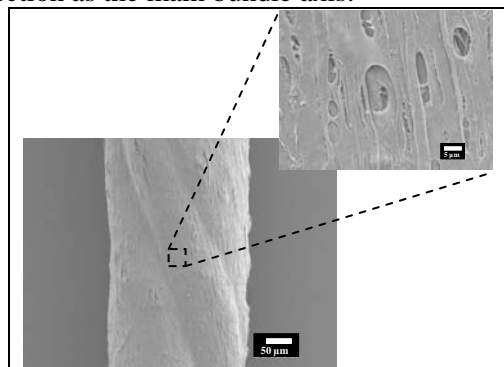


Fig. 1 – SEM micrographs demonstrating cell attachment and orientation on the 3D bundle surface

Mechanical loading of the scaffolds demonstrated 3D bundles to have superior tensile properties compared to 2D aligned and 2D random fibrous scaffolds (Table 1).

Scaffold Structure	Modulus (MPa)	Tensile Strength (MPa)
2D Random Fibres	1.54 (±0.26)	0.45 (±0.09)
2D Aligned Fibres	4.84 (±0.13)	1.30 (±0.14)
3D Fibrous Bundle	14.11 (±3.76)	4.74 (±1.64)

Table 1 – Mechanical properties of different polycaprolactone scaffold structures

DISCUSSION & CONCLUSIONS: The 3D bundles conferred contact guidance and appropriate biomimicry to the seeded tenocytes. The tensile properties highlighted a clear difference in scaffold strength depending on fibre orientation. We have developed a technique to electrospin aligned, degradable 3D nanofibrous scaffolds, which mimic the morphology of natural tendon.

REFERENCES:

- [1] Sharma P, et al. *The Surgeon*, 2005, 3(5)
- [2] Kidoaki S, et al. *Biomaterials*, 2005, 26:37-46
- [3] Smith, RKW, et al. *Comp. Biochem. and Phys. Part A*, 2002, 133:1039–1050
- [4] Miedema HS, et al. *Rheumat*. 1998, 37(5):555-561
- [5] Maffulli N, et al. *J R Soc Med* 2004, 97(10):472-476

ACKNOWLEDGEMENTS: The Authors would like to thank The UMIP Premier Fund and RegeNer8 for funding this research.

Development of an integrated collagen gel system for studying cellular interfaces following spinal cord injury

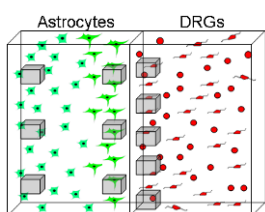
E East, J.P. Golding and J.B. Phillips

The Open University, [Department of Life Sciences](#), Walton Hall, Milton Keynes, MK7 6AA.

INTRODUCTION: Many current bridging devices aimed at spinal cord injury (SCI) repair contain or become populated by Schwann cells. These PNS glia can trigger resident CNS glia called astrocytes to become reactive and growth inhibitory, preventing regenerating axons from crossing the Schwann cell-astrocyte transition zone^{1, 2}. This cellular interface is also like that seen at the dorsal root entry zone (DREZ). In order to improve strategies to overcome this inhibitory interface, we have developed a 3D collagen gel culture model.

METHODS: Postnatal rat GFP positive astrocytes (4 million/ml) and wild type DRGs (20 dissociated/ml; containing PNS glia and neurons) were seeded into two separate collagen gel mixtures (2mg/ml) before pipetting into a stainless steel mould in which the cell types were separated by a divider. The divider was removed after 2 min, ensuring integration of the collagen gels as they set, whilst keeping the cell populations segregated. Cultures were maintained for 5, 10 or 15 days before fixing and immunostaining for GFAP (reactive astrocytes) and β III tubulin (neurons). Confocal microscopy of gels was performed in a systematic manner and astrocyte reactivity (hypertrophy) was quantified by GFP and GFAP cell volume (Volocity software, Improvision)³. Neurite outgrowth from DRG cells was also quantified.

Figure 1. Astrocytes and dissociated DRGs seeded in 2 separate collagen gels, which integrate to form a cellular interface. Volumes for quantification were $400 \times 400 \times 40 \mu\text{m}$ (xyz).



RESULTS: Astrocytes at the interface with DRG cells became significantly hypertrophic over the 15 day time course (Figure 2i A-C), with increased GFP and GFAP cell volume (Figure 2ii and iii). Astrocytes away from the interface did not become reactive over the 15 days (Figure 2i D-F), and showed no changes in GFP and GFAP cell volume (Figure 2ii and iii). A significant twofold increase in cell density was observed at the interface, indicating astrocyte migration and/or proliferation (data were

corrected for these differences). The system also permitted detailed analysis of the interaction of neurons with astrocytes. Neurites extended in 3D but did not penetrate the astrocyte interface.

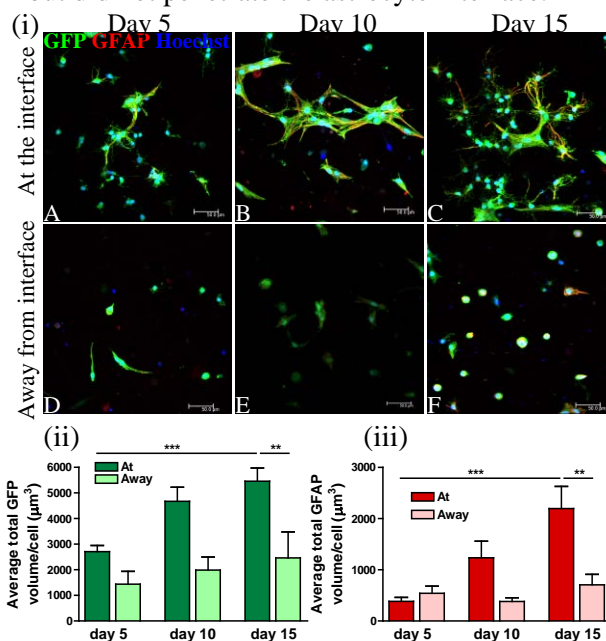


Figure 2. (i) GFP+ astrocytes stained for GFAP and Hoechst after 5, 10 and 15 days in culture at and away from the interface with DRGs. GFP (i) and GFAP (ii) cell volume quantification.

DISCUSSION & CONCLUSIONS: A model was successfully developed using collagen gels in which an integrated 3D interface formed between astrocytes and DRGs. DRG cells conferred a reactive phenotype on astrocytes, which become hypertrophic and upregulated reactivity markers in a time-dependent manner over 15 days. This interface was also inhibitory to neuronal growth, thus providing a useful model system in which strategies aimed at repairing sites of spinal cord injury can be tested.

REFERENCES: ¹ Adcock KH *et al.* (2004) *Eur J Neurosci.*20:1425-35. ² Wilby MJ *et al.* (1999) *Mol Cell Neurosci.*14:66-84. ³ East E *et al.* (2009) *J Tiss Eng Regen Med.* 3:634-646.

ACKNOWLEDGEMENTS: This research was funded by the Wellcome Trust.

Development of an alternative to the amniotic membrane for delivering cultured epithelial cells to the cornea using poly(lactide-co-glycolide) electrospun scaffolds

P Deshpande¹, R McKean², KA Blackwood¹, RA Senior¹, A Ogunbanjo¹, AJ Ryan² & S MacNeil¹

¹Kroto Research Institute, [Department of Engineering Materials](#), University of Sheffield, UK

²[Department of Chemistry](#), University of Sheffield, UK

INTRODUCTION: One of the many causes of loss of corneal transparency is limbal stem cell deficiency caused by alkali burns, Aniridia, Steven Johnson syndrome, radiation and multiple surgeries. In the last 15 years several procedures have been developed to use laboratory expanded corneal cells to prevent blindness occurring due to this disease. Most commonly cells are transferred on a donor amniotic membrane. While results can be good, there is a disease risk in using the human amniotic membrane and inter-donor variation exists..

The aim of this work was to develop an alternative delivery system for transferring laboratory expanded limbal epithelial cells for treatment of the cornea. The approach explored was the use of biodegradable poly (lactide-co-glycolide) 3D polymeric scaffolds as an alternative to the amniotic membrane.

METHODS: PLGA 3D scaffolds were electrospun, sterilised¹ and seeded with primary rabbit limbal epithelial cells. After 2 weeks in culture the scaffolds were examined using confocal microscopy, cryosectioning and scanning electron microscopy. The tensile strength of the scaffolds was also studied on annealing and sterilisation of the scaffolds as well as the handling of the scaffolds.

RESULTS: The cells had formed a continuous on the surface of the scaffolds (Figure 1a,b,c). Also the scaffolds showed the onset of degradation within 2 weeks in culture². The scaffolds could be easily handled as well as sutured onto a grid (Figure 1d).

The tensile study showed that the wet annealed scaffolds led to a more brittle sheet of fibres and it was noted that annealing the scaffolds increased the stiffness (Young's modulus) of the dry scaffolds ($p < 0.05$) (Table 1). Also sterilising the scaffolds with peracetic acid led to a significant reduction in tensile strength ($p < 0.01$) but reduced the stiffness of the scaffolds (Table 1).

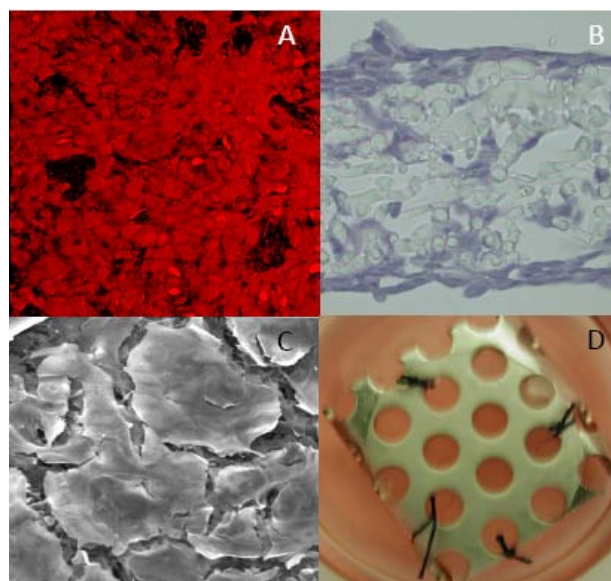


Fig. 1: Front view of confocal microscopy (A), cryosection (B), scanning electron microscopic images (C) of the scaffold with cells after 2 weeks in culture and an image of the scaffold with limbal epithelial cells on day 0 sutured to a metal grid (D).

Table 1. Mechanical properties of the scaffolds

		Max. yield (MPa)	Max. strain	Young's modulus (10^6) N/m ²
Non heat-treated	Dry	0.53±0.19	26%±14%	5.1±2.3
	Wet	0.29±0.08	17.7%±6.5%	3.8±1.32
Heat-treated (60°C for 3 hours)	Dry	0.88±0.28	22.4%±3.2%	10.5±2.2
	Wet	0.38±0.29	9%±4.7%	7.6±2.9

Dry-no treatment, wet-sterilised with 0.01% peracetic acid for 3 hours prior to testing

CONCLUSIONS: We suggest this carrier scaffold could be used as a replacement for the human amniotic membrane in the treatment of limbal stem cell deficiency lowering the risk of disease transmission to the patient.

REFERENCES:

¹Blackwood et al. (2008) *Biomaterials* **29**: 3091-3104.

²Deshpande et al. (2010) *Regen. Med.* In Press.

Endothelial cell migration and aggregation in response to hypoxia-induced signalling

Cheema, U.^{1*} Hadjipanayi, E.¹, Mudera, V.¹, Deng, D.², Liu, W.², Brown, R.A.¹

¹UCL Division of surgery and interventional sciences, Tissue Repair and Engineering Centre, London, HA7 4LP, UK

²Department of Plastic and Reconstructive Surgery, Ninth People's Hospital and National Tissue Engineering Center of China, Shanghai Jiangtong University School of medicine, Shanghai 200011, PR China.

Introduction

The vascularisation of any graft, engineered implant or injury site is a key factor for optimal repair and regeneration. New blood vessel formation is a physiological response to tissue hypoxia, through upregulation of angiogenic factor signalling. We engineered cell-mediated hypoxia in a convenient cell type, human dermal fibroblasts (HDFs), to form a population of Hypoxia-Induced Signalling (HIS) cells and showed that HIS responses by HDFs induce endothelial cell (EC) migration and tubule formation both *in vitro* and *in vivo*.

Materials and Methods

Capillary-like structure formation by EC's (HUVEC'S) in response to the HIS response by HDF's was measured in a 3D collagen matrix assay. This assay tested EC migration (up to 1 cm) and aggregation towards a HIS cell source (fig.1). EC capillary-like structure (CLS) formation was monitored over 14 days. Constructs containing HIS cells were also seeded *in vivo* and the functionality of invading vessels was verified by real-time monitoring of O₂ in the core of implanted constructs.

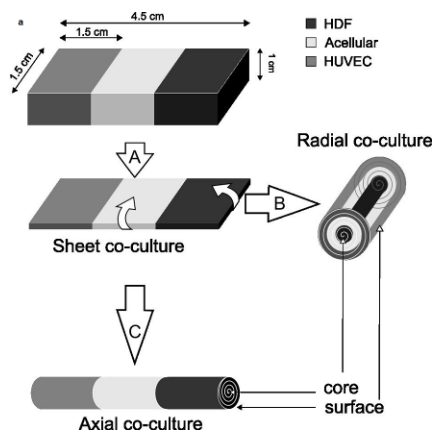


Fig. 1 Schematic showing construction of 3D collagen matrix with spatially positioned cells. Maximal protein was found in the core.

Results

By positioning HIS cells and ECs in distinct locations within 3D collagen constructs, we were able to quantify CLS formation by EC's in response to HIS cells, which induced directional EC sprouting *in vitro* (fig.2). Furthermore, depots of HIS cells, positioned in the core of 3D collagen constructs could direct host vessels deep into the matrix within 1 week *in vivo* implantation in rabbits.

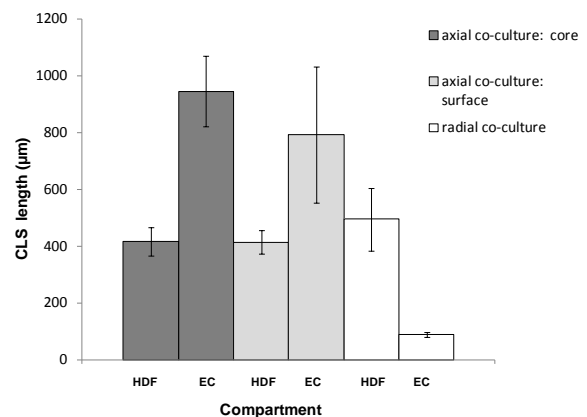


Fig. 2. Graph showing CLS formation mainly in the EC/HUVEC region of the axial co-culture. In the radial co-culture this CLS formation was inhibited due to decreased diffusion of angiogenic proteins through multiple collagen layers.

Discussion and Conclusions

These findings unravel the angiogenic potential of HIS cells with important implications for *in vitro* tissue modelling, as well as devising implant vascularisation strategies and potent angiogenic therapies for ischaemic diseases.

Acknowledgments

UC is a BBSRC David Phillips Fellow and this work has been funded through this route.

Hyaluronan as a potential mechanotransduction mediator

Hayley L Morris, John W Haycock & Gwendolyn C Reilly.

Department of Engineering Materials (Kroto Research Institute), University of Sheffield, Sheffield UK.

INTRODUCTION:

Osteocytes are believed to be the cells within bone which are sensitive to mechanical stimulation [1]. Osteocytes are embedded within bone matrix and bathed in pericellular fluid. This fluid has been shown to move when bone is mechanically loaded. Mechanosensitivity is proposed to result from the application of shear forces from the fluid movement on the osteocyte cell membrane. However, the molecular mechanisms of flow induced signal transduction in bone are poorly understood. The glycocalyx which connects between the cell membrane and the wall of the bone matrix has been proposed as a potential mediator of mechanical forces in bone. Hyaluronan (HA) has been described as a key component of the osteocyte pericellular matrix [2] and has been shown in previous investigations on MLO-Y4 cells to be important in mechanotransduction [3]. This investigation aims to elucidate further mechanisms by which the HA glycocalyx moderates mechanotransduction in MLO-A5 osteoid osteocyte cells.

METHODS:

Using a parallel plate flow chamber (Ibidi, μ slide VI) we investigated the effects of removal of HA on flow induced collagen production and NF- κ B activation in MLO-A5 osteoid osteocytes. Static culture was also utilised to investigate possible pathways linking Ca^{2+} responses, NF- κ B activation and long term collagen production.

RESULTS:

Short periods of laminar fluid flow at 0.8Pa shear stress significantly increased collagen production and induced translocation of the NF- κ B subunit, p65, to the cell's nuclei in 65% of the cell population. Blocking of CD44, the principle receptor of HA and removal of the HA coat by hyaluronidase had no effect on the translocation of p65 but eliminated the fluid flow induced increase in collagen production. In statically cultured MLO-A5 cells addition of ionomycin, to stimulate a Ca^{2+} response, appears to reduce the lipopolysaccharide (LPS) stimulated activation of p65.

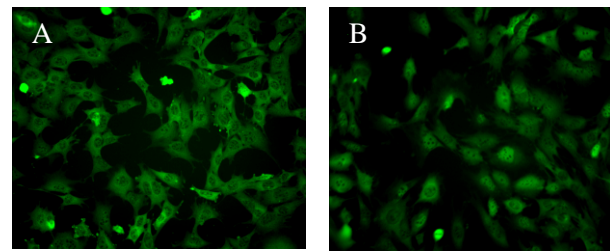


Figure 1: MLO-A5 cells labelled for the NF- κ B p65 subunit **A)** No Flow, labelling concentrated in the cytoplasm showing no nuclear activation. **B)** 2hr laminar flow at 0.8Pa, labelling concentrated in the nucleus indicating activation and transcription of target genes.

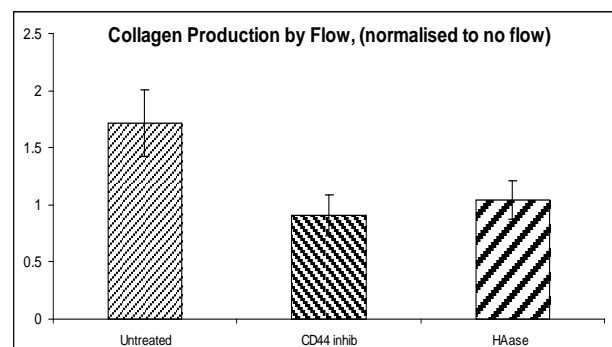


Figure 2: Collagen production after subjecting cells to laminar fluid flow (0.8Pa). Pre-treating cells with a CD44 blocking antibody or hyaluronidase reduced the collagen production compared to the untreated control.

DISCUSSION & CONCLUSIONS: Hyaluronan and CD44 appear to play a role in transducing long term flow signals that modulate collagen production but do not effect short term flow-induced activation of NF- κ B. It is likely that multiple signaling events are initiated upon the commencement of fluid flow in tissue engineered bone and ongoing work is seeking to elucidate which of these contribute predominantly to a matrix forming response [4].

REFERENCES: 1. LE Lanyon. *Calcif Tissue Int.* (1993) 53S102-6. S102-7. 2. JM Tarbell, MY Pahakis. (2006) *J. Int. Med* 259, 339-350. 3. GC Reilly et al. *Biorheology* (2003) 40(6) 591-603. 4. HL Morris, CI Reed, GC Reilly & JW Haycock (2010). *Proc I Mech E, Pt H: J Eng Med* (In press).

ACKNOWLEDGEMENTS:

We acknowledge the EPSRC, EXPERTISSUES and the White Rose Doctorial Training Centre for funding.

Characterisation of Mesenchymal Stem Cell Responses to Titanium Nanopillars for Orthopaedic Applications

LE McNamara¹, T Sjöström³, K Burgess², ROC Oreffo⁴, B Su³, MJ Dalby¹

¹ Centre for Cell Engineering and ² Sir Henry Wellcome Functional Genomics Facility, Faculty of Biomedical and Life Sciences, University of Glasgow, UK. ³ Department of Oral and Dental Science, University of Bristol, UK. ⁴ Bone and Joint Research Group, Institute of Developmental Sciences, University of Southampton, UK.

INTRODUCTION: Topographically structured surfaces have great potential for the direction of apposite cell responses in regenerative medicine, but most research is conducted with polymeric materials with poor load strength. In this study, the cellular response of mesenchymal stem cells (MSCs) to titanium nanostructures (Ti), a clinically relevant material with excellent loading properties, has been examined. A range of nanopillar heights were evaluated to allow selection of the optimal surface features for osteoinduction, by quantification of focal adhesion formation, which has previously been linked with modulation of differentiation [1]. The global metabolic profile of MSCs was investigated using metabolomics.

METHODS:

Fabrication: Ti nanopillars were fabricated to different heights (15, 55, 90 nm) by through-mask anodisation of a sputter-coated layer of aluminium on Ti substrates (discussed in [2]). Planar Ti surfaces were used as controls.

Cell adhesion and proliferation assay: STRO-1+-enriched MSCs (passage 2-3) were cultured for 3d on the Ti nanosurfaces or polished controls, pulse-labelled with 5'-bromo-2'-deoxyuridine to identify S-phase cells, and co-immunostained for vinculin and actin.

Metabolomics: Solvent-extracted metabolites were examined following 7d and 14d culture using a Fourier Transform Orbitrap mass spectrometer to identify differentially abundant metabolites.

RESULTS:

To examine cell adhesion in a cell population in a single phase of the cell cycle (and avoid artefacts in enumeration of adhesions due to cell-cycle stage), focal adhesions were quantified in S-phase cells. The results suggest that the height of Ti nanostructures altered the cell morphology, in addition to the number and size of adhesions.

Metabolomics was used to evaluate changes in the cellular metabolites with culture period. A number of metabolites, including glutathione and 1'-

Acetoxyeugenol acetate were consistently differentially abundant in MSCs after 7d and 14d.

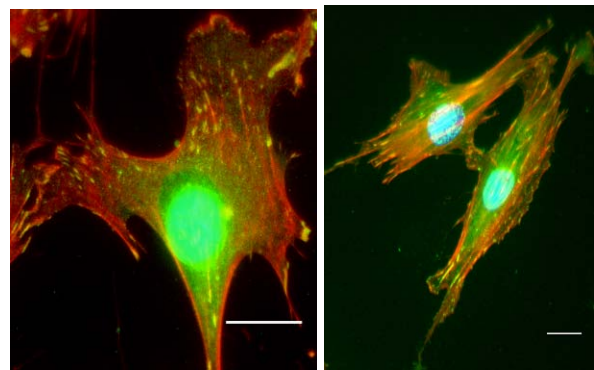


Fig. 1: MSCs cultured on 15 nm Ti nanopillars (left) and planar control (right). Note that cells were well spread on both surfaces, with particularly numerous focal adhesions on 15 nm nanopillars. Key: Red - Actin, Green - Vinculin, Blue - S-phase nuclei. Bars - 20 μ m.

DISCUSSION & CONCLUSIONS: These results support the use of nanostructured Ti as an osteogenic substratum, and illustrate that different feature heights affect focal adhesion formation and cell morphology. Metabolomics offers a novel means of characterising the molecular response of cells to biomaterial substrates.

REFERENCES:

¹ M.J.P. Biggs, R.G. Richards, S. McFarlane et al (2008) *J. R. Soc. Interface* **5**:1231-42.

² T. Sjöström, M.J. Dalby, A. Hart et al (2009) *Acta Biomaterialia* **5**:1433-41.

ACKNOWLEDGEMENTS: This work was funded by the EPSRC. The authors would like to thank Dr. A. Pitt, Miss R. McMurray, Dr. M. Tsimbouri, Dr. V. Chintapalli, Dr. M. Kurowska-Stolarska, Dr. J. Wang and all in CCE for their assistance and helpful discussion.

Interaction of Bioactive Glass Nanoparticles with Mesenchymal

Stem Cells *In Vitro*

S.Labbaf, O.Tsigkou, M. Stevens, A.E Porter, J.R Jones

Imperial College London, South Kensington, London SW7 2AZ (s.labbaf07@imperial.ac.uk)

Introduction: Bioactive glasses (BG) are promising for hard tissue regeneration because of their rapid bone bonding, controlled biodegradability and their ability to stimulate osteogenesis [1]. BG nanoparticles have the potential to be injected directly into the defect site to allow healing and regeneration of bone tissue. Also, regardless of the great potential of BG as porous scaffolds for bone regeneration concerns arise on their long term fate in the body as small particles may be released after implantation, which could lead to undesirable reactions to surrounding cells, hence investigations on such nanoparticles is crucial. Nanostructured materials possess unique properties that are strongly dependent on size, chemistry and shape, which are of particular interest considering many biological processes occur at nanoscale. As mesenchymal stem cells (MSCs) are precursors to osteoblasts, the effect of nanoparticles on their behaviour is critical. In this study 80S20C (80 mol% SiO₂ and 20 mol% CaO) BG nanoparticles, have been synthesised and characterized for the first time. The BG nanoparticle's uptake and distribution inside MSCs using confocal microscopy and transmission electron microscopy (TEM) was also assessed. The effect of the BG nanoparticles on cell viability, metabolic activity and proliferation as a result of particle uptake was also determined.

Materials and Methods: The Stöber process [2] was applied to produce sol-gel derived BG nanoparticles. To follow the internalisation and intracellular distribution of the BG nanoparticles inside MSCs (Lonza, UK) in 3D, cells were exposed to BG nanoparticles at a concentration of 100µg/ml in cell medium (Dublecco's Modified Eagle Medium (DMEM) supplemented with 10% fetal bovine serum and 1% penicillin streptomycin (all from Invitrogen, UK) for 24 h. For confocal microscopy the actin cytoskeleton was stained with Alexa Fluor conjugated phalloidin (molecular probes, UK). TEM was also used to monitor the uptake and distribution of the nanoparticles (100µg/ml) inside MSCs after 24 h exposure. Cells were fixed, osmicated and the samples were embedded in resin and sectioned. The effect of the nanoparticles on cell viability and proliferation was determined by exposing MSCs to three different BG nanoparticle concentrations: 100, 150 and 200 µg/ml in cell medium (DMEM) for 24h and their response monitored over of the period of 1, 4 and 7 days using LIVE/DEAD (Molecular Probes,

UK), MTT 3-(4,5-Dimethylthiazol-2-yl) 2,5diphenyltetrazolium bromide (Sigma, UK), total DNA using Hoechst (Sigma, UK) (and Lactate dehydrogenase (LDH) Cytotox-one™ (Promega, UK).

Results and Discussion: The processing route for the synthesis of the BG nanoparticles was successful as it resulted in spherical and dense particles with a composition of SiO₂ and CaO. The uptake and intracellular localization of the BG nanoparticles inside MSCs was confirmed by confocal microscopy and TEM. TEM demonstrated nanoparticles entrapped in endosomes/ lysosomes after 24 h exposure. Furthermore, the uptake of the nanoparticles by MSCs was captured, for the first time, using TEM (Fig.1). The dissolution behaviour and break-up of the nanoparticles inside cells were also observed using TEM. No significant level of cytotoxicity was observed for the nanoparticles at all concentrations. At the concentrations of 100 and 150 µg/ml, the particles were seen to increase metabolic activity of human MSCs. Effect of the BG nanoparticles on MSC differentiation will also be presented.

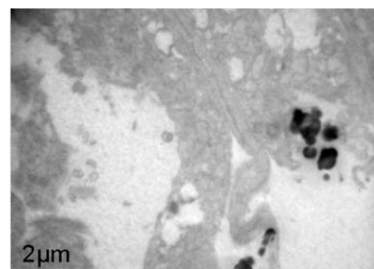


Figure 1: TEM image of MSCs exposed to 100µg/ml of BG nanoparticles for 24 h.

Conclusions: Spherical bioactive glass nanoparticles of 80S20C composition with controlled sizes were produced. In this study we successfully showed that BG nanoparticles were able to be internalised by MSCs. The viability and proliferation assays confirmed that none of the BG nanoparticle concentrations tested induced any major toxicity to MSCs.

Acknowledgements:

Royal Academy of Engineering and EPSRC (funding).

References:

1. Hench, L.L., Journal of American Ceramic Society 1991. **74**: p. 1487-1510.
2. Stöber W *et al*, Journal of Colloid and Interface Science, 1968. **26**(1): p. 62-69.

Adipose-derived stem cells (ASCs) for peripheral nerve repair

¹R Kaewkhaw, ²AM Scutt & ¹JW Haycock

¹Departments of Engineering Materials (Kroto Research Institute) & ²Medicine, University of Sheffield, UK.

INTRODUCTION: The use of primary Schwann cells in conjunction with nerve guidance conduits has been shown to improve regeneration and remyelination of injured peripheral nerve [1]. However, clinical application of primary Schwann cells for nerve repair is limited due to the requirement of nerve biopsies, and slow growth of Schwann cells *in vitro*. Adipose-derived stem cells (ASCs) may be an optional cell source for derivation towards Schwann-like cells. In this study adipose-derived stem cells from three anatomically different sites were explored for differentiation towards a Schwann phenotype which included protein expression, morphology and function.

METHODS: Stem cells were isolated from: i) subcutaneous; ii) perinephric adipose and iii) epididymis adipose tissue of adult male Wistar rats according to the method of Bjornorp *et al* [2]. Plastic-adherent multipotent cells were then cultured according to an experimental differentiation protocol using β -mercaptoethanol, retinoic and growth factors. The protein markers S100 β , GFAP and p75NGFR were studied by Western blotting, together with phenotypic changes. A Transwell co-culture system containing NG108-15 neuronal cells and ASCs was employed to study the promotion of neurite growth. Neurite extension was determined after co-culture. Soluble neurotrophins contributing to neurite growth in co-culture medium was analyzed by ELISA.

RESULTS: Western blotting demonstrated an up-regulation of the Schwann cell marker S100 β , GFAP and p75 NGFR in perinephrium-ASCs. However, only S100 β expression was up-regulated in subcutaneous-ASCs while GFAP and p75NGFR were up-regulated in epididymis-ASCs. In addition, differentiated cells from all ASC sources formed an elongated shape, whereas undifferentiated cells displayed a polygonal and flattened morphology. A functional assay demonstrated that differentiated ASCs could stimulate neurite extension of NG108-15 neuronal cells by $36.44\mu\text{m} \pm 1.55\mu\text{m}$ (subcutaneous), $40.93\mu\text{m} \pm 2.02\mu\text{m}$ (perinephrium) and $27.29\mu\text{m} \pm 2.63\mu\text{m}$ (epididymis). This was in comparison with undifferentiated ASCs which stimulated neurite growth by $13\mu\text{m} \pm 0.98\mu\text{m}$, $18\mu\text{m} \pm 0.96\mu\text{m}$ and $13\mu\text{m} \pm 1.07\mu\text{m}$. In addition, the neurotrophins NGF and BDNF (but not NT-3) were

detected in the co-culture medium. Subcutaneous-, perinephrium- and epididymis-ASCs produced NGF at 26.5-fold, 23.7-fold and 10.2-fold higher and BDNF 6.9-fold, 5-fold and 5-fold higher than undifferentiated-ASCs, respectively.

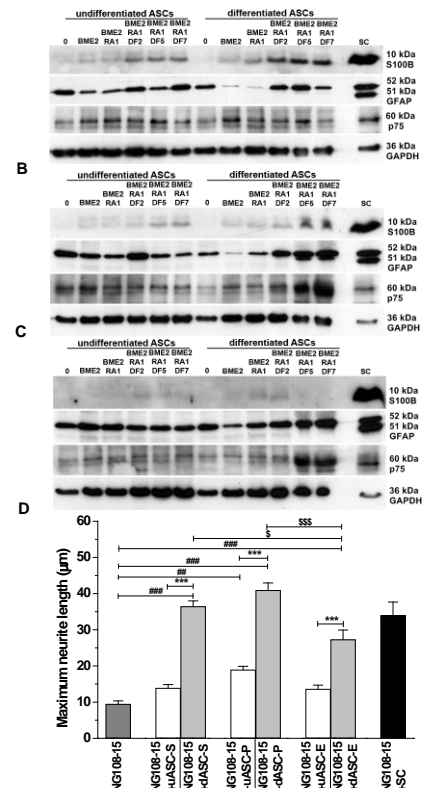


Figure 1. Differentiation of adipose-derived stem cells (ASCs) into Schwann-like cells. **A-C.** Western blotting for S100 β , GFAP and p75 proteins of **A)** subcutaneous-, **B)** perinephrium- and **C)** epididymis-ASCs. **D.** The promotion of neurite elongation from NG108-15 neuronal cells by ASCs or primary Schwann cells (SC). ### or *** or \$\$\$ $P < 0.001$, \$ $P < 0.05$.

DISCUSSION & CONCLUSIONS: The use of ASCs as an alternative to Schwann cells for peripheral nerve repair shows good potential. Differentiated ASCs from three different anatomical fat sources showed an up-regulation of Schwann markers to varying extents. However, all differentiated ASCs were able to support neurite elongation in co-culture, mediated by neurotrophin secretion. This work forms the basis for extending work towards the use of injury models *in vivo*.

REFERENCES:

1. T Hadlock *et al.*, *Tissue Eng*, 6, 119–127 (2000).
2. P Bjornorp *et al.*, *J Lipid Res*, 19, 316-324 (1978).

ACKNOWLEDGEMENTS: SFR Scholarship programme (Thailand) for financial support.

A NOVEL, FEEDER FREE, AUTOLOGOUS SYSTEM FOR MAINTENANCE OF HUMAN EMBRYONIC STEM CELL PHENOTYPE

F C Lewis¹, N.P. Rhodes¹, J.A. Hunt¹

¹ UKCTE, Clinical Engineering, School of Clinical Sciences, University of Liverpool, Liverpool, UK

INTRODUCTION: Human embryonic stem cells (hESCs) are pluripotent, having the potential to differentiate into all cell types of an organism. Self renewal of hESCs is classically maintained on feeder layers, which secrete an undefined, variable array of soluble factors required for population expansion. Here we report a novel, feeder-free, platelet poor plasma (PPP) derived culture system which is able to support the self-renewal and pluripotency of hESCs without the potential xeno-contamination inherent with using feeder layers.

METHODS: The hESC line, HUES7, was kindly donated by Harvard University and maintained under serum-free conditions. Blood was isolated from 5 healthy donors of both genders under informed consent and citrated immediately following collection. Whole blood was spun at 800g for 20 minutes and the PPP subsequently separated. The PPP hydrogel was prepared from 10% citrated PPP and hESC suspension both of which were pre-warmed to 37°C. Calcium ions in the hESC culture medium initiated the rapid conversion of fibrinogen to a cross-linked fibrin network, forming a stable hydrogel with hESCs embedded within.

Fluorescent microscopy –hESCs were fixed in situ using 4% paraformaldehyde and blocked in 10% animal serum for 1 hour at room temperature. Primary antibodies were diluted in 10% triton X-100, 1% serum and applied to hESCs overnight at 4°C. Primary antibody working concentrations were: Oct4 1:500, Nanog 1:200, Sox2 1:100. Appropriate conjugated secondary antibodies were applied for 2 hours at 37°C. Finally hESCs were mounted in Vectashield mounting medium containing DAPI. At 72 hours post seeding hESCs were visualised using a Carl Zeiss inverted fluorescent microscope.

qRT-PCR analysis - Total cellular RNA was purified using an RNeasy Kit. Reverse transcription was performed on 2µl of RNA using SuperScript III™ reverse transcriptase and random primers. RT-PCR was carried out on 2µl of cDNA template with SYBR Green master mix. All PCR reactions were performed for 50 cycles.

RESULTS: This unique PPP-derived hydrogel system successfully maintained the proliferation of hESCs *in vitro*, with hESCs encapsulated within the hydrogel, forming colonies and displaying typical hESC morphology. After repeated passaging no significant change in hESC morphology or viability occurred.

Immunohistochemical analysis demonstrated clear nuclear staining of the cellular construct for Oct4, Nanog and Sox2 all of which are typically expressed by undifferentiated hESCs.

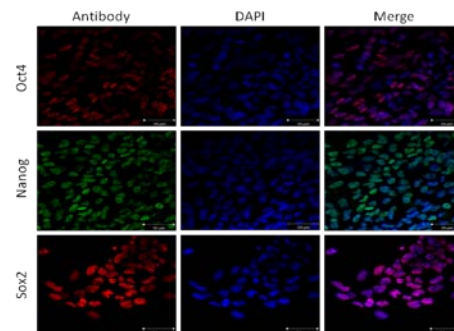


Fig. 1: Fluorescent microscopic observation of hESCs passage 7 stained with Oct 4, Sox2 and Nanog, cell nuclei stained with DAPI after 72 hours under PPP-hydrogel culture conditions.

qRT-PCR analysis revealed no significant difference between the gene expression levels of Oct4, Nanog and Sox2 between hESCs cultured under standard culture conditions and the PPP-derived hydrogel system.

DISCUSSION & CONCLUSIONS: This investigation has demonstrated, for the first time, the maintenance of hESCs in an undifferentiated state using a feeder-free, PPP-derived hydrogel culture system, which has the potential for being autologous. This system retained both hESC pluripotency and self renewal capacity *in vitro*. Therefore the combination of hESCs with this autologous system method may provide an ideal candidate for tissue engineering solutions.

ACKNOWLEDGEMENTS: Funding from the EPSRC for this study is gratefully acknowledged.

Directed Differentiation of Human Embryonic Stem Cells to Functional Cardiomyocytes by Defined Factors

James E. Dixon, Emily Dick, Maria Munoz, David Anderson, Chris Denning[§], Kevin M. Shakesheff[§]
Wolfson Centre for Stem Cells, Tissue Engineering and Modelling (STEM), University of Nottingham, NG7 2RD, UK.; [§]To whom correspondence should be addressed: Kevin.Shakesheff@nottingham.ac.uk or Chris.Denning@nottingham.ac.uk

INTRODUCTION: Lineage commitment and differentiation are considered permanent cellular processes, however recent work has impressively demonstrated reprogramming of differentiation potential (iPSCs)¹ or conversion of lineages (iN)² by the ectopic activity of specific transcription factors (TFs). As damaged or diseased hearts cannot regenerate direct generation of new cardiomyocytes (CMs) would be beneficial to cell therapy strategies and therefore we tested whether a combination of TFs could directly produce induced CMs (iCMs) from pluripotent cells. We employed a pool of 15 genes and identified a combination of 4 that rapidly and efficiently induce the differentiation of human embryonic stem cells (hESCs) into functional beating CMs *in vitro*. This demonstrates a potentially important method for controlling cardiac differentiation and programming of large populations of iCMs for regenerative purposes. Our data also indicates that this approach may be useful for differentiating large numbers of other tissue-types required for significant tissue engineering projects.

METHODS: A HUES7 hESC cell-line (MYH6-mRFP) was created which reports CM differentiation by expressing mRFP (monomeric red fluorescent protein). cDNAs were cloned into the pSIN-IRES-PURO lentiviral vector³. Lentiviruses were created by HEK293T transfection. hESCs were infected (10 μ gml⁻¹ polybrene) and selected with 300ngml⁻¹ Puromycin after 48h. Combinations and permutations of 15 viruses were transduced and CM differentiation assayed by TMRM staining (HUES7s) or mRFP-fluorescence (MYH6-mRFP hESCs), QPCR and immunofluorescence.

RESULTS: A combination of 4 lentiviruses directed the rapid CM differentiation under standard monolayer hESCs conditions. A time course experiment showed that the differentiation events mirrored normal differentiation. Beating iCM clusters (10-200 cells) were readily identified 15 days post infection (Fig. 1) and these may be

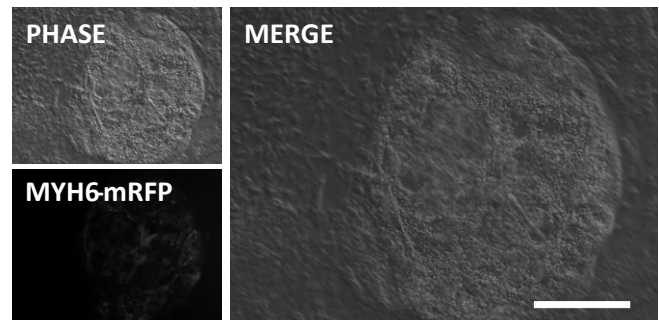


Figure 1. iCM by defined factors. MYH6-mRFP expressing iCM cluster 15 days post-infection. Bar=400 μ m

dissociated with collagenase B. iCMs show normal electrical activity (patch clamp and MEA analyses) and pharmacology.

DISCUSSION & CONCLUSIONS: This is the first demonstration that defined factors can direct hESCs to iCMs. iCMs express multiple CM-specific proteins, are electrically active and form beating clusters. We are now beginning testing of these factors for activity to directly convert human somatic lineages to iCMs. The generation of large numbers of functional iCMs is important for large-scale cardiac tissue engineering projects, and these cells will be employed to generate functional tissue constructs. Furthermore we will employ human induced pluripotent cells (iPSCs) to create large quantities of patient-matched iCMs. These experiments will have important implications for cardiac disease modelling, aid cell therapy approaches and validate drug screening in more physiological patient-specific contexts.

REFERENCES: ¹K. Takahashi, et al. (2006) *Cell*, **126**: 663-76. ²T. Vierbuchen, et al. (2010) *Nature*, **463**: 1035-1041. ³J. Yu, et al. (2007) *Science* **318**: 1917-1920.

ACKNOWLEDGEMENTS: We would like to thank Tissue Engineering/Stem Cell research teams for reagents, advice and technical assistance. We would also like to thank the BBSRC, MRC, BHF and Stem Cells for Safer Medicine for funding.

Application of Self-Assembling, β -sheet Forming Octapeptides to Stem Cell Culture

K Meade, R Holley, C Merry and A Saiani

School of Materials, The University of Manchester, The Materials Science Centre, Grosvenor Street, Manchester, M1 7HS

INTRODUCTION: Phenylalanine based octapeptides (FEFEFKFK and FEFKFEFK) self-assemble into anti-parallel β -sheets, which in turn assemble to form self-supporting hydrogels composed of three dimensional (3D) networks of nanofibres (fibre diameter of 3-5nm)¹. The hydrated nanofibrillar environment has great therapeutic potential, replicating the architecture of the extracellular matrix and enabling homogenous distribution of cells within the gel, creating a truly 3D environment for stem cell culture. Pluripotent embryonic stem (ES) cells have the unique capacity to form any adult cell phenotype. However, effective differentiation into organised tissue constructs is limited by current two dimensional (2D) culture techniques. Culture of stem cells on and within the gels will assist in determining the biological and structural cues necessary to manipulate cell behaviour, creating an instructive matrix that either maintains the pluripotent/multipotent state or assists the formation of mature cell phenotypes.

METHODS: Mouse ES cells were cultured as previously described². For culture on the hydrogel surface, 10mg/ml FEFEFKFK was dissolved in H₂O for 2 hours at 85°C. The pH was adjusted to pH9 and solutions transferred to well plates and allowed to set. Gels were covered in a film of ES media and incubated for 24 hours. Mouse ES cells were then seeded onto the surface (1×10^4 cells/cm²). For 3D culture, peptide was dissolved in 1 x PBS and treated as described above. Cells were added in mouse ES media (supplemented with FCS) and mixed with the unset gel at a gel: cell suspension ratio of 4:1. The final peptide concentration was 17.5mg/ml with 3×10^6 cells/ml of gel. LIVE/DEAD viability assay (Invitrogen) was used following the manufacturers protocol.

RESULTS: Mouse ES cells attached to the surface of FEFEFKFK hydrogels, forming spherical heaped aggregates (Figure 1, A). Encapsulated mouse ES cells were dispersed homogeneously within the hydrogels (Figure 1, B). Encapsulated ES cells remained viable after 4 days in culture (Figure 2, A). Cells were effectively removed from the scaffold by disrupting the gel

with gentle pipetting. Rescued cells were viable, forming ES cell colonies on gelatin 24 hours after replating (Figure 2, B).

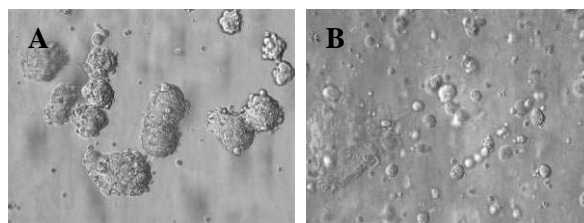


Figure 1. Light microscope images of mouse ES cells cultured on the surface (A) and within (B) FEFEFKFK hydrogels for 48 hours.

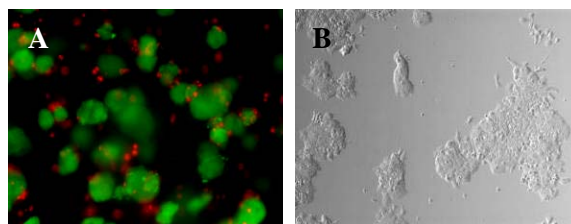


Figure 2. LIVE/DEAD staining of mouse ES cells cultured within FEFEFKFK hydrogels for 4 days highlighting live (green) and dead (red) cells (A). Light microscope image of mouse ES cells removed from gels (B).

DISCUSSIONS & CONCLUSIONS: FEFEFKFK peptide hydrogels provided a nanofibrillar surface for attachment and growth of mouse ES cells. ES cells were successfully incorporated within the gels, remaining viable after 4 days of culture. Cells were successfully retrieved from the gel, with rescued cells forming colonies and retaining ES cell morphology. Further research will focus on assessing ES pluripotency and growth within the octapeptide gels. Methods to functionalise the basic gel structure will also be explored with an aim to create an environment that facilitates the differentiation of both pluripotent and multipotent stem cells towards particular cell phenotypes.

REFERENCES: ¹A. Saiani et al (2009) *Soft Matter* **5**: 193-202. ²C. M. Ward et al (2002) *Lab. Invest.* **82** (12): 1765-1767.

ACKNOWLEDGEMENTS: This work is part of the BIOSCENT EU FP7 project for cardiovascular repair.

The use of Immobilised Protein Coated Surfaces to Direct Nucleus Pulposus Cell Attachment, Spreading, and Function

[E.A.Mitchell](#)¹, [A.Berta](#)¹, [A.M. White](#)¹, [S.Richardson](#)¹, [J.A.Hoyland](#)¹

¹ [School of Biomedicine, The University of Manchester, Manchester, England.](#)

INTRODUCTION: In tissue engineering good cell attachment, distribution and appropriate differentiation/function on a scaffold is a prerequisite for stronger associations between a biomaterial implant and native tissue *in vivo* and as such will ultimately improve the success of an engineered implant. Methods to achieve this include the specific immobilisation of proteins on biomaterial surfaces thus providing appropriate chemical cues to seeded cells.

The bone morphogenic proteins (e.g. BMP 2, 7, 13 and 14) have been shown to be important in regulating extracellular matrix synthesis in the intervertebral disc (IVD) and as such may have a role in directing relevant cell behavior in IVD tissue engineering strategies when attached to appropriate scaffolds. However, in order to assess the feasibility of such an approach proof of concept studies are needed to investigate the effect of these immobilised protein motifs on IVD cells. Here we describe the use of a TollAIII fusion expression system to immobilise BMP motifs on gold surfaces to investigate the effects on nucleus pulposus (NP) cells.

METHODS: Short functional motifs were identified from sequences of BMP 2, 7, 13 and 14 and the recombinant forms expressed in *E. coli* and purified by metal affinity chromatography. Proteins were immobilised on gold surfaces (Orla Protein Technologies) and spaces between the proteins filled with a hydroxyl terminated thiol¹. Human NP cells were incubated on surfaces (glass cover slips, bare gold cover slips, bare gold cover slips with full-length BMP added to the media following cell seeding, Tol surface without the BMP motif, Toll BMP motif coated surfaces) in the absence of serum for twenty four hours. Samples were then taken for RNA extraction or cells fixed with 4% paraformaldehyde. Cells were stained for DNA and actin cytoskeleton and imaged by epi-fluorescent microscopy.

RESULTS: Cell number: Tol-BMP surfaces supported adhesion of cells and there was no

significant difference in the number of cells adhered to these surfaces compared to when exogenous full lengths BMPs were present in media.

Cell Morphology: BMP2 and 13 coated surfaces displayed cells which were circular with a chondrocyte-like NP morphology. On BMP7 surfaces cells were more elongated, suggesting that the phenotype of NP cells had been altered. Cells on BMP14 coated surfaces appeared to be smaller indicating less cell adhesion and reduced spreading.

Gene Expression: Preliminary studies suggest that individual BMP motifs have different effects on NP gene expression and that the BMP13 motif is the most potent BMP in up regulation of NP phenotypic markers and extracellular matrix gene expression.

CONCLUSION: Cell morphology and gene expression was affected by immobilisation of short BMP motifs on surfaces with immobilisation of BMP13 leading to an enhanced NP phenotype. Interestingly this study suggests that the immobilised BMP motifs may be more potent than the exogenous factors, possibly due to the potentiation of signal. Importantly this system can provide an insight into the role of protein immobilisation on IVD cell physiology and thus will aid in the development of functionalised biomaterials for future tissue engineering strategies for repair of the degenerate IVD.

REFERENCES: ¹Chaffey et al, Journal of Nanomedicine, 2008, 3: 287-293.

ACKNOWLEDGEMENTS: Thanks to Arthritis Research UK for funding this study.

Effects of nanotopography on cell adhesion, morphology and differentiation

PM Tsimbouri¹, N Gadegaard², ROC Oreffo³ & MJ Dalby¹

¹ Centre for Cell engineering, Faculty of Biological & Life Sciences, Joseph Black Bld, University of Glasgow, Glasgow G12 8QQ, UK, ² Centre for Cell engineering, Department of Electronics and Electrical Engineering, Rankine Bld, University of Glasgow, Glasgow G12 8QQ, UK, ³ Bone and Joint Research Group, University of Southampton, Southampton, SO16 6YD, UK

INTRODUCTION: Topography and its effects on cell adhesion, apoptosis and differentiation have been well documented. Current advances with the use of nanotopography provided us with promising results in the field of regenerative medicine (Dalby et al 2007). Examining closely the effects of nanotopography on cell adhesion and morphology and the consequences of cell shape changes in the nucleus and gene expression we will be a step closer to understand and even control stem cell differentiation. In doing so, a molecular approach was used in combination with immunostaining studies and data will be presented.

METHODS: Stro-1 selected skeletal stem cells were used to study early time-point (3day) events in mechanotransduction. To study this, nanopits (120 nm diam, 100 nm depth) that were ordered (300 nm centre-centre square) and also with a controlled degree of nanodisorder (± 50 nm from centre of square) were used and compared to planar controls. These surfaces are known to change stem cell fate and to examine mechanotransductive events, cell, nucleus and adhesion morphology has been quantified and microarray analysis performed. Transcriptional changes were analysed with Ingenuity Pathway Analysis (IPA). Several inhibition studies have also been performed. Furthermore, the organization of the interphase nucleus has also been considered by lamin nucleoskeletal staining and chromosome territory analysis using FISH.

RESULTS: The results clearly show large changes in cell adhesion, nucleus and lamin morphologies in response to the different surfaces. Furthermore, these changes relate to changes in packing of chromosome territories within the interphase nucleus. IPA shows a wide range of signalling pathway regulatory changes hinging around hub signalling effectors such as ERK (extracellular receptor kinase). This, in turn, leads to changes in transcription factor activity and functional (phenotypical) signalling.

DISCUSSION & CONCLUSIONS:

Nanotopography is a very useful non-invasive tool for studying cellular mechanotransduction, gene and protein expression patterns, through its effects

on cell morphology. The different nanotopographies resulted in different morphological changes in the cyto- and nucleoskeleton as well as the chromosomes. Consequences of these changes have possibly contributed to the genomic changes observed. We propose that both indirect (biochemical) and direct (mechanical) signaling is important in these early stages of tuning stem cell fate. The work presented here provides us with a better understanding of cell-surface interaction and possibly new insights of how to control cell differentiation with future applications in areas like regenerative medicine.

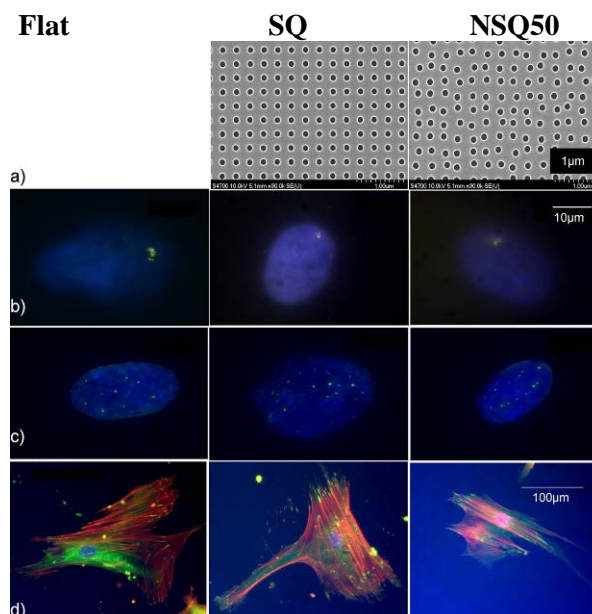


Fig. 1: Effect of different nanotopography patterns (a) on Chromosome 1 territory (FISH) (b) Lamin A staining shows differences in the organisation of the interphase nucleus (c) cell attachment /morphology using Actin (red filaments)/Vinculin (green adhesions) /DAPI (nucleus) staining

REFERENCES:

¹Dalby MJ, Gadegaard N., Tare R, Andar A., Riehle M.O., Herzyk P., Wilkinson C.D.W., Oreffo R.O.C. The Control of Mesenchymal Stem Cell Differentiation Using Nanoscale Symmetry and Disorder. (2007) Nature Mat.

ACKNOWLEDGEMENTS: This project is funded by BBSRC grant BGG0088681.

Recording & Evaluating the Effect of Silicon-substitution on Protein Adsorption/Desorption to Hydroxyapatite

M.-K. Mafina^{1,2}, A.C.Sullivan² & K.A. Hing¹

¹ School of Engineering and Materials & IRC, and ² School of Biological & Chemical Sciences Queen Mary & Westfield College, University of London, E1 4NS, UK

INTRODUCTION: The aim of this study was to develop a method which would facilitate the evaluation & comparison of individual & competitive protein adsorption on silicate-substituted hydroxyapatite (SA) & stoichiometric hydroxyapatite (HA). The initial objective was to evaluate whether it was possible to synthesise a fluorescent label fluorescein isothiocyanate (FITC) for covalent attachment to individually target proteins (albumin-BSA, fibronectin & osteopontin) and to use fluorescence to monitor individual & competitive binding.

METHODS: SA & HA powders (Apatech Ltd, UK) were calcined at 700 °C, pressed into 12 mm diameter dense discs (DD) at a pressure of 88.4 MPa, and sintered at 1300 & 1250 °C, respectively. Porous granules (PG) were also investigated. FITC was extended with a methyl-aminocaproate ester (ACA-OMe, Sigma-Aldrich, UK) spacer to provide covalent bonding to bovine serum albumin (BSA, Sigma-Aldrich, UK) *via* the lysine residue. BSA & FTCA-BSA solutions (1.5 ml) were placed in glass vials, and samples (1 DD /0.50 g PG) were added to analyse **adsorption**, 100 µl aliquot of the solution was removed at time intervals of 1, 5, 10 and 15mins. After 15 minutes, the test materials were placed in another vial to remove loosely bound BSA. Test materials were then placed in fresh PBS (1.5 ml) to analyse **desorption**, 100 µl aliquots were removed at time intervals of 5, 60, 240 and 1440mins. Protein concentrations in adsorption and desorption studies were doubly analysed (in triplicate) using the Quant-it kit assay (Invitrogen) and by measurement of FTCA-labelled protein fluorescence intensity (excitation/emission, nm) to verify accuracy of the technique.

RESULTS: Good correlation was found between Quant-it and FTCA-BSA data on HAD (Fig.1). Data obtained for FTCA-BSA adsorption and desorption at 37°C (Fig.2) showed BSA adsorption to be sensitive to temperature, chemistry and porosity of biomaterials.

DISCUSSION & CONCLUSIONS: This data indicates that FTCA-labelled proteins may be used to monitor protein adsorption & desorption. Initially, the data indicates that both substrate chemistry and its morphology affect the protein the

adsorption and desorption profiles, especially when porosity is introduced. Delayed adsorption is initially observed, which may reflect time for BSA diffusion to occur into the pore structure.

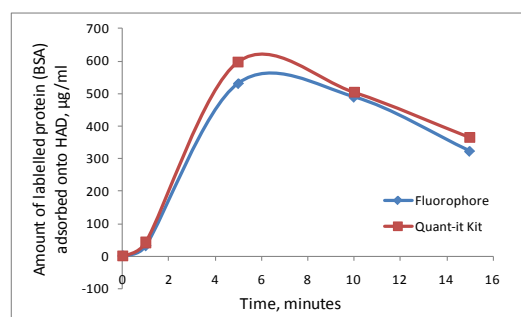


Fig. 1: Amount of FTCA-BSA adsorbed onto HAD calculated using the Quant-it kit & Fluorophore at RT

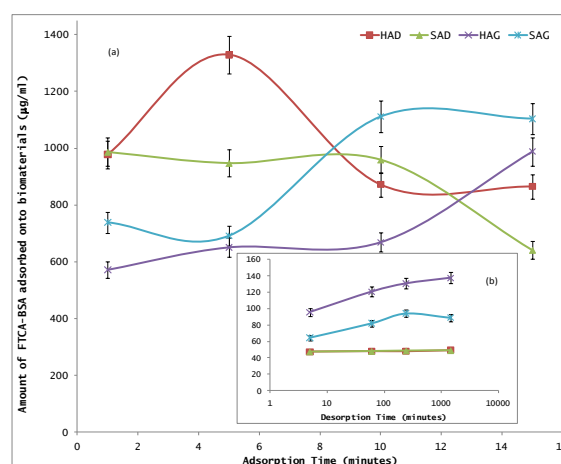


Fig. 2: (a) Adsorption & (b) desorption profiles of FTCA-BSA onto biomaterials at 37°C

Desorption, however, was instantaneous from PG with greater desorption from HA, suggesting protein is more tightly bound to SA-PG. Very little desorption occurred from DD, suggesting flat surfaces may facilitate tighter bonding of BSA.

REFERENCES: ¹ A.S. Abuelyaman, et al. (1994) *Bioconjugate Chem* 5:400-405 ² D.J. Fabrizio-Homan, et al (2000) *J Biomater Sci Polymer Edn* 3:27-47.

ACKNOWLEDGEMENTS: Thanks to EPSRC for MKMs studentship funding and ApaTech Ltd for providing the biomaterials.

Raman spectroscopy reveals material differences between pharmaceutically-treated bone nodules *in vitro*

B White^{1,2}, E Gentleman^{1,2} & M M Stevens^{1,2}

¹ Department of Materials and ² Institute of Biomedical Engineering, Imperial College London, UK

INTRODUCTION: Raman spectroscopy is a non-invasive optical imaging technique which can be used to rapidly and accurately characterise the biomolecular composition of live cells, without requiring the use of labelling or fixation procedures. In recent work [1] our group has used Raman spectroscopy to demonstrate that the material characteristics of tissue-engineered bone depend significantly on the cell type used: mesenchymal stem cells and osteoblasts were found to produce a material that mimicked many of the characteristics of native bone, while embryonic stem cells generated a material that was deficient in its mineral composition and ultrastructural organisation. To extend these results, we have studied the effects of several clinically important pharmacological and physiological interventions on the bone-like nodules formed *in vitro* by cultured primary mouse osteoblasts. Using Raman spectroscopy, we detect key differences in the resultant tissue structure. Our work suggests novel approaches to the characterisation of pharmaceutical effects, and may support the emerging use of small molecules to enhance cell-based regenerative medicine [2].

METHODS: Primary osteoblasts were isolated from neonatal mice and cultured *in vitro* using standard osteogenic medium which was further supplemented with a variety of treatments.

Intermittent parathyroid hormone exposure [3] and pamidronate [4] were selected as representative pharmaceutical treatments. Varying concentrations of extracellular ATP were also added to the osteogenic medium in order to characterise the effects of metabolic conditions on bone formation. Cell culture was conducted on individual MgF₂ substrates, due to the low background Raman signal of this material and its excellent compatibility with cells. After 10 days in culture, dense "bone nodules" began to form on the surface of the substrates; these substrates were thus imaged at 14 and 28 days in order to study the mineralisation process of the bone-like material.

Phase contrast microscopy was used to study the morphology of the bone nodules, while Alizarin Red S staining was used to confirm the

development of mineralisation and presence of calcium. Raman imaging was performed with a Renishaw InVia system, using a 785nm illuminating laser wavelength and a Leica microscope with 63 N.A. immersion lens.

RESULTS: All treatments appeared similar when stained with Alizarin Red S. However, differences in bone nodule properties as determined by Raman spectral analysis were observed between all treatment types and with controls; the pharmaceutical treatments produced a bone material that differed in relative composition to native bone, while high (micro-molar) concentrations of extracellular ATP were found to modify the proteinaceous components of the bone nodule environment. Use of ATP instead of β -glycerophosphate in osteogenic medium was also found to be able to produce bone nodules. In addition, pamidronate treatment seemingly inhibited the overall number of bone nodules formed *in vitro*.

DISCUSSION & CONCLUSIONS: We have shown that Raman spectroscopy can distinguish the effects of pharmaceutical treatments on an *in vitro* model of bone tissue formation, and that such differences cannot easily be identified with current staining protocols. These results suggest that Raman spectroscopy may provide a novel approach to validating pharmaceutical interventions in diseases such as osteoporosis. Furthermore, these observations suggest that a promising avenue for tissue engineering may be to combine the use of small molecules to "fine tune" the cellular properties in tissue-engineered constructs with the subsequent use of Raman spectroscopy to characterise the material thereby obtained.

REFERENCES: ¹ E. Gentleman et al. (2009) *Nature Materials* **8**:763-770 ² Y. Xu, Y. Shi, and S. Ding (2008) *Nature* **453**:338-344 ³ R. Skripitz, T.T. Andreassen, and P. Aspenberg (2000) *J Bone Joint Surg* **82-B**:138-41 ⁴ I.R. Orriss et al. (2009) *J Cellular Biochem* **106**:109-118

Targeted Drug Delivery *In Vitro*

F.Leng^{1,2} & S. Webb², J.E Gough¹

¹ School of Materials, ² Manchester Interdisciplinary Biocentre, University of Manchester, Manchester, UK

INTRODUCTION: Creating biomaterials that replicate the complex structure and functions of tissue has so far proved to be challenging. The possible applications of such mimics are vast, ranging from subcutaneous drug delivery to tissue engineering. Furthermore the aggregation of vesicles (simple cell mimics) can give an insight into cell-cell adhesion. They can also act as active stores with drugs encapsulated, ready for controlled release.¹

METHODS: Vesicle gels are a new type of biomaterial composed of: vesicles with membranes doped with biotinylated ligands, which are crosslinked with magnetic nanoparticles by avidin and embedded in a hydrogel. The inclusion of the magnetic functionality allows non-invasive magneto-spatial control of vesicle-nanoparticle assemblies in the gel, and facilitates the magnetic release of the contents of the vesicles into the surrounding area (Fig 1). The vesicle-nanoparticle assemblies are added to a biological mixture of a hydrogelator with fibroblasts or chondrocytes, in a 3D cell culture well.

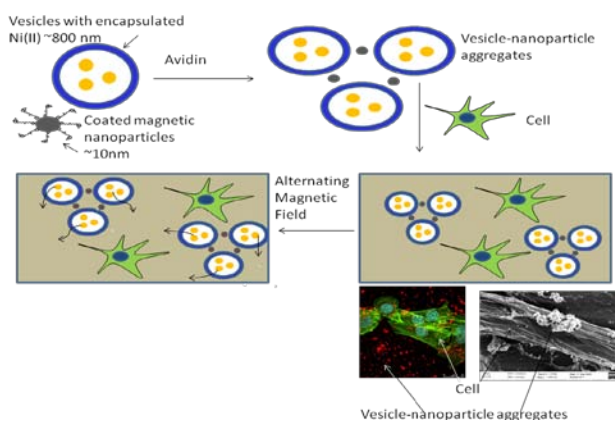


Fig. 1: Formation of vesicle-nanoparticle assemblies (top) and the magnetic release of cell stimuli from vesicle gels (bottom.)

When the vesicle gel is placed in an alternating magnetic field the alternating field has no

effect on the cells but the contents of the vesicles are released, which diffuse through the gel and triggering a cell response. To this end small molecules such as nickel chloride have been used to gain proof of principle.

RESULTS: Release from the vesicle gels is targeted by utilising the alternating magnetic field. This releases the compounds stored in the vesicles. The cell stimuli used are nickel which has been shown to have high toxicity in to 3T3 fibroblasts and ascorbic acid which is required for collagen production by chondrocytes. The vesicle-nanoparticle aggregates with encapsulated nickel chloride can be held in the gel block in close proximity to the cells with no adverse effects seen until placed in the alternating magnetic field which releases the contents and kills the cells. Similarly ascorbic acid has been encapsulated and the vesicle nanoparticle aggregates held in close proximity to chondrocytes in ascorbic acid deficient media. Once the magnetic field is applied the ascorbic acid is released and the cells begin to produce collagen. If the aggregates are not placed in the alternating magnetic field no collagen is produced.

DISCUSSION & CONCLUSIONS: Alginate gel is non-toxic and easily manipulated cell scaffold, and does not insert into or interrupt the vesicle membrane showing low percentage loss of the encapsulated molecules over time without stimulus. This system has promise in the on-demand release of biomolecules for specific responses tailored to specific cell types.

ACKNOWLEDGEMENTS: The BBSRC for funding and Mike Faulkner for SEM microscopy work.

REFERENCES

1.Mart RJ, Liem KP, Webb SJ, (2009) *Chem. Commun.* **33**:2287-2289.

HIGHLY ORIENTED ARRAYS OF CELLULOSE NANOWHISKERS GUIDE MYOBLAST MORPHOLOGY AND ORIENTATION

J M Dugan, J E Gough and S J Eichhorn

School of Materials, The University of Manchester, UK

INTRODUCTION: The natural hierarchical structure of native cellulose can be exploited to produce cellulose nanowhiskers (CNWs) - high aspect ratio crystals of cellulose with nearly monodisperse diameters of ~10nm [1]. Nanotopography has been shown to affect the morphology, differentiation and gene expression of various cell types [2,3]. In spite of their extremely small size, we have shown that CNWs can be utilised to direct the morphology of skeletal muscle cells (myoblasts) and, more generally, that the spatial arrangement of features as small as 10nm can impose order on proliferating mammalian cells.

METHODS: CNWs were prepared from the tests of *styela clava* tunicates by partial hydrolysis with sulfuric acid followed by dialysis, filtration and ultrasonication to yield a stable aqueous suspension of whisker-like nanoparticles with net anionic surface charge [1]. Arrays of CNWs were prepared by spin coating. Pieces of glass were cleaned with piranha solution and treated with 0.6% (w/v) polyallylamine hydrochloride. An aqueous suspension of CNWs (0.5% w/w) was then spin coated onto the clean cationic glass. A high spin speed of 6000 RPM achieved a high degree of orientation (samples designated CNW6000) whereas a slower speed of 500 RPM gave arrays with a much lower degree of orientation (designated CNW500).

The CNW arrays were characterised using AFM in tapping mode. C2C12 myoblasts were cultured using standard methods [4]. Cells were seeded to the arrays and fixed after 12 hours before staining with fluorescamine and propidium iodide. Morphological image analysis was carried out to quantify the orientation of the CNWs and myoblasts.

RESULTS: The CNW arrays were homogeneous and uniform with average feature height of ~10nm. The CNWs were highly oriented radiating from the centre of the CNW6000 samples. Much lower orientation was observed on the CNW500 samples as confirmed by image analysis. The myoblasts attached to the arrays and were well spread relative to control. For many cells the main axis of

elongation was oriented in line with the radial axis indicating contact guidance from the CNW6000 arrays. This effect was not observed on the CNW500 samples or the glass controls.

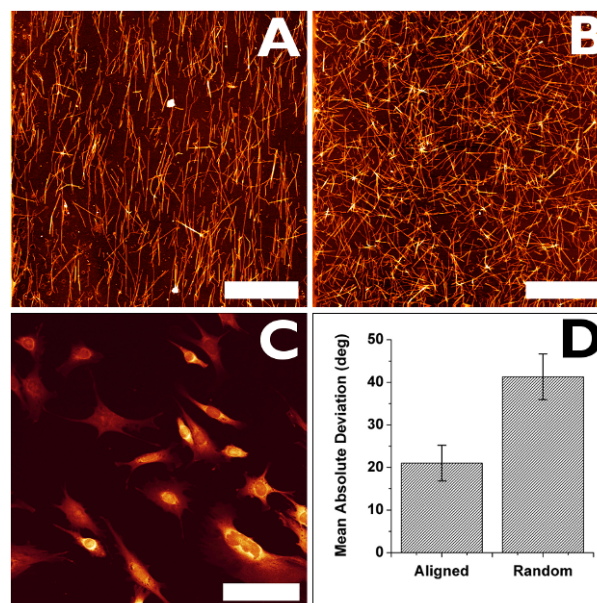


Fig. 1: (a) AFM topography image of CNW6000 and (b) CNW500 array. Bar=5 μ m. (c) Confocal micrograph of fluorescamine stained C2C12 cells on CNW6000 array. Bar=100 μ m. (d) Mean absolute deviation of CNW orientation..

DISCUSSION & CONCLUSIONS: We have shown that features of only ~10nm induce contact guidance in myoblasts. This indicates that myoblasts may be a particularly sensitive cell type to topographical cues and that cellulose may be a valuable material for applications in regenerative medicine and tissue engineering. Moreover, we believe that the preparation method may be scalable as a bioactive coating technology for medical devices.

REFERENCES: ¹Van den Berg et al. (2007), *Biomacromolecules* (2007), 8, 1353. ²Biggs et al. (2008) *J.R.Soc.Interface*, 5, 1231. ³Biela et al. (2009) *Acta Biomaterialia* 5, 2460. ⁴Huang et al. (2006) *Nano Lett.* 6, 3, 537.

ACKNOWLEDGEMENTS: Tunicin CNWs were kindly donated by Dr Laurent Heux, CERMAV, Grenoble, France.

Analysis of myotube-motoneuron interaction within an *in vitro* 3D collagen-based model of skeletal muscle.

A.S.T.Smith^{1,2}, V. Mudera³, L.Greensmith¹ & M.P. Lewis²

¹ Sobell Department of Motor Neuroscience and Movement Disorders, UCL Institute of Neurology.

² Muscle Cellular and Molecular Physiology Group, Institute of Sport and Physical Activity Research, Bedford and UCL Eastman Dental Institute.

³ Division of Surgical and Interventional Sciences, UCL Institute of Orthopaedics and Musculoskeletal Sciences.

INTRODUCTION: In seeking to further our understanding of skeletal muscle physiology and function in both healthy and diseased tissues, there is a strong need to develop *in vitro* culture systems that better represent the *in vivo* condition. This project is aimed at developing an innervated 3D *in vitro* model of skeletal muscle. It is hoped that the incorporation of primary motoneurons into a 3D model of skeletal muscle established in our lab will promote myofibre development towards an adult phenotype and improve the biomimicry of the system. Furthermore, the formation of neuromuscular junctions (NMJ) within a 3D *in vitro* setting should allow for testing of the effects of neuromuscular agents in culture, thereby reducing the need for *in vivo* experimentation. Here we present data characterising the development and maturation of this 3D co-culture system in comparison to conventional 2D cultures and discuss the implications for the future of skeletal muscle tissue culture techniques.

METHODS: Muscle derived cells (MDCs) isolated from P1 neonatal rat pups were seeded in neutralised type-1 rat tail collagen and plated into standard dimension chamber slides (TTP Lab Tech). The slides each held a custom built floatation bar (termed “A-frame”) at either end. Once the collagen gelled, it was cut away from the sides of the chamber and suspended in growth medium (20% fetal calf serum in high glucose DMEM). This provided two attachment points within the culture so that, as the cells attached and contracted, lines of isometric tension developed along the long axis of the construct. This tension provided sufficient mechanical stimulus to promote the realignment of the MDCs in a single plane. The result was a 3D tissue possessing uniaxially aligned and differentiated myotubes capable of performing directed contraction. These models were cultured for 7 days before plating primary E14 rat motoneurons on top. The co-cultures were maintained for a further 7 days before being either a) immunostained for myogenic (eg desmin)

neuronal (eg MAP-2) and/ or NMJ (eg alpha-bungarotoxin, synaptophysin) markers or b) prepared for PCR analysis.

RESULTS: Immunohistochemical stains confirmed the alignment of MDCs in culture and their capacity to differentiate into primary myotubes. The capability of neurons to survive in the system was also verified. Ability for exploratory neurites to penetrate the collagen matrix and run parallel to the cultured MDCs was also observed (Fig. 1).

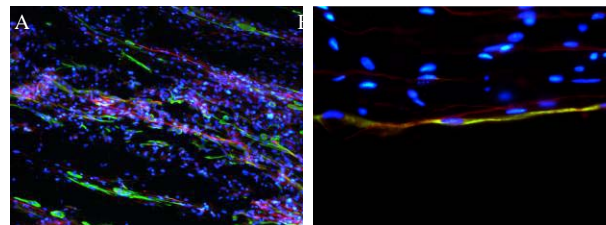


Fig. 1: 25 µm sections through the 3D collagen construct, stained for desmin (green) and MAP-2 (red, a neuronal marker) with a DAPI counterstain. Images taken at x20 (A) and x64 (B).

No significant difference was found by PCR in myogenin expression between 2D and 3D cultures, indicating that the fusion capability of MDCs in 3D is at least equal to that in standard cultures. The expression of synaptic markers synaptophysin, agrin and acetylcholine receptor suggests cells within this system are capable of forming synaptic contacts.

DISCUSSION & CONCLUSIONS: Though the formation of functional NMJs in this 3D model has yet to be established, our preliminary data indicates the presence and co-localisation of both pre and postsynaptic elements of NMJs. The survival of cells isolated from the ventral horn of E14 rat embryos within this system has been verified.

ACKNOWLEDGEMENTS: A.S.T. Smith is in receipt of an MRC studentship.

Alignment of Axonal Outgrowth on Microgrooved Devices

T.Dejardin , L.Ross, A.Hart and M. Riehle

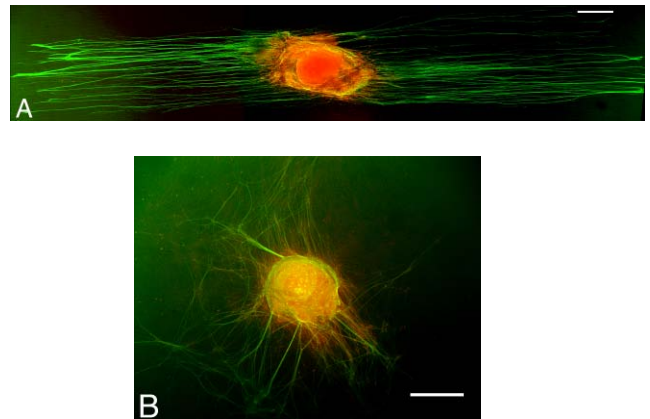
Centre for Cell Engineering, Dept of Molecular and Cell Biology, University of Glasgow UK.

Introduction: The use of “nerve tubes” which are in this context tubular conduits, that aim to connect the two opposing ends of a severed nerve and that guide axons across the gap, are a promising alternative to autologous nerve graft repair, which is currently the gold standard treatment. Nerve tubes are being used mostly in the repair of small diameter nerves with the defects being smaller than 3cm¹. Currently available nerve tubes are made of different biomaterials using various fabrication techniques and featuring different properties². Modifications to the common hollow nerve tube, like the addition of supportive cells^{3,4}, neurotrophins⁵, frameworks⁶ and electronic components⁷ are currently investigated in order to increase the gap length that can be bridged and to achieve better clinical outcomes. Here we focus on the effect of the microgrooved framework on the nerve outgrowth.

Method: Dorsal roots ganglia (DRG) were isolated from 2 days old neonates Wistar rats. There were then seeded either on poly-L-lysine (sigma) coated coverslip or 30s plasma treated Polydimethylsiloxane (PDMS) devices featuring 5µm depth and either 12.5, 25 µm width microgrooves. DRGs are then grown for 15 days in L15 media (sigma) supplemented by 10% FBS, 10ng/ml NGF 2.5S (Invitrogen), 50µg/ml n-acetyl-cystein and 1% antibiotics antimycotic (PAA p11-002). After 15 days growth, cells were fixed and immunostained for β-tubulin (ms anti-TU-20 Santa Cruz) & S100 (rb S100 Abcam). The samples were viewed by fluorescence microscopy.

Results: The axons outgrowth is guided by the microstructures. The outgrowth on the flat coverslip is randomly oriented and leads to a final ovoid or round neuronal network whereas on both microgrooved devices (12.5, 25µm) the outgrowth length is dramatically

increased to the edges of the 13mm long devices, the outgrowth follows the patterns to the end. The migration of Schwann cells and the formation of column of Bunker can be followed on both substrates.



DRG after 15 days culture on PLL in L15 NGF(10ng/ML) 10% FBS, 37°C 5%CO₂ (A) on 12.5µm width 5µm depth microgrooved PDMS device (B) on flat glass; red:s100; green:β-tubulin; scale 500µm

Discussion and conclusion: These initial results are encouraging for the design of a future nerve repair device because they shows how the inner topography of such a tube can provide a good guidance for outgrowing axons. The challenge is now to find the best way to integrate this topography in the design of a nerve guidance conduit in order to obtain the best clinical outcomes for patients.

Acknowledgement: We would like to thank the Steven Forrest Trust for funding, and EPSRC for support (DTC fellowship for LR).

- 1.Dahlin LB, Lundborg G. Use of tubes in peripheral nerve repair. *Neurosurg Clin N Am.* 2001 Apr;12(2):341-5
- 2.de Ruyter GC, Malessy MJ, Yaszemski MJ, Windebank AJ, Spinner RJ. Designing ideal conduits for peripheral nerve repair. *Neurosurg Focus.* 2009 Feb;26(2):E5.
- 3.di Summa PG, Kingham PJ, Raffoul W, Wiberg M, Terenghi G, KalbermattenDF. Adipose-derived stem cells enhance peripheral nerve regeneration. *J Plast Reconstr Aesthet Surg.* 2009 Oct 12.
- 4.Guo BF, Dong MM. Application of neural stem cells in tissue-engineered artificial nerve. *Otolaryngol Head Neck Surg.* 2009 Feb;140(2):159-64.
- 5.Gordon T. The role of neurotrophic factors in nerve regeneration. *Neurosurg Focus.* 2009;26(2):E3.
- 6.Hadlock T, Sundback C, Hunter D, Cheney M, Vacanti JP. A polymer foam conduit seeded with Schwann cells promotes guided peripheral nerve regeneration. *Tissue Eng.* 2000 Apr;6(2):119-27.
- 7.Gordon T, Brushart TM, Chan KM. Augmenting nerve regeneration with electrical stimulation. *Neurol Res.* 2008 Dec;30(10):1012-22.

Development of a Perfused Bioreactor System with Multiple Mini-chambers for the Culture of Cells on Biomaterials: Applications to Constructs Aimed at Spinal Cord Repair

T Sun^{1*}, P Donoghue², J R. Higginson², Susan C. Barnett², Nikolaj Gadegaard³, Mathis O. Riehle^{1*}
¹Centre for Cell Engineering, Joseph Black Building, ²Glasgow Biological Research Centre, ³Department of Electronic Engineering, University of Glasgow, UK

INTRODUCTION: It has been proposed that the repair of spinal cord injury will require a combination of strategies such as integrating the biological influence of glial cells together with physical guiding cues. Previously we demonstrated the effectiveness of micro-grooved ϵ -polycaprolactone (PCL) scaffold in conjunction with astrocytes on axon¹ and fabricated tubular PCL constructs ('Swiss-roll') with a wide range of micro- and nano- topographies². Before preparing aligned astrocytes within the 'Swiss-rolls' at relatively large scale, various scale up issues need to be addressed. Thus, the aim of this study was to design and evaluate a bioreactor system with multiple mini-chambers in 6-well plate, which can be used to bridge the gap between small scale static culture and relatively large scale perfused culture by investigating various scale-up issues.

METHODS: *Cell culture:* Astrocytes were purified and cultured in DMEM supplemented with 10% foetal bovine serum (FBS) and L-glutamine (2mM) as described previously³. *Design and fabrication of the bioreactor system* As illustrated in Fig. 1A, the bioreactor system consisted mainly of two commercially available 6-well tissue culture plates situated in two plastic boxes respectively, an 8-channel Ismatec peristaltic pump, 8 medium reservoirs (2.5ml) and 3-way valves. Corresponding to the 8 channels of the peristaltic pump, 8 mini perfusion chambers were fabricated in the 6-well plates as illustrated in Fig. 1B-C. Prior to experimentations, each perfusion system was sterilised by perfusing 70% (v/v) ethanol / 30% (v/v) sterile water overnight, washed with PBS for 60 minutes (at 1 ml/minute) and subsequently filled with cell culture medium. The perfusion chamber was then seeded with either astrocytes or fibroblasts using a syringe through the 3-way valves. The entire system was subsequently placed in a tissue culture incubator (37°C, 95% air/5% CO₂). After incubated statically for various amounts of time to allow cell attachment to the PCL substrates, the cells were then subjected to medium perfusion with varying flow rates for certain periods of time. During cell culture, the cells in both systems were monitored using either phase contrast microscope or time lapse video microscope. After cell culture, both systems were disassembled and the cells/substrates removed

for various analyses. **RESULTS:** Perfusion using the bioreactor suggested that cells could be detached by medium perfusion from untreated PCL, while plasma treatment combined with collagen coating (P-COL) could prevent this. Based on systematic investigations, an optimal bio-process was then proposed and aligned astrocytes were obtained successfully on P-COL treated micro-grooved PCL substrates.

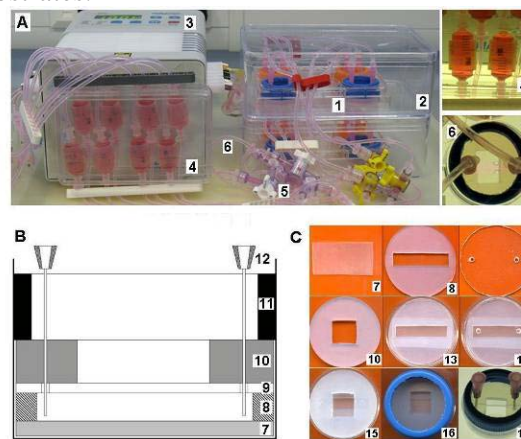


Fig. 1(A) The bioreactor system with multiple mini perfusion chambers. (B) Schematic diagram and (C) components of the mini perfusion chamber.

DISCUSSION & CONCLUSIONS: The bioreactor displayed technical and operational advantages, which will be of significance for systematic investigation of scale-up issues such as cell-cell and cell-scaffold interactions under different conditions (perfusion regime, dimensionality of scaffold, cell type etc), which is crucial for the transfer of static cultures to perfused cultures at relative large scale.

REFERENCES: ¹ Sørensen A et al, 2007. Long-term neurite orientation on astrocyte monolayers aligned by microtopography. *Biomaterials* 28:5498-5508. ² Gadegaard et al, 2003. Arrays of nano-dots for cellular engineering. *Microelectronic Engineering* 67:162-168. ³ Sørensen et al, 2008. Astrocytes, but not olfactory ensheathing cells or Schwann cells, promote myelination of CNS axons in vitro. *Glia* 56:750-763.

ACKNOWLEDGEMENTS:

We gratefully acknowledge financial support of BBSRC (UK) for this study.

Bioartificial Livers: a Modelling Approach to Hollow Fibre Bioreactor Design

A J Davidson, M J Ellis and J B Chaudhuri

Centre for Regenerative Medicine, Department of Chemical Engineering, University of Bath, UK

INTRODUCTION: Bioartificial Livers (BALs) aim to support liver function in patients until recovery or a liver transplant is available. Their design is based on the interaction of the patient's blood or plasma with cultured liver tissue. Several variations of the BAL have undergone clinical trials, although none have as yet acquired clinical acceptance¹. As liver cells are highly metabolic and often not directly-perfused, the mass transport of oxygen is critical. Mass transport equations are solved and the results presented in a way that allows conclusions over suitable bioreactor design to be made. The design methodology presented here could be adapted for use within other tissue engineering applications.

METHODS: The BAL model considered is based on a hollow fibre bioreactor where the fibres act as a scaffold for the liver cells. A mathematical model based on Krogh cylinders² is used to describe mass transport in the fibre bundle. In addition, operating constraints are defined on the system – cells should not experience hypoxia and the cell population should be of adequate size. By combining Comsol Multiphysics modelling results (Fig. 1) with these operating constraints and presenting the results graphically, 'operating region' charts can be constructed for the hollow fiber BAL (HF-BAL). The effects of varying operating conditions are then established.

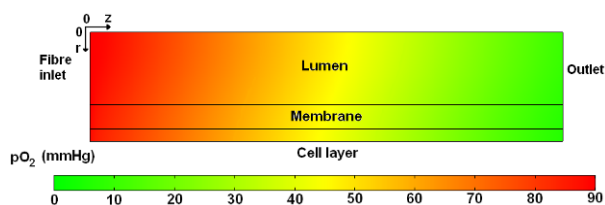


Fig. 1: A Comsol model solution, the colour map representing the distribution of oxygen partial pressure within a hollow fibre and surrounding cell layer

RESULTS: The operating region charts are defined by maximum and minimum possible fibre numbers as a function of fibre lumen radius. These charts were produced for varying plasma flow rate, cell number, fibre length and cell layer and membrane thicknesses (Fig. 2). The relative sizes of the operating regions were calculated as a measure of design flexibility and margin for error

in the model. A flow rate of 200 ml/min was enough to adequately oxygenate a population of 10 billion cells, or 10% of the adult liver cell mass, within the device. A double layer of cells adherent to the fibre caused the operating region to contract compared to the single layer model.

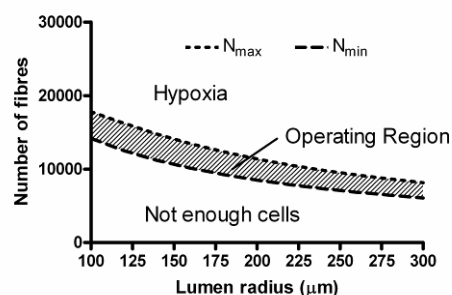


Fig. 2: An operating region chart for a hollow fibre bioartificial liver. The shaded area represents viable configurations

CONCLUSIONS: Studies on oxygen transport in BALs have been carried out before, however usually with existing commercial bioreactor designs. This work aims to connect mathematical models to bioreactor designs and operating conditions which result in a functional replacement liver. The results suggest for example it is preferable to use numerous narrow-bore fibres of short length to provide attachment area for the liver cells. Under the right conditions up to 20 billion liver cells can be supported, a therapeutically relevant cell mass³. The mathematical models discussed in this work can be adapted for other hollow fibre based tissue engineering applications, such as tissue-engineered bone and the bioartificial pancreas.

REFERENCES: ¹ N.L. Sussman, B.M. McGuire, and J.H. Kelly (2009) *Curr Gastroenterol Rep* **11**:64-68. ² A. Krogh (1919) *J Physiol* **52**(6):409-415. ³ H.I. Pryor, J.P. Vacanti (2008) *Frontiers in Bioscience* **13**:2140-2159.

ACKNOWLEDGEMENTS: This work was funded by the Engineering and Physical Sciences Research Council (EPSRC).

Development of a tissue-engineered skin model for detecting irritants

J Chunthapong, S MacNeil & JW Haycock

¹Department of Engineering Materials (Kroto Research Institute), University of Sheffield, UK.

INTRODUCTION: Chemical, cosmetic and pharmaceutical products are routinely evaluated for safety prior to release into the market, with the Draize rabbit skin and eye tests being the most commonplace [1]. However wide-spread scientific and ethical concerns have surrounded the use of these tests for a number of years. The European Council Directive 76/768/EEC, which has been enforced since March 2009, prohibits the use of animals for irritation, corrosive and phototoxicity tests when alternative means are available. Several *in vitro* 3D culture models have been developed as alternatives for chemical testing [2]. While they are typically expensive and largely confined to epidermal only models, they do not provide information beyond basic toxicity assessment. The aim of this project is therefore to develop a more accurate 3D skin model based on paracrine inflammatory interactions between human keratinocytes and fibroblasts with detection of IL-1 α , IL-6, IL-8 and NF- κ B as measured endpoints.

METHODS: Keratinocytes (NHK) and fibroblasts (HDF) were isolated from human skin obtained from abdominoplasty or breast reduction operations (under ethically approved guidelines). HaCaT keratinocytes were also used to explore the possibility of replacing NHKs. The effect of sodium dodecyl sulphate (SDS) and potassium diformate (Formi[®]) as model chemical irritants were studied on the release of IL-1 α , IL-6 and IL-8 by ELISA. Activation of NF- κ B in HDFs, based on translocation of its p65 subunit was investigated by immunofluorescence staining and confocal microscopy. MTT-ESTA assay was also performed in parallel to determine the cytotoxic effect of both model chemical irritants.

RESULTS: Subtoxic concentrations of SDS and Formi[®] induced the release of IL-1 α in normal human keratinocytes and HaCaT cells. Fibroblast cells also responded to human recombinant IL-1 α with sensitive and rapid activation of NF- κ B and responded to 24h incubation with IL-1 α by releasing a five-fold to twelve-fold increase of IL-6 and IL-8 into culture medium. Thus a link between irritant driven inflammatory signalling via IL-1 α and IL6/8 has been detected in skin cells.

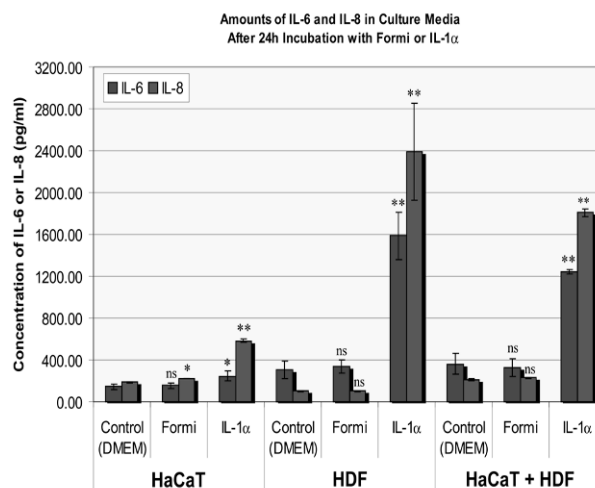


Figure 1: IL-1 α promotes IL-6 and IL-8 secretion by human dermal fibroblasts. Subconfluent cultures were challenged for 24h with 20 mM Formi[®] or 100 pg/ml IL-1 α . Conditioned media were collected ELISA assay performed to measure the amount of IL-6 and IL-8. Data are expressed as mean \pm SD, n = 2. * P < 0.05 and ** P < 0.01.

DISCUSSION & CONCLUSIONS: A 3D co-culture model is being developed to as an alternative for animal testing. The present work underpins the validity of the model whereby chemical test agents that come into contact with keratinocytes stimulate the release of IL-1 α . Subsequently, fibroblasts respond by the activation of NF- κ B and the release of IL-6 and IL-8 at much higher levels (and are therefore more readily detectable) compared to IL-1 α released by keratinocytes. In conclusion, fibroblasts are an essential part of paracrine signalling and we suggest must be integrated into such models [3, 4].

ACKNOWLEDGEMENTS: We acknowledge funding from BBSRC and Thailand's Strategic Scholarship for Frontier Research Network (to JC).

REFERENCES:

1. JH Draize et al (1944) *J Pharmacol Exp Ther* 82:377-390.
2. T Welss et al (2004) *Toxicol In Vitro* 18 (3):231-243.
3. I Cantón I, EH Kemp, AJ Ryan, S MacNeil, JW Haycock (2010). *Biotech Bioeng* (In press).
4. I Cantón, U Sarwar, EH Kemp, AJ Ryan, S MacNeil, JW Haycock (2007). *Tissue Eng*, 13 (5): 1013-1024.

Challenges of Cell Based Cartilage Repair

Tim Hardingham
University of Manchester

Damage and degeneration of articular joints is a major health care concern due to the high incidence of trauma and degenerative disease in an ageing population. Joint replacement is very successful, but with limited lifetime, so for younger patients there is great interest in developing biological repair. One of the key questions is what cells we can use. We have investigated primary human chondrocytes (HCAC) from osteoarthritic patients and found that they retain the potential to provide a source of autologous cells for cartilage repair at early passage. Adult human bone marrow stem cells (hMSC) provide an alternative source of cells and we have shown strong cartilage matrix assembly during in vitro chondrogenesis of hMSC scaffold-free in Transwell cultures. Some of the lessons learnt in vitro, such as the inhibitory affects of cell attachment on chondrogenesis, help guide the design of scaffolds for cell based cartilage repair. For future application a major issue to be resolved is the use of allogeneic rather than autologous cells, as this would enable much wider application of cell-based clinical treatments and at lower cost.

Designing materials to direct stem cell fate

Matthias Lutolf

Laboratory of Stem Cell Bioengineering, Lausanne, Switzerland

Proper tissue maintenance and regeneration relies on robust spatial and temporal control of biophysical and biochemical microenvironmental cues, instructing stem cells to acquire particular fates. Biomaterials are being rapidly developed to display and deliver stem cell regulatory signals in a precise and near-physiological fashion, serving as powerful artificial microenvironments (or ‘niches’) to study and manipulate stem cell fate both in culture and in vivo. In this talk I will highlight recent efforts in my laboratory to develop microarrayed artificial niches based on a combination of biomolecular hydrogel and microfabrication technologies. These platforms allow key biochemical characteristics of adult stem cell niches to be mimicked and the physiological complexity deconstructed into a smaller, experimentally amenable number of distinct signaling interactions. The systematic deconstruction of a stem cell niche may serve as a broadly applicable paradigm for defining and reconstructing artificial niches to accelerate the transition of stem cell biology to the clinic.

RESORBABLE COMPOSITE SCAFFOLDS FOR BONE TISSUE ENGINEERING

M A Woodruff¹, D W Hutmacher¹

¹ *Regenerative Medicine Group, Institute of Health and Biomedical Innovation, Queensland University of Technology, Australia, Kelvin Grove 4059.*

INTRODUCTION:

Bone loss associated with trauma osteo-degenerative diseases and tumors has tremendous socioeconomic impact related to personal and occupation disability and health care costs. Bone grafting is often critical to surgical therapies. Autogenous bone is presently the preferred grafting material; however, this holds several disadvantages such as donor site morbidity. In the present climate of increasing life expectancy with an ensuing increase in bone-related injuries, orthopaedic surgery is undergoing a paradigm shift from bone-grafting to bone engineering, where a scaffold is implanted to provide adequate load bearing and enhance tissue regeneration.

We have developed, characterised and evaluated polycaprolactone/tricalcium phosphate (PCL/TCP) composite scaffolds for low load-bearing bone defects. These scaffolds are being further developed for application in higher load bearing sites. Our approach emphasizes the importance of the biomaterials' structural design, the scaffold architecture and structural and nutritional requirements for cell culture. These first-generation scaffolds made from medical grade PCL (mPCL) have been studied for more than 5 years within a clinical setting¹. This paper describes the application of second-generation scaffolds in small and large animal bone defect models and the ensuing bone regeneration as shown by histology and μ CT.

METHODS:

mPCL/TCP scaffolds (80/20 wt%) were fabricated using fused deposition modelling. Scaffolds were cut to size using either biopsy punches for rat cranial defect studies or were custom made to 1x1.5x2cm implants for pig cranial implantations. All defects sites were pre-established to be "critical sized" and empty defects were used as a control. Pig experiments are detailed schematically in Fig 1 (A, B). Cells were dispersed within fibrin glue and injected during implantation into selected scaffold/defect sites to compare bone regenerative capabilities of cell versus cell-free scaffolds.

Figure 1: BMSC extraction (A) and scaffold implantation into critical sized defect (B). After 2 years implantation, the scaffolds plus surrounding host bone were explanted (C) and analysed using μ CT (D) and histology (E-J).

RESULTS:

Histological assessment using von kossa staining for mineralised bone (black areas E,G,H) showed extensive bone regeneration throughout the entire scaffold, supported by μ CT analysis (D). Goldners trichrome staining showed clear osteocytes embedded within mineralised matrix and active osteoblasts present around scaffold struts (F,H,J). Cell groups performed better than cell-free scaffolds.

DISCUSSION & CONCLUSIONS:

Bone regeneration within defects which cannot heal unassisted can be achieved using PCL/TCP scaffolds, and this is improved by the inclusion of autogenous BMSCs. Further work will include the inclusion of growth factors including BMP-2, VEGF and PDGF. Using knowledge of drug delivery and biomaterial science, multifunctional scaffolds, where the three-dimensional (3D) template itself acts as a biomimetic, programmable and multi-drug delivery device can be designed to emulate the structure and function of the anatomical site which provides the ultimate tool in successful bone tissue engineering.

REFERENCES:

¹ Woodruff MA, Hutmacher DW (2010) *The return of a forgotten polymer: PCL in the 21st century.* Prog. Polym. Sci.

Modelling the niche: Analyses of Mesenchymal Stem Cells in 3D

Paul Genever

Department of Biology, University of York, York, UK

Human multipotent mesenchymal stromal cells or mesenchymal stem cells (MSCs) are found in adult tissues such as bone marrow and are able to differentiate into osteogenic, chondrogenic and adipogenic tissues. There is intense interest in determining how MSCs may be used in future cell-based therapies, including gene therapy and tissue engineering, and as in vitro models for fundamental research and drug discovery. However, better understanding of MSC biology and the factors that regulate MSCs in their 3D microenvironment or niche is required. These factors are likely to include cell-cell and cell-matrix interactions, oxygen tension, mechanical influences and nutrient diffusion. To address this, we have developed simplified methods for cultivating human MSCs under non-adherent conditions to promote cell-cell interactions to form 3D microtissue-like structures. Under precisely defined conditions, we observe a significant increase in expression of pluripotent markers and enhanced MSC differentiation capacity. To determine the function of a putative vascular MSC niche and heterotypic cell-cell signalling, we have studied the effect of endothelial cells on MSCs activity using a 3D self-assembling co-culture model. Our 2D and 3D models have been used to determine pathways that regulate MSC differentiation using in vitro conditions that may reflect more accurately in vivo intercellular connectivity.

Harnessing Material Induced Cell interactions to Develop Cost Effective Regenerative Medicine Solutions: The Journey from Bench to Body

J.M. Curran,

UKCTE Clinical Engineering, The University of Liverpool. U.K.

INTRODUCTION: Current strategies in regenerative medicine and tissue engineering have been born out of the belief that for the vast majority of materials must be more than passive entities that are sealed off by the host with a minimal inflammatory reaction, but instead should play an active role in dictating the host response. This can be through control of protein adsorption, cell selection and adhesion resulting in induction of selected cell signalling pathways to produce a pre-determined cell response. To design and develop such materials requires a fundamental understanding of what factors control initial host responses, i.e. levels of selected reactions that then go on to determine a specific cell response, but more importantly what variables we can control on a surface that will result in our desired cellular behaviour. To achieve this we need a thorough understanding of the cells and also a high level of control of the cell presenting surface. There is a significant level of research activity relating to the design of highly specified surfaces that can be used to induce definitive cellular responses, and a large volume of knowledge has been collected regarding how we can use material factors to control the cells. These surfaces are often model surfaces allowing the control of one single variable, a practice that is invaluable in isolating specific factors that can be used, but the problem often comes when transferring the model surfaces to useable 2- and 3-dimensional tissue scaffolds. The information presented within this talk will encompass the derivation of data regarding the role of functional chemistries, relating specifically to cell/material interactions, and how we can use these modifications to design and produce cost effective, commercially viable solutions to an array of unmet clinical needs.

METHODS: An array of silane modified surfaces were produced using previously described methods [1]. Protein and cell adhesion, and subsequent cell responses including MSC differentiation, to these bulk coated surfaces (-CH₃, -OH, -COOH and -NH₂) were used as a preliminary screen for direct comparison of functional chemical nano-arrays.

Nano-patterned substrates were produced using Dip Pen Nanolithography (DPN®) systems [2]. A number of thiolated inks that presented distinct chemical functionalities (-CO₂H, -NH₂, -CH₃, -OH) were used. In order to investigate the effect of feature size (area of modification), spacing (centre-to-centre distance between adjacent groups), array (square versus hexagonal arrays) and the terminating chemical functionality of the fabricated nanostructures, several nanopatterned surfaces were prepared. Fundamental data derived from these studies was used to design surfaces with dynamic surface chemistries that controlled the contextual presentation of the functional group; cell selective and expansion properties of these novel materials were evaluated using an array of autologous stem cell sources.

RESULTS: Data confirmed that functional chemistries can be used to induce stem cell differentiation in the absence of exogenous biological factors. Chemical arrays produced by DPN systems significantly enhanced material induced cell differentiation by control of density and nano-spacings of functional groups, effectively controlling integrin binding and clustering. Manipulating the contextual presentation of the chemical group, i.e. dynamic surface chemistry using bulk coating techniques, over a finite set of parameters can be used to transfer the fundamental model data obtained from DPN studies to useable biomedical substrates.

ACKNOWLEDGEMENTS: NanoInk Inc. for their collaborative contribution to this research.

REFERENCES:

1. Curran JM, Chen R, Hunt JA. Biomaterials 2006 Sep;27(27):4783-4793.
2. Curran JM, Stokes R, Irvine E, Graham D, Amro NA, Sanedrin RG, et al.. Lab Chip Apr 14, Vol 10 (13).

Control of corneal fibroblast orientation and behaviour by nanofibers

M Ahearne¹, AJ El Haj¹, S Rauz² & Y Yang¹

¹*Guy Hilton Research Centre, Institute for Science & Technology in Medicine, Keele University UK*

²*Academic Unit of Ophthalmology, School of Immunity & Infection, Birmingham University UK*

INTRODUCTION: Control of cell orientation is vital to the development and function of several engineered tissues included cornea, tendon, nerve and muscle. Certain cell types, such as corneal fibroblasts, are believed to align naturally in-vitro under certain culture conditions [1]. Here we investigated if the application of aligned nanofibers can be used to dictate the orientation and improve alignment of the corneal fibroblasts cultured over several weeks in-vitro.

METHODS: Polycaprolactone dissolved in a chloroform solution was electrospun to form nanofibers using the electrospinning apparatus described previously [2]. Aligned nanofiber meshes were collected and adhered to glass slides (25 x 50mm) which had been coated using rat-tail collagen type-1 (BD Bioscience). The slides were UV sterilized before use with cells.

Human corneal fibroblasts were cultivated as previously described [3]. The fibroblasts were seeded onto glass slides both with and without nanofibers attached. 200,000 cells were seeded onto each slide. 1mM of ascorbic acid was added to the culture media for some of the cells to examine if it enhanced or affected cell alignment. The cells were cultivated for 4 weeks and media was changed every 3-4 days. After 4 weeks cells were viewed using a light microscope and stained using a live-dead staining kit (Fluka) and viewed using a confocal microscope.

RESULTS: After 4 weeks in culture, corneal fibroblasts on glass slides with nanofibers all aligned in the direction of the nanofibers (Fig 1b). Fibroblasts on slides without nanofibers contained localised regions of aligned cells but there was no one direction all the cells appeared to orientate towards (Fig 1a). Interestingly a second layer of cells on slides without nanofibers appeared to grow at an angle to the underlying layer, a phenomena not seen on slides with nanofibers (Fig 2). Ascorbic acid did not appear to have any significant affect on the cell orientation. Live-dead images appeared to show higher levels of cell viability on slides with nanofibers than those without nanofibers.

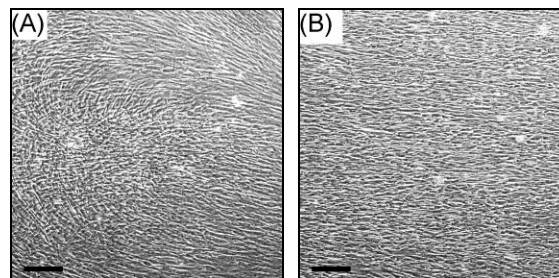


Fig. 1: Light microscopy images of corneal fibroblasts cultured on a (A) glass slide only and (B) glass slide with aligned nanofibers attached for 4 weeks (scalebar = 250µm).

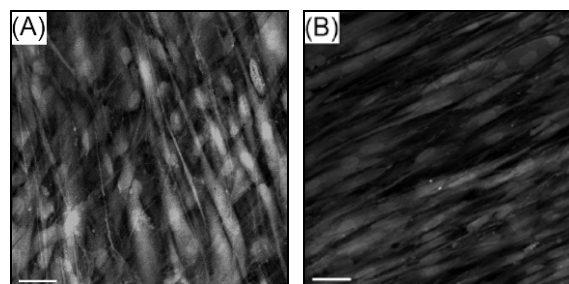


Fig. 2: Live-dead fluorescently stained corneal fibroblasts cultured on (A) glass slide only and (B) glass slide with aligned nanofibers attached for 4 weeks (scalebar = 50µm).

DISCUSSION & CONCLUSIONS: It has been demonstrated that nano-topography can be used to dictate the direction of cell growth. These findings can be applied to engineering several tissues which require cells and fibers to be orientated in a particular direction. Further investigation is required to determine the influence aligned nanofibers have on cell proliferation and extracellular matrix production.

REFERENCES: ¹X. Guo, A.E.K. Hutcheon, S.A. Melotti et al (2007) *Invest Ophthalmol Vis Sci* **48**:4050-60. ²I. Wimpenny, K. Hampson, Y. Yang, (2009) *Tissue Eng C* (In Press). ³M. Ahearne, Y. Yang, K.Y. Then et al (2008) *Br J Ophthalmol* **92**:268-71.

ACKNOWLEDGEMENTS: This research was funded by BBSRC (BB/F002866/1).

Introducing stable microgrooves in to fluid-leaving surface of plastic compressed collagen by embossing.

Tijna Alekseeva¹, Frank Tully², Jonathan C. Knowles³, Robert A. Brown¹

¹UCL, Institute of Orthopaedics-TREC, Stanmore Campus, London UK, ²The Automation Partnership (Cambridge) Ltd, Royston, Hertfordshire, UK, ³UCL, Eastman Dental Institute, London, UK

INTRODUCTION: Micropatterning of polymers is a technique used in tissue engineering to create additional features on the surface usually to manipulate cell behaviour. However, methods used for fabrication of such features on the surface of synthetic polymers are not always suitable for natural polymers. Here we describe a method of embossing developed for plastic compressed collagen constructs. Plastic compression (PC) of collagen is a technique that allows cell-independent fabrication of dense, tissue-like collagen constructs without compromising viability of resident cells (1). Method of PC creates potential anisotropy of the opposite surfaces – stiffer fluid leaving (closest to the blotting elements) and more elastic non-fluid leaving surface. We hypothesized that embossing into these surfaces will give more stable features on the fluid-leaving surface (FLS) as opposed to non fluid-leaving surface (NFLS). Objectives were to develop methods of embossing onto both surfaces, assess these features and to determine stability of the embossed pattern over time with and without cells. Slow-dissolving phosphate-based glass fibers were used as the embossing template in this study as fiber diameter and spacing is easily controlled.

METHODS: Collagen type I (acid-soluble, rat-tail, FirstLink, UK) was neutralized and set prior to plastic compression. Glass fibers (diameter 35-40 μm , average spacing 70 μm) were pressed into the collagen gel during standard PC, into the FLS or NFLS (Fig1) for pattern embossing.

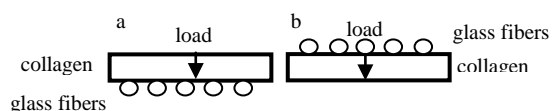


Fig1. Schematic representation of the PC embossing on to the FLS (a) and NFLS (b). Arrow – direction of fluid flow.

Constructs were fixed and features analyzed using SEM and routine wax histology. Stability of the grooves embossed on to FLS was then tested by culturing acellular and cellular (seeded with human corneal fibroblasts, 5×10^5 per construct) constructs in the standard culture medium

(DMEM) for two weeks. Grooves dimensions were measured at days 1, 7 and 14 using SEM and wax histology. Data are presented as mean \pm SD. Statistical analysis was carried out using non-parametric unpaired t-test (GraphPad Prism 3.0 software, USA); value of $p < 0.05$ was considered significant.

RESULTS: Embossing of the glass fibers on to PC collagen resulted in deeper, more pronounced grooves on the FLS as opposed to the NFLS (Fig.2a, b). Measured depth of the indentations was almost 3 fold greater in the FLS ($23 \pm 3.8 \mu\text{m}$) than NFLS ($8.2 \pm 2.2 \mu\text{m}$).

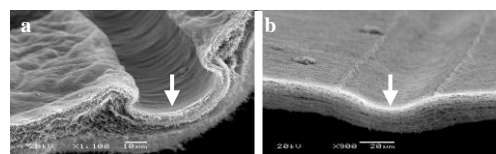


Fig. 2. SEM images of features, embossed in to the PC collagen (arrows). a- FLS, b-NFLS

Importantly, the depth of grooves embossed on to FLS did not change significantly over two weeks culture period in either cellular or acellular constructs (Fig.3a, b).

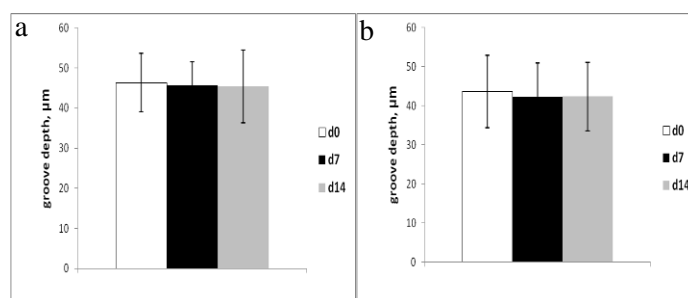


Fig.3 Average depths of the grooves embossed on to FLS of a – acellular PC collagen constructs b - seeded with corneal fibroblasts. Measured at days 1, 7 and 14 in culture.

DISCUSSION & CONCLUSIONS: Embossing of the predictable microfeatures is more effective on to the FLS of the PC collagen and features are stable for at least 2 weeks culture regardless of cell activity.

REFERENCES: ¹Brown R.A. et al. (2005) *Adv. Funct. Mater.* **15(11)**, 1762-1770

ACKNOWLEDGEMENTS: TSB-EPSC for funding, George Georgiou for technical help.

Electrospinning highly oriented elastomeric fibres for skeletal muscle regeneration

K. Aviss, J. Gough, & S. Downes

School of Materials, The University of Manchester, Manchester UK

INTRODUCTION: The strict hierarchy and parallel arrangement of myofibres within skeletal muscle tissue has made *in vitro* regeneration of this tissue difficult. Creating a biodegradable template scaffold to encourage myoblast and consequent myofibre alignment may be beneficial. This work focuses on electrospinning of the elastomeric polymer PLGA to create highly aligned fibres to provide the correct topographical contact guidance for myoblast alignment and bipolar elongation. Differentiating myoblasts have been known to spontaneously contract. This contraction often leads to cellular detachment away from their substrate¹. Previous studies have found that altering the substrate stiffness can affect how myoblasts detach as they differentiate². PLGA is an elastomeric polymer that when electrospun fits into the acceptable range of elasticity optimal for myoblast differentiation^{3,4}.

METHODS: PL85GA15 was dissolved in HFIP to form a 20% w/v solution. This was then pumped at 1 ml/hour through a blunted needle with 25 kV applied to it. The rotating mandrel collector plate was 12 cm away from the needle, rotating at 300 RPM for randomly oriented fibres and 1500 RPM for aligned fibres. SEM was utilised to visualise fibrous scaffold meshes. C2C12 murine myoblasts were cultured in DMEM with 20% FBS and 1% penicillin/streptomycin. Differentiation was induced with 2% horse serum. Myoblasts were seeded on electrospun scaffolds and glass coverslips. They were then fixed and stained for f-actin; using FITC-conjugated phalloidin, or sarcomeric myosin using A1025, a gift from Dr. Michelle Peckham, or fast myosin heavy chain, and nuclei using DAPI prolong. Alexa Fluor 546 was used for sarcomeric staining; Alexa Fluor 488 was used for fast myosin heavy chain.

RESULTS: Myoblasts responded to the aligned topography by showing a more elongated morphology compared to the random fibres and glass control after 30 minutes culture (see fig 1). This elongation was quantified by measuring the cells' aspect ratio and found that cells on aligned fibres had significantly more elongation than on random fibres or the glass control ($P = 0.05$).

Immunostaining of differentiation marker fast myosin heavy chain showed that cells cultured on the aligned fibres had significantly more differentiation than those on random fibres and glass control. Immunostaining of sarcomeric myosin showed that the correct sarcomeric array of proteins is present, indicating that these cells would be able to contract given correct stimuli.

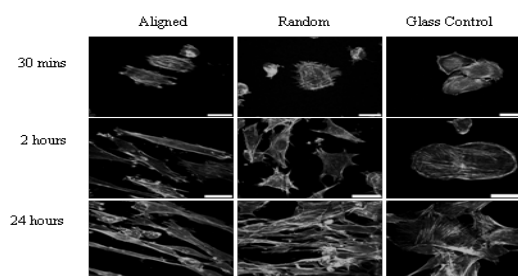


Fig. 1: Elongation of myoblasts on electrospun fibres and a glass control³.

DISCUSSION & CONCLUSIONS:

Electrospinning of PLGA into aligned fibres provides an adequate template for myoblast alignment. This alignment is maintained longer term³. The aligned fibres encouraged myoblast differentiation compared to random fibres and glass control³.

REFERENCES: ¹S. A. Riboldi, M. Sampaolesi, P. Neuenschwander, G. Cossu, S. Mantero, 2005, Electrospun degradable polyesterurethane membranes: potential scaffolds for skeletal muscle tissue engineering, *Biomaterials*, 4606-4015. ²A. J. Engler, M. A. Griffin, S. Sen, C. G. Bonnemann, H. L. Sweeny, D. E. Discher, 2004, Myotubes differentiate optimally on substrates with tissue-like stiffness: pathological implications for soft or stiff microenvironments, *The Journal of Cell Biology*, **166**:877-887. ³K. J. Aviss, J. E. Gough, S. Downes, Aligned electrospun polymer fibres for skeletal muscle regeneration, 2010, *eCM*, Article in Press. ⁴M. Levi-Mishali, J. Zoldan, S. Levenberg, 2009, Effect of scaffold stiffness on myoblast differentiation, *Tissue Engineering Part A*, **15**:935-944.

ACKNOWLEDGEMENTS: Thanks to the BBSRC for funding this project.

FT-IR Study on Bone Nodules Formation

H M Aydin, B Hu, A J El Haj, Y Yang¹

Institute for Science and Technology in Medicine, School of Medicine, Keele University

INTRODUCTION: As one of the promising approach in bone regeneration, tissue engineering of bone has been one of the focal areas for years due to the ageing population. We reported that primary osteoblastic cells and stem cells are capable of mineralization up to certain levels in vitro [1]. In scaffold based approaches, it is important to obtain cell-material constructs which are capable of producing high amounts of matrices. In this study we investigated the nodule formation capacity of osteoblasts on different substrates and culturing conditions. FT-IR analyses were used to identify the structure of generated inorganic matrices.

METHODS: An osteoblastic cell line (MLO-A5) was used to generate cell aggregates and inorganic nodules. Cells were seeded onto three different substrate surfaces and cultured in the presence of two different media (undifferentiated and osteogenesis) for 40 hours. Coatings were prepared either on suspension cell flasks or normal adhesive cell culture plates by using PEO Pluronic F127 (BASF, Germany). Types of the substrate surfaces and the media used are summarized in Table 1. Then the formed cell aggregates were transferred to normal 6-well cell culture plates (cell adhesive) for further cell proliferation and mineralization. The osteogenesis medium was used for the further culture. At the end of the study, cell aggregates along with the produced nodules were collected and analyzed with TGA and FT-IR. TGA gave the quantitative analysis of the minerals. Then the FTIR spectra of the samples which were ashes from the previous TGA analysis were recorded by Bruker ALPHA-P FT-IR spectrometer with a diamond ATR cell (Bruker, UK) in the range of 4000-400 cm^{-1} . Representative FT-IR spectrum of the nodules is given in Figure 1.

RESULTS: Within 40 hour culture, osteoblasts generated high and homogeneous cell aggregates on commercial suspension plates with average aggregate size of 100 μm ; whilst they generated few but much bigger cell aggregates in PEO coated culture flasks. The XRD analysis of nodules confirmed hydroxyapatite crystals and TGA showed that the minerals quantity was much higher in the group 3A. FT-IR analysis showed the formation of hydroxyapatite crystals.

Table 1. Substrate surfaces and the media used in the groups.

Group	Media	Flask Surfaces
1A	Normal	Non-adhesive suspension
1B	Osteogenic	Non-adhesive suspension
2A	Osteogenic	PEO (10 mg/ml) coated normal cell culture
2B	Osteogenic	PEO (20 mg/ml) coated normal flask
3A	Osteogenic	PEO (10 mg/ml) coated non-adhesive
3B	Osteogenic	PEO (20 mg/ml) coated non-adhesive

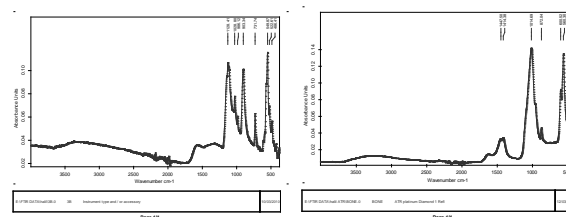


Fig. 1 Representative FT-IR spectra of the nodules produced in 3B group (left) and of native bone (right).

DISCUSSION & CONCLUSIONS: An osteoblastic cell line can form cell aggregates and induce enhanced mineral formation. Interestingly, the minerals from the nodules contains high phosphate crystals amount comparable to native bone, although there were small other peaks in the mineral peak range (mineral crystallinity appearing in 1030-1020 cm^{-1}). Hence, the sequential culturing of osteoblasts has a potential to enhance mineralization.

REFERENCES: ¹ Y. Yang, J. Magnay, L. Cooling, J.J. Cooper, A.J. El Haj (2004), *Effects of Substrate Characteristics on Bone Cell Response to the Mechanical Environment*. Medical and Biological Engineering and Computing. 42(1):22-29. ² A. Boskey, N.P. Camacho, (2007). *FT-IR Imaging of Native and Tissue Engineered Bone and Cartilage*. Biomaterials 28:2465-2478.

ACKNOWLEDGEMENTS: FP7 IEF Marie Curie action (PIEF-GA-2009-237762). We would like to thank Professor Lynda Bonewald, USA for kind donation of MLO-A5 cell line.

CELLULAR RESPONSES TO PHOSPHONATE CONTAINING POLYMERS

Anita Bassi, J Gough, M Zakikhani & S Downes

The University of Manchester, The School of Materials, Materials Science Centre, Grosvenor Street, Manchester, M1 7HS, UK

INTRODUCTION: Osteoporosis is a chronic illness that affects an estimated 200 million people worldwide¹. The homeostatic imbalance between bone resorption and bone deposition by osteoclasts and osteoblasts, respectively, leads to a decrease in bone mass. Osteoporotic patients are more prone to fracture compared to healthy individuals; there are approximately 150,000 osteoporotic fractures in the UK every year. Fracture repair and prosthesis implantation can be problematic due to diminishing bone stock; bone grafts are often required². There is a clinical need for a synthetic bone graft substitute that can be implanted at the site of surgery; one that could reduce the activity of osteoclasts and consequently increase bone mass at the site. This could be achieved by functionalising a biocompatible polymer with a drug mimic.

METHODS: Polycaprolactone (PCL) fibrous scaffolds were produced through the electrospinning process (Electrospinning parameters: flow rate of 0.05ml/min, voltage 20kV and distance from needle to collector plate of 15cm) and treated with a novel drug mimic. Osteoclast pre-cursor cells (Lonza, UK) were treated with RANK-L and M-CSF and after 7 days there was mature osteoclast formation. Osteoclasts were seeded onto scaffolds and cultured for 14 days. Cell apoptosis was assessed by cell counting and using the commercially available Apopercantage assay (Biocolor Ltd, UK) at day 14. Osteoclast morphology was evaluated using scanning electron microscopy (SEM) at day 1 and day 7. Glass cover slips and untreated PCL were used as a control.

RESULTS: After 14 days in culture there was a decrease in osteoclast number on the drug mimic when compared to the untreated PCL and glass. The apoptosis assay confirmed the presence of a higher number of apoptosing cells in the presence of the drug mimic. There was no significant difference in the number of apoptosing cells between glass and untreated PCL. SEM confirmed the presence of osteoclasts on all surfaces at day 1. At day 7 there were multinucleated cells present on glass and untreated PCL however there were fewer cells on surfaces containing the drug mimic. There was also evidence of cell debris.

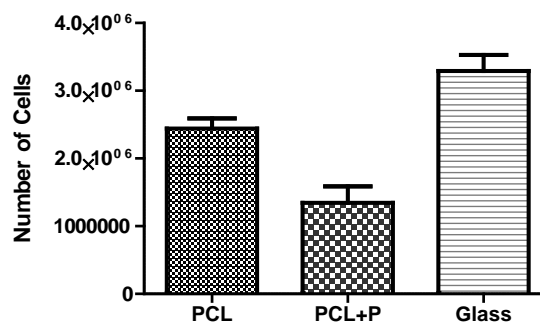


Fig. 1: After 14 days in culture there was a decrease on osteoclast number in the presence of the drug mimic when compared to untreated PCL and glass.

DISCUSSION & CONCLUSIONS: The decrease in osteoclast number in the presence of the drug mimic suggests that the drug mimic is causing cell apoptosis. The drug mimic contains a P-C pendant group. The P-C pendant group mimics the P-C-P backbone found in bisphosphonates, a group of drugs used to treat osteoporotic patients. It is suggested that the P-C group is internalised by resorbing osteoclasts. Once internalised it is reported that bisphosphonates inhibit farnesyl pyrophosphate (FPP) synthase, which is a major enzyme in the mevalonate pathway. This inhibition leads to the disruption of osteoclast activities such as attachment, resorption and eventually leads to cell apoptosis³. Previous *in vitro* testing using osteoblast cells has shown an increase in metabolic activity and an increase in the rate of mineralisation. The novel scaffold has shown to elicit an enhanced osteoblast response and decrease in osteoclast number therefore could possibly be used to increase bone mass at local sites in osteoporotic patients.

REFERENCES: ¹ B. Gullberg, O. Johnell, and J.A Kanis (1997) *Osteoporos Int* **7**: 407-413. ² C.G Finkemeier (200) *J Bone Joint Surg Am* **84**: 454-464. ³ F.P Coxon, K. Thompson, and M.J Rogers (2006) *Curr Opin Pharmacol* **6**: 307-312.

ACKNOWLEDGEMENTS: The author would like to thank her supervisors for their advice and support and the BBSRC for funding the PhD project.

Biological characterization of bioactive glasses functionalized with alkaline phosphatase

E. Battistella¹, L. Rimondini¹, S. Ferraris² and Enrica Vernè²

¹Department of Medical Sciences, University of Eastern Piedmont, Novara, Italy

²Material Science and Chemical Engineering Department, Politecnico di Torino, Italy

INTRODUCTION: Bioactive glasses can be used in bone tissue engineering. Their composition promote a chemical bond to bone through a hydroxyapatite layer developed on material surface in physiological fluids. Sometimes, their surface is functionalized with biological and chemical molecule to improve biocompatibility⁽¹⁾. In this case the grafting of the enzyme alkaline phosphatase (ALP) was performed on the glasses surface. It has been demonstrated that it is possible to successfully graft ALP to surface of reactive glasses maintaining its activity. The osteoblast cell line MG63 was used and propagated on bioglass scaffolds for the biological characterization.

METHODS: Two different bioglasses were functionalized: SCNA, simple composition and low bioactivity index, and CEL2, more complex composition and high bioactivity index. The functionalization was performed using two methods: direct grafting of ALP on the surface (SCNA+ALP; CEL2+ALP) and grafting with a spacer (3-amino-propyl-silane) between the bioglass surface and the ALP (SCNA+SIL-ALP; CEL2+SIL-ALP). Both sterility and enzymatic activity have been tested before and after sterilization, using the method of Lowry⁽²⁾.

MG63 cells (human osteosarcoma) were maintained in MEM (Minimum Essential Medium) supplemented with FBS 10%, 100 U/ml of penicillin and 100 µg/ml of streptomycin at 37°C in a 5% CO₂. Cells were sub-cultured twice a week. Medium was replaced every 3 days.

Cells were seeded on every bioglass at the density of 175.000 cells/ml (T0). After seeding, the culture was left untouched for 2 hour at 37°C to promote cell attachment. Then, the wells were rinsed with the medium.

The proliferation analysis, osteocalcin and osteopontin production and mineralization of extracellular matrix analysis were performed.

Each experimental condition was analyzed in triplicate.

RESULTS: Bioactive glasses were synthesized and successfully functionalized with ALP. The chemical-physical characterization of the glasses showed that ALP maintains its activity after sterilization with gamma Xrs.



Fig. 1: The bioglass

The proliferation assay and the extracellular matrix deposition showed some differences between the controls (SCNA; CEL2) and the functionalized glasses (SCNA+ALP and SCNA+SIL-ALP; CEL2+ALP and CEL2+SIL-ALP). In particular, the more activity were observed for the bioglass SCNA+SIL-ALP.

DISCUSSION & CONCLUSIONS: In conclusion, it is possible to graft ALP on the bioglass surface successfully. The two methods (direct and with a spacer) are both useful. However, the grafting with a spacer seems to improve bioactivity of the bioglass. It is probable that ALP results more available for the cells: this lead to more integration and tissue regeneration after implant.

The results can be useful to study the grafting of another family of protein involved in bone integration, which are BMP.

REFERENCES: ¹E. Vernè, S. Ferraris, C. Vitale Brovarone et al. Acta Biomater. 2010 Jan;6(1):229-40

²Lowry O.H., Roberts N.R., WU M.L., et al. J. Biol. Chem. 1954 Mar;207(1):19-37

ACKNOWLEDGEMENTS: Thanks to Prof.ssa L. Rimondini and Prof.ssa E. Vernè for their support as supervisors.

OPTIMISING THE PRODUCTION CRITERIA OF 'SMART MATRIX' FIBRIN BASED SCAFFOLD

K A Blackwood, A Taheri, J Dye

The RAFT Institute, The Leopold Muller Building, Mount Vernon Hospital, Northwood, Middlesex UK

INTRODUCTION: Our aim is the design of next-generation dermal scaffold to address the clinical need for a robust, reliable synthetic dermis for full thickness dermal repair and regeneration. Current research has shown that the fibrin based Smart Matrix composite biomaterial shows clinical potential, by rapid integration via cellular ingress and particularly, rapid vascularisation.

While Smart Matrix has shown good potential to fulfil the role of a full thickness dermal repair scaffold there is scope to further improve the functionality of the scaffold by optimisation of its structure and repeatability of production.

METHODS: The basis of Smart Matrix is a cross linked fibrin/alginate composite material, as previously established. We investigated the use of a blend of different combinations of stabilisers and surfactants to alter the physical structure of the Smart Matrix (details confidential). A coagulation assay showed the effect different blends had on the clotting of fibrin, and scaffolds were analysed by histology and SEM for structural characteristics. Any toxic effect of the supplements added to the Smart Matrix was assessed by a MTS assay.

RESULTS: The addition of stabilisation agents and specific blends of surfactants we were able to prevent excessive precipitation of protein from the solution as observed by optical density @425 nm. While these supplements had an inhibitory effect upon the speed of coagulation (Fig. 1) they had no detectable effect upon the quality of the gel being formed.

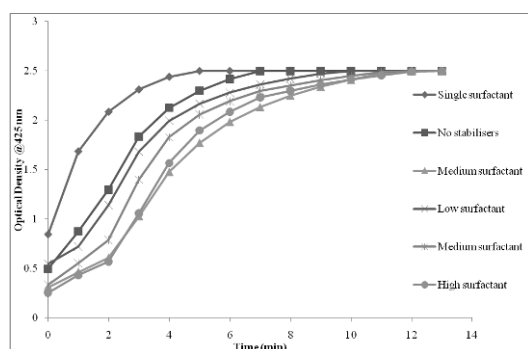


Fig. 1. Optical density readings of the coagulation of Smart Matrix with different blends of foaming agents.

MTS toxicity testing of PBS soaked with the scaffold for 4 hours showed no negative effects compared to the PBS control.

Eosin staining of the scaffold revealed similar structural features found in all scaffolds, with varying pore size and fiber thickness dependent upon the amount of surfactant present (Fig 2.). Importantly the porosity of the supplemented Smart Matrices remained consistent throughout the depths of the scaffolds.

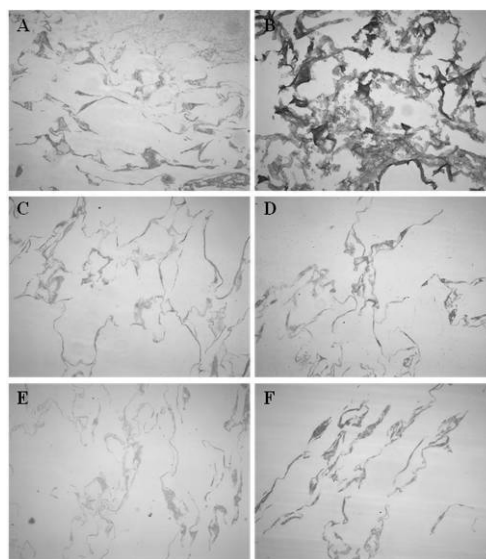


Fig. 2. Eosin stained scaffolds, (A) Single surfactant, (B) No stabiliser, (C) Medium surfactant, (D) Low surfactant, (E) Medium surfactants, and (F) High surfactant.

DISCUSSION & CONCLUSIONS: Successful scaffold design for treatment of full thickness skin defects requires multiple intersecting criteria that must be satisfied. Smart Matrix fibrin based scaffolds have already shown good cellular penetration from wound beds.

This work shows that porosity of the produced scaffolds can be controlled with a blend of surfactants and stabilising agents without adversely affecting the inherent structural features of the Smart Matrix scaffold or producing any form of toxic response.

ACKNOWLEDGEMENTS: This work is supported in part by an HTD LINK grant.

Micronisation and encapsulation of biologically active rhBMP2 into PLGA microspheres and its sustained release for bone tissue engineering applications

A Boussahel¹, FRAJ Rose¹ & KM Shakesheff¹

¹Wolfson Centre for Stem Cells, Tissue Engineering and Modeling (STEM), School of Pharmacy, University of Nottingham, UK

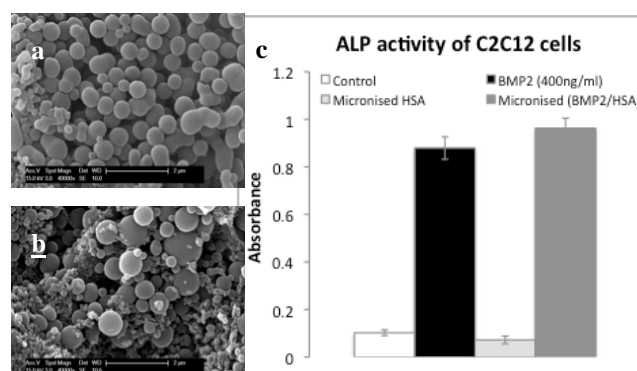
INTRODUCTION: Musculoskeletal conditions affect one of every seven Americans, posing a huge burden on health services and costing the United States \$215 billion per year [1]. Applying osteoinductive growth factors with tissue-engineered scaffolds is currently a promising strategy for reconstructing bone defects. In particular, recombinant human bone morphogenetic protein 2 (rhBMP2) has been extensively investigated for this purpose [2]. Recent progress in recombinant gene technology renders such therapeutic proteins widely available. However, with a short half-life and potential toxicity at systematic levels, a drug delivery system such as polymer particles is imperative [3]. This project investigates the encapsulation of rhBMP2 into Poly(lactic-co-glycolic) acid (PLGA) microparticles using a solid in oil in water dispersion method (S/O/W) to develop a sustained delivery system.

METHODS: We used S/O/W to encapsulate model proteins into PLGA microspheres. Each protein was first micronised with PEG through phase separation of two polymer systems induced by freezing-condensation. This produced small protein microspheres in the size range 500 nm-2 µm, which were then encapsulated into PLGA microspheres. The effect of two parameters on the micronisation and encapsulation efficiency (EE) was investigated using SEM images and BCA assay respectively. The optimised parameters were then used to micronise rhBMP2 with HSA as a carrier protein at different ratios. Maintaining the amount of HSA constant and varying the rhBMP2 amount allowed for dose alteration. The activity of micronised rhBMP2 was confirmed using both an ELISA and a C2C12 cells/Alkaline Phosphatase (ALP) biological activity assay. HSA/rhBMP2 was then encapsulated into PLGA microspheres with the developed S/O/W method.

RESULTS: Both the PEG molecular weight (mwt) and the PEG:protein ratios had an effect on the micronisation step and subsequent EE. Increasing the PEG:protein ratio from 0.5 to 4 produced small protein microspheres with low aggregation that encapsulated with a 60% to 80% EE. Increasing PEG mwt from 2 to 20 kD and using pluronic with a mwt of 8.4 kD produced large protein microspheres (Figure 1a, 1b). The

lowest mwt of PEG led to the formation of small aggregating protein microspheres, which decreased the EE. The maximum EE was achieved with a PEG mwt of 6 kD and PEG:protein ratio of 4.

An ELISA showed that micronised rhBMP2 was active at all HSA/rhBMP2 ratios, and when compared to a positive control (rhBMP2 alone), it stimulated C2C12 cell differentiation towards a bone cell-like lineage (Figure 1c). The micronised HSA/rhBMP2 was then encapsulated into PLGA microspheres with an EE of between 60-80%. We are currently investigating the rate of rhBMP2 release from these particles and its activity after



release.

Fig. 1: (a & b) SEM images of micronised BSA, (c) ALP activity of C2C12 cells following stimulation with micronised rhBMP2.

DISCUSSION & CONCLUSIONS: High EE of model proteins was obtained by controlling two processing parameters of the S/O/W method. rhBMP2 was successfully micronised with HSA and encapsulated within PLGA microspheres with a maximum 80% EE whilst retaining protein activity. Initial results suggest that a sustained release of rhBMP2 from these particles could be achieved. Future studies will focus on optimising the release kinetics and determining the biological activity of released rhBMP2 through *in-vitro* cell differentiation studies. The ultimate aim is to develop an injectable scaffold for bone regeneration using a mixture of optimised rhBMP2 containing microparticles and cells.

REFERENCES:¹ S.L. Weinstein (2000) *J Bone Joint Surg Am* **82**: 1-3. ² M.F. Termaat, F.C. Den Boer, F.C. Bakker, et al (2005) *J Bone Joint Surg* **87**:1367-78. ³ J.E. Babensee, L.V. McIntire, and A.G. Mikos (2000). *Pharm Res* **17**: 497-504.

Synergistic Cell Type Specific Effect of Substrate Topography and Shear Flow on Cellular Alignment

Faika Bozankaya¹, Tao Sun^{2*}, Susan C. Barnett³, Nikolaj Gadegaard⁴, Mathis O. Riehle^{2*}

¹MRes in Biomedical Sciences, FBLs, ²Centre for Cell Engineering, FBLs, ³Dept Clinical Neuroscience, Medicine, ⁴Department of Electronic Engineering, University of Glasgow, UK

INTRODUCTION: Sever injury to the spinal cord will lead to permanent damage as the spinal cord is not able to regenerate itself. It has been proposed that the repair of spinal cord injury will require a combination of strategies such as integrating the biological influence of glial cells together with physical guiding cues on three-dimensional (3D) scaffold. Before preparing glial cells within in complex 3D scaffolds at relatively large scale for spinal cord injury, various scale-up issues need to be addressed. Thus, the aim of this project was to look at the influences of substrate topography and medium perfusion on various cellular behaviours using mini-bioreactor systems.

METHODS:

Cell culture: Type I astrocytes were purified and cultured in DMEM supplemented with 10% foetal bovine serum (FBS) and L-glutamine (2mM) as described previously¹.

Mini-bioreactor system: A mini bioreactor system consisted mainly of two commercially available tissue culture plates situated in two plastic boxes respectively, an 8-channel Ismatec peristaltic pump, 8 medium reservoirs (2.5ml) and 3-way valves. Corresponding to the 8 channels of the peristaltic pump, up to 8 perfusion chambers were fabricated and seeded with either astrocytes or fibroblasts. The entire system was then placed in a tissue culture incubator (37°C, 95% air/5% CO₂) and the cells subjected to medium perfusion with varying flow rates for defined periods of time.

RESULTS

Serial perfusion cultures of astrocytes and/or fibroblasts using the mini bioreactor system indicated that the supply of medium was crucial for the survival of the cells in closed mini chambers (volume = 0.125 ml). Systematic investigations demonstrated that aligned astrocytes and fibroblasts can be achieved on micro-grooved ε-polycaprolactone (PCL) substrates, and that this alignment is maintained throughout perfusion culture. More interestingly, it was also found that medium perfusion increased alignment of

fibroblasts and influenced placement compared to static as more fibroblasts were observed to 'hide' in the grooves and could only rarely be found on ridges (Fig 1). In contrast astrocytes although aligned were not significantly influenced by flow (Fig 2).

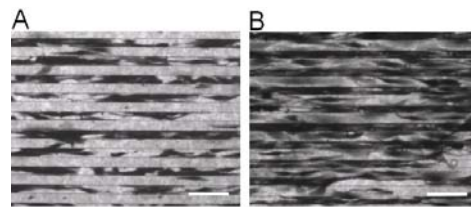


Fig. 1: The distributions and alignment of fibroblasts on microgrooved PCL substrates in (A) perfusion and (B) static cultures. bar=100µm.

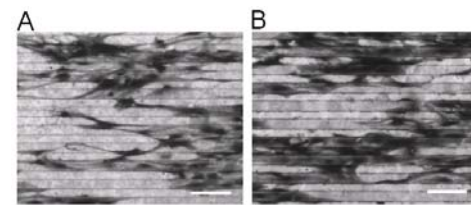


Fig. 2: The distributions and alignment of astrocytes on microgrooved PCL substrates in (A) perfusion and (B) static cultures. bar=100µm.

DISCUSSION & CONCLUSIONS:

Our research demonstrated that:

(A) The susceptibility to respond to a combination of microtopographic, and physical cues is cell type dependant, with fibroblasts being responsive, whereas the astrocytes were not.

(B) The mini bioreactor systems can be used for systematic investigation of various scale-up issues in tissues engineering.

REFERENCES:

¹ Sørensen et al. (2008) Astrocytes, but not olfactory ensheathing cells or Schwann cells, promote myelination of CNS axons in vitro. *Glia* 56:750-763.

ACKNOWLEDGEMENTS:

We gratefully acknowledge financial support of BBSRC (UK) for this study.

Modelling of a Perfusion Bioreactor using Lattice Boltzman Technique

Sarah H. Cartmell,¹ Tim J. Spencer² Lila A. Hidalgo-Bastida¹, Ian Halliday², Chris M. Care²
¹Institute for Science and Technology in Medicine, Keele University, Staffordshire, UK. and ²Materials & Engineering Research Institute, Sheffield Hallam University, Sheffield, UK.

INTRODUCTION:

Bone tissue can be engineered in the laboratory using a bioreactor in which culture medium is perfused through a porous three dimensional (3D) scaffold. One important feature in bone tissue engineering is the configuration of placing the cells onto a porous 3D scaffold at the start of the culture period to create the tissue engineered construct. A perfusion bioreactor may be utilized to deliver cells at the start of culture. Mathematical modelling offers scientists assistance with regards to reducing the number of physical laboratory experiments needed for experimental characterisation and optimising cell seeding. We are utilising incompressible lattice Boltzmann (IB) modelling to investigate the parameters of culture for optimal cell adhesion and distribution.

METHODS:

Our first approach was to use microCT images of porous polylactic acid scaffolds to generate the 3D structure for the IB model. This approach modeled the hydrodynamics of the porous scaffold without cells to measure typical flow velocities, wall shear stress, scaffold permeability and tortuosity. The second approach coupled advection diffusion reaction equations to the IB method in order to model key components of the culture medium. Moreover, we considered dissolved oxygen, carbon dioxide and mesenchymal stem cell species together with a receptor ligand model of cell attachment. Simulations were performed to reproduce experimental findings and begin the optimization process.

RESULTS:

It was found that flow is highly inhomogeneous and the PLA scaffolds are anisotropic. These findings highlight that homogenous Darcy flow models must be used with caution in a bioreactor environment [1].

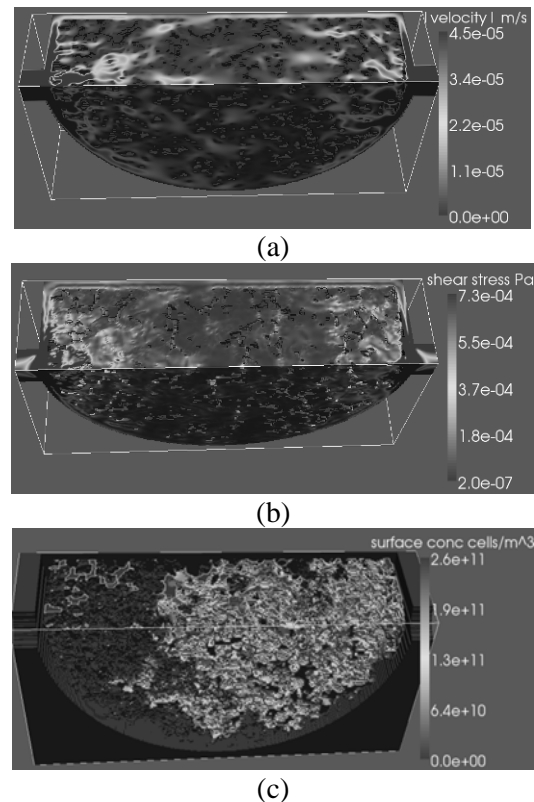


Fig. 1. Plots over a one quarter segment of the bioreactor and scaffold showing the (a) culture medium velocity, (b) culture shear stress and (c) cell attachment concentration.

DISCUSSION & CONCLUSIONS:

LB code setup for this perfusion system was able to produce models for pressure profile, mass transport and shear stress in the scaffold placed in the bioreactor chamber. Laboratory experiments are now underway to validate the predicted cell attachment.

REFERENCES:

¹ WHITTAKER, R. ET AL., (2009) Journal of Theoretical Biology 256(4), 533.

ACKNOWLEDGEMENTS:

BBSRC grant BB/F013892/1.

Behaviour of Fibronectin on Interaction with Stoichiometric and Silicate Substituted Hydroxyapatite Bone Graft Substitutes

V. Castagna^{1,2}, A. Sullivan² & K.A. Hing¹

¹School of Engineering & Material Sciences & IRC, and ²School of Biological & Chemical Science, Queen Mary & Westfield College, University of London E1 4NS UK

INTRODUCTION: Fibronectin (Fn) is one of the most important proteins involved in cell adhesion and its Arg-Gly-Asp peptide (RGD) sequence is identified as a cell attachment site; it has a central role in cell adhesion and spreading and promotes binding of osteogenic cells to silicon-substituted (SA) and stoichiometric hydroxyapatites (HA)¹. The aim of this study was to evaluate the behaviour of Fn both labelled and unlabelled with a fluorophore on dense discs (DD) and porous granules (PG) of HA and SA.

METHODS: Initially the Fn was labelled with the fluorophore FTCA (fluorescein derivative with aminocaproic acid spacer) so that it was possible to quantify the amount of the protein by fluorescence analysis at the wavelength of 494 nm. A Fn solution in phosphate buffered saline (PBS) (1.5 ml) of known concentration was transferred into a vial containing either DD or PG and samples taken for analysis after 1, 5, 10 and 15 mins to assess Fn adsorption via depletion. Additional experiments were performed where the fluorescence intensity of a known concentration of as-lyophilized unlabelled Fn and Fn exposed to HA-DD or SA-DD for up to 15 mins was also investigated.

RESULTS: Calibration curves showed good correlation (Fig. 1) and monitoring of fluorescence indicated that Fn adsorption peaked within seconds of exposure before finding a lower equilibrium level, however samples exhibited a higher fluorescence intensity as compared to the stock solution resulting in negative 'adsorption' values (Fig. 2). Investigation of Fn auto-fluorescence demonstrated a significant effect on exposure to both HA and SA which persisted over the 15min incubation period (Fig 3).

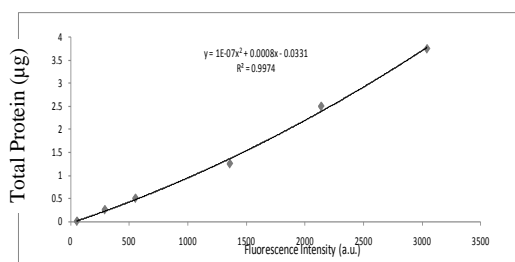


Fig.1: FTCA-Fn fluorescence intensity vs. total protein in 96 well plate (i.e. per 200µl).

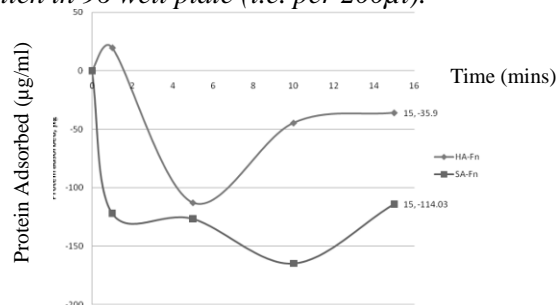


Fig.2: Amount of adsorbed protein as a function of time with HA-DD and SA-DD.

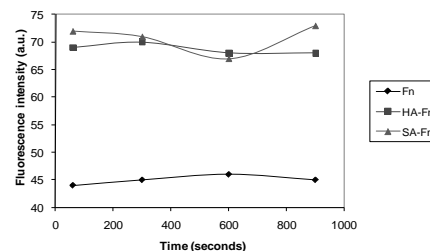


Fig 3: Fluorescence intensity of Fn as function of time with HA-DD, SA-DD and individually.

DISCUSSION & CONCLUSIONS: The results clearly demonstrate the rapid rate of interaction between Fn, HA and SA surfaces. What was surprising was the effect on auto-fluorescence at 494 nm. This result confirms the hypothesis that Fn is subject to a significant conformational change when in contact with HA and SA surfaces¹. Furthermore this effect appears to be at least partly preserved on desorption. This has implications with regard to exposure of the RGD and other functional motifs and warrants further investigation.

REFERENCES: ¹K. Guth, et al. (2010), *Advanced Engineering Materials* **12**; B26-B36. ²G. Mabileau, et al. (2007), *Tissue Engineering* **13**; 1388-1388. ³M.D. Pierschbacher et al. (1984). *Nature* **309**:30-33.

ACKNOWLEDGEMENTS: Thanks to my sponsor ApaTech Ltd., and my colleagues M.-K. Mafina and A. Parish.

Neuronal Growth and Patterning on Diamond Like Carbon Substrates

F Claeysens¹, EM Regan², JB Uney², AD Dick³, JP McGeehan⁴, S Kelly²

¹Dept. of Engineering Materials, The Kroto Research Institute, North Campus, University of Sheffield, Broad Lane, Sheffield S3 7HQ ²Henry Wellcome L.I.N.E., Clinical Sciences South Bristol, University of Bristol, BS1 3NY, UK. ³Bristol Eye Hospital, University of Bristol, Lower Maudlin Street, Bristol BS1 2LX, UK., ⁴Centre for Communications Research, Faculty of Engineering, University of Bristol, Merchant Venturers Building, Woodland Road, Bristol BS8 1UB.

INTRODUCTION: For more than a decade diamond like carbon (DLC) has been explored as an attractive biocompatible material for coating implantable devices. These devices have been predominantly confined to vascular stents, cardiac valves and replacement joints. Work on these areas has led to significant advancement of the understanding of how DLC interacts with the mammalian immune and inflammatory systems. Modifying DLC by the addition of dopant materials, e.g. phosphorous or silicon, has been shown to modulate cell adhesion, cell activation and blood compatibility in vitro – making DLC a versatile substrate material.

The aim of this study is to assess the suitability of modified DLC for the coating of neural implants. Neuronal adhesion and cytocompatibility of DLC substrates were assessed using primary central nervous system neurones and neuroblastoma cells. Additionally, methods of patterning other neural cells (both neurones and glia) are achieved by utilisation of the varying adhesion properties of the different DLC substrates, and by chemical surface modifications

METHODS: DLC was prepared using pulsed laser deposition. [1] The output of an Argon Fluoride (ArF) excimer laser (Lambda Physik, Compex 201, laser wavelength 193 nm) was focused on a target located in a stainless steel vacuum chamber maintained at 10^{-6} Torr. Thin films of DLC and P:DLC (20% P) were deposited onto glass coverslips. UV:DLC samples were subjected to 18hrs of UV exposure.[2]

Dissociated cortical neurones and dorsal root ganglion explants were cultured from E18 wistar rats on substrates using standard tissue culture protocols [1]. Prior to plating, substrates were sterilised in ethanol and coated with poly-D-lysine (70,000–150,000 MW). U-87 astroglial cells were grown in DMEM media containing 10% FCS, L-Glutamine and penicillin/streptomycin.

RESULTS: MTT assays of cortical neural cell growth on DLC indicates that untreated DLC is a bioinert material, and that both doping with phosphorus or irradiating the material with UV

light greatly improves neural adhesion on the DLC surfaces. This finding was exploited to produce neuronal pattern via patterned deposition/UV exposure of the samples. An example of a cortical neuronal cell pattern achieved via this technique is illustrated in Figure 1. Additionally we have studied patterned growth of dorsal root ganglion cells and human neural progenitor cells.

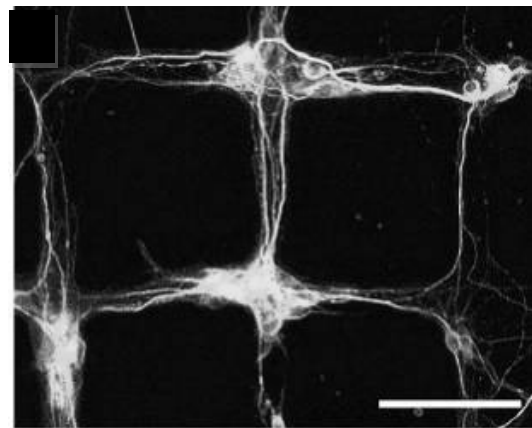


Fig. 1: Preferential patterning of cortical neurones (green = MAP2 stain, blue = dapi) along P:DLC tracks. Scale bar: 90 μ m

DISCUSSION & CONCLUSIONS: Our data highlight that DLC is a modifiable substrate suitable for coating brain implants. We describe patterned growth of several neural cell types on P:DLC & UV:DLC. We also show preliminary data showing an approach that could reduce the brains inflammatory response to brain implants.

REFERENCES: ¹ E.M. Regan et al. (2008) Patterned growth of neuronal cells on modified diamond-like carbon substrates *Biomaterials* 29(17):2573-80. ² E.M. Regan et al. (2010) Differential patterning of neuronal, glial and neural progenitor cells on phosphorus-doped and UV irradiated diamond-like carbon *Biomaterials*, 31 (2), 207-15

ACKNOWLEDGEMENTS: FC thanks EPSRC for his Life Sciences Interface Fellowship (EP/C532066/1) and ER thanks Micron Foundation for provision of a scholarship.

Response of Dermal Fibroblasts to Dynamic Tensile Loading

R.M. Delaine-Smith, G. Reilly & S. MacNeil

Kroto Research Institute, Department of Engineering Materials, University of Sheffield, UK.

INTRODUCTION: Most tissues in the human body are subjected to mechanical forces including load bearing (bone, tendon) and non-load bearing tissues (skin). The functional form of each tissue type is strongly influenced by the forces that they experience and the constituents and structure of the tissues are continually adapting and remodelling due to growth and response to the mechanical environment [1]. For example, cyclic mechanical strain was carried out on fibroblasts using flexible membranes resulting in an increase in collagen expression [2]. Recently, our group has developed a model for mechanical conditioning of cell-seeded constructs and showed that dynamic cyclic compressive loading of scaffolds containing osteoblasts increased matrix production [3]. This loading system can also be used to create tensile forces, which is more representative of the loading environment of tissues that stretch such as skin or tendon. The aim of the present work was to investigate the response of human dermal fibroblasts (HDFs) to dynamic tensile loading.

METHODS: Polyurethane foam scaffolds were cut into ASTM standard 'dog bone' shapes with a depth of 5mm and seeded with 2.5×10^5 HDFs per scaffold. Cell-seeded scaffolds were subjected to dynamic tensile loading in a biodynamic chamber at 5% strain, 1Hz and 5400 cycles for 4 days over a 20 day period. Mechanically conditioned and non-loaded control scaffolds were assayed for cell viability (MTS) and collagen production (Sirius Red) at day 20. Cell coverage and morphology were also observed using DAPI and TRITC-Phalloidin fluorescent staining on an AXON ImageXpress.

RESULTS: Loaded scaffolds showed a significant increase in cell number as well as cell coverage when compared with non-loaded control scaffolds (Fig.1). However, there did not appear to be any differences in cell morphology or orientation. Cell viability and total collagen production of loaded scaffolds was significantly higher than the control scaffolds (Fig. 2). The amount of collagen produced per cell (SR/MTS) was almost double in loaded scaffolds compared with the non-loaded controls.

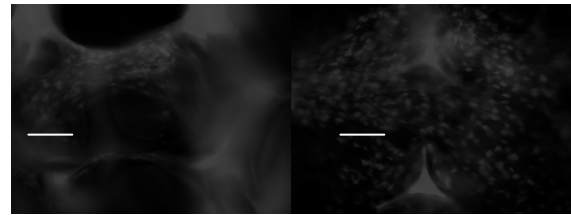


Fig. 1: DAPI & TRITC-Phalloidin staining of HDFs on loaded (left) and non-loaded (right) scaffolds. Scaffold auto-fluorescence is also observable. Scale bar = $50 \mu\text{m}$

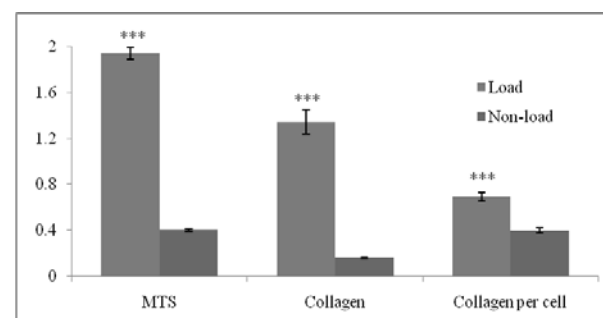


Fig. 2: Relative responses of HDFs on dynamically loaded and non-loaded scaffolds. Results are mean \pm SD for $n=3$. *** $P < 0.001$ using student's *t*-test.

DISCUSSION & CONCLUSIONS: We have demonstrated that human fibroblasts respond to short bouts of mechanical loading with a significant increase in collagen production and increased cell coverage of the scaffold. This information has implications for the design of a mechanical conditioning regime in a bioreactor for the growth of collagenous tissues. The polyurethane scaffold used here was highly porous with randomly orientated elements. We are currently synthesising orientated and non-orientated fibrous scaffolds with smaller pores, by electrospinning, to identify whether similar loading protocols can upregulate collagen in clinically relevant scaffolds.

REFERENCES: ¹ J.A. Pederson *et al*, *Annals of Biomedical Engineering*, 33(11): 1469-1490, 2005. ² E.C. Breen, *Journal of Applied Physiology*, 88(1): 203-209, 2000. ³ A. Sittichockechaiwut *et al*, *Bone*, 44: 822-82, 2009

ACKNOWLEDGEMENTS: We gratefully acknowledge financial support from EPSRC (UK).

Physical and Biological Characterisation Of A Novel Injectable Scaffold Formulation

A. Dhillon¹, C. Rahman², L. White², B.E. Scammell¹, K.M. Shakesheff²

¹ Division of Orthopaedic and Accident Surgery, University of Nottingham, Queens Medical Centre, NG7 2UH

² School of Pharmacy, University of Nottingham, NG7 2RD

INTRODUCTION: Injectable scaffolds which also deliver cells and bioactive molecules to augment bone healing may overcome many of the limitations associated with current bone graft substitutes¹. The aim of this study was to develop and test a novel injectable scaffold that self-assembles isothermally *in situ* to form a biodegradable porous osteoconductive material. In addition, an assessment of the viability of human mesenchymal stem cells (hMSC) seeded onto the scaffold was made.

METHODS: Rheological assessment was performed on three different molecular weights (Mw) of poly(lactic-co-glycolic acid) (PLGA) (26kDa, 53kDa and 92kDa) combined with differing ratios of polyethylene glycol (PEG) to control the temperature required for scaffold self-assembly. The strength (MPa) and stiffness (Young's Modulus) patterns of the scaffolds were assessed in compression. The cell viability, proliferation and distribution patterns of hMSCs seeded within the scaffold microparticle mixture prior to injection and self assembly were assessed using Alamar Blue[®], confocal microscopy and micro-CT. hMSC differentiation in osteogenic media was characterised by the identification of specific bone formation markers (e.g. alkaline phosphatase).

RESULTS: Rheological assessment identified a stepwise control of the trigger-temperature (37°C) required for scaffold self-assembly through adjustment of PLGA Mw and PLGA/PEG ratios. Mechanical analysis of the most competent scaffolds after 2 hours at 37°C revealed compressive (1-2MPa) and stiffness (Young's Modulus of 3.5-5.5 MPa) strengths similar to that of cancellous bone. Confocal microscopy analysis of LIVE/DEAD[®] assays conducted on cell-seeded scaffolds demonstrated the scaffold's biocompatibility post-injection/assembly. This is further complemented by subsequent cell proliferation assays of the viable hMSCs present.

Identification of bone formation markers further supported the scaffold's potential to provide a supporting osteoconductive environment for bone formation and deposition.

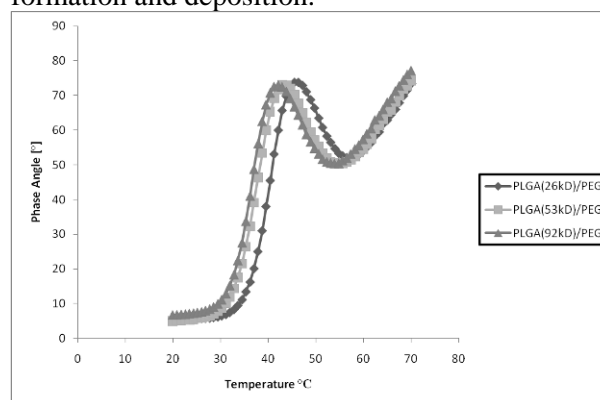


Fig. 1: Rheology Profiles of the most mechanically competent PLGA (26kd, 53kd and 92kd) PEG formulations that self-assemble at 37°C

DISCUSSION & CONCLUSIONS: This study has confirmed specific injectable scaffold formulations that self-assemble at physiologically relevant temperatures and possess compressive and stiffness strengths in the range of cancellous bone. It is possible to tailor the architecture/mechanical/biodegradable properties of the scaffold through manipulation of PLGA Mw and PEG ratios. This injectable scaffold system provides a 'potential' means of delivery for hMSCs (and growth factors or antibiotics) and is an architecturally suitable 3D scaffold that has the potential to not only be osteoconductive, but also osteoinductive and osteogenic.

REFERENCES: ¹ Q. Hou, P.A. De Bank, K.M. Shakesheff (2004) *J. Mater. Chem.* 14:1915-1923

ACKNOWLEDGEMENTS: Funding from the University of Nottingham Medical School (School of Clinical Sciences).

The Influence of Substrate Features on CNS Development; Relevance for the Design of a Scaffold to Treat Spinal Cord Injury

P.S. Donoghue¹, R. Lamond¹, T. Sun², N. Gadegaard³, M.O. Riehle², S.C. Barnett¹

¹ Glasgow Biomedical Research Centre, University of Glasgow, G12 8QQ, UK

² Centre for Cell Engineering, University of Glasgow, G12 8QQ, UK

³ Department of Electronics and Electrical Engineering, University of Glasgow, UK

INTRODUCTION: Spinal cord injury (SCI) is a complex injury of the central nervous system (CNS), characterised by a loss of innervation and a localised glial scar, presenting a physical and molecular barrier to functional regeneration. To overcome this obstruction, numerous bridging strategies are being considered, but due to the complexity of the CNS, the slightest change in substrate or surface treatment can have significant effects on the cellular response. Using an in vitro culture ("myelinating cultures") that can model the intact CNS we discuss how the development of a ϵ -polycaprolactone scaffold and different surface treatments affect the properties of the cell.

METHODS: *Preparation of the PCL:* Constructs were prepared by spin coating 15% PCL dissolved in chloroform on a blank silicon wafer to produce a non-porous membranes, which was subsequently hot embossed with a microtopography. The finished membrane was then attached to polycarbonate and subjected to oxygen plasma treatment and either PLL, collagen, fibronectin, or laminin coating.

Preparation of the myelinating culture; The myelinating culture generated from dissociated embryonic E15 rat spinal cords (Sprague-Dawley, SD) has a supporting confluent layer of astrocytes derived from striatal neurospheres. Spinal cords were dissected, enzymatically dissociated and seeded onto the confluent astrocyte monolayer. Cultures were maintained for 28 days in vitro (D.I.V) in defined serum free media with regular feeding¹.

RESULTS: Previously we have shown that myelinating cultures plated onto micro-patterned PCL results in aligned axonal outgrowth¹. However, the substrate, and the addition of a micro-pattern appears to reduce the amount of myelinated fibres when compared to glass cover slips. We have treated PCL with extra-cellular matrix (ECM) proteins to further see if we can overcome enhance myelination and ensure the substrate is supportive for the ingrowth of axons and myelinating glia after transplantation.

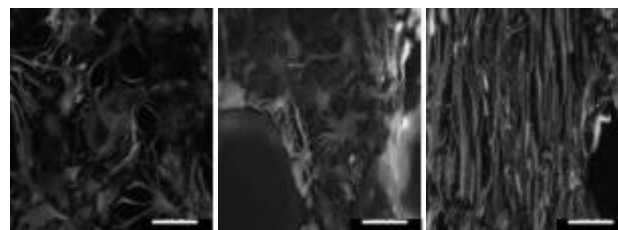


Fig. 1: The effect of surface changes on astrocyte reactivity at 7 D.I.V. L-R: Flat PCL, porous PCL, porous micro-patterned PCL. Stained for glial fibrillary acidic protein (GFAP, Red) and nestin (green). Astrocytes appear more reactive, with a greater GFAP intensity. Scale bar: 100 μ m

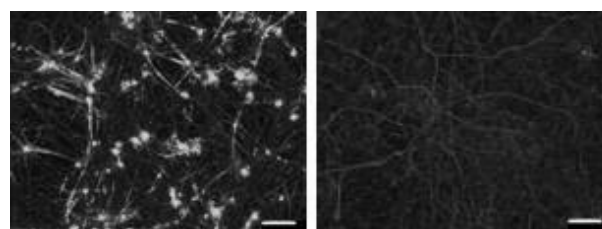


Fig. 2: Effect of substrate on myelination at 28 D.I.V. L: Myelinating culture on control glass coverslip; R: Myelinating culture on PCL. Stained for neurites (SMI31, Red) and myelin (proteolipid protein, green). The marked absence of PLP on the PCL substrate being an indicator of a lack of myelinating oligodendrocytes. Scale bar: 100 μ m

DISCUSSION & CONCLUSIONS: An aligned micro-pattern on PCL, induces aligned cell growth, but may affect the underlying cell substrate, reducing axonal myelination, compared to control glass coverslips. This work addresses strategies where we attempt to alleviate this effect through surface modification.

REFERENCES: ¹Sørensen A, Alekseeva T, Katechia K, Robertson M, Riehle M.O, Barnett SC. *Biomaterials* 2007 **28** (36):5498-5508.

ACKNOWLEDGEMENTS: This work is funded by the BBSRC and a Lord Kelvin-Smith Scholarship from the University of Glasgow.

***In Vitro* Evaluation of Plasma Modified Polymer Spheres for use in Novel Injectable Scaffold Systems**

S. Fawcett¹, J.M. Curran¹, L.G. Hamilton², N.P. Rhodes¹, K.M. Shakesheff², J.A. Hunt¹

¹ *Division of Clinical Engineering, UKCTE, University of Liverpool*

² *School of Pharmacy, University of Nottingham*

INTRODUCTION: PLGA spheres were plasma treated with four surface-modifying chemical groups (Hexane, Allyl alcohol, Allylamine, and Acrylic acid). The aim was to alter the surface characteristics of the spheres, including surface energy and chemistry in order to direct stem cell differentiation following culture in direct contact. . When used as part of a 3D scaffold, it is anticipated that the surface modifications of the spheres will promote tissue regeneration as a 3D platform.

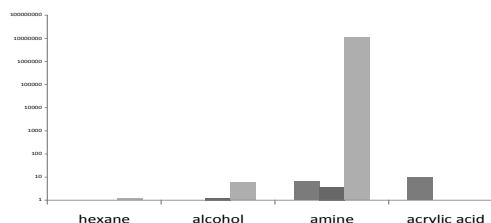
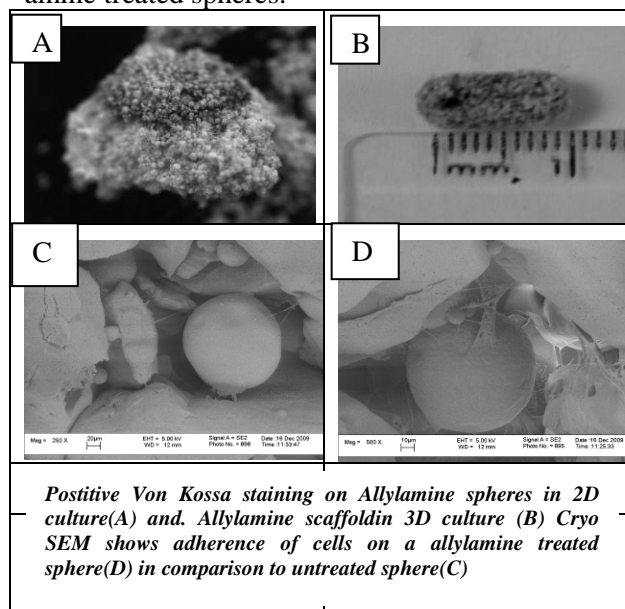
METHODS: Prior to introducing modified particles to the 3D system the ability of the materials to induce differentiation in 2D systems was evaluated. 0.1g of treated and untreated spheres were seeded with well characterized hMSCs (Lonza, UK). Samples were then incubated for 14 and 28 days under standard basal conditions. Osteogenic and chondrogenic differentiation was evaluated using von Kossa and Van Geison tinctural stains.

The scaffolds were produced when treated particles were mixed with an adhesive component and compacted into a mould with a volume of 140µl. 100µl of serum free media containing 2x10⁵ hMSC (as above) were infiltrated into the compressed mixture and the sample was cured at 37°C. The resulting scaffolds were removed from moulds and placed in a 6 well plate with basal MSC media (Lonza, UK), and cultured dynamically on a shaker plate at 37°C with 5% CO₂ for 7, 14 and 28 days. Cell viability was quantified using LDH assays (Promega UK). Cellular infiltration and attachment to particles within the scaffolds was evaluated by Cryo SEM.

Evaluation of cell phenotype was determined using combinations of real time PCR (quantification of an array of osteogenic and chondrogenic markers) and tinctural staining *i.e.* Von Kossa to determine levels of calcified extra cellular matrix production.

Results: Allylamine treated scaffolds demonstrated increased osteogenic differentiation with positive von Kossa staining in 2 and 3 dimensional tests, and an increase in osteogenic markers at the mRNA level. Cryo SEM

demonstrated the cellular infiltration of the cells into the scaffold, and preferential adherence to amine treated spheres.



An increased expression of osteonectin on the allylamine treated scaffold, at 7 (blue), 14 (red) and 28 (green) days when normalised to a control untreated scaffold, and β -Actin housekeeping gene.

DISCUSSION & CONCLUSIONS: Preliminary results indicated that the introduction of -NH₂ groups using specialised plasma treatment is a valid tool for increasing the efficiency of osteogenic differentiation when MSC are cultured in contact with PLGA spheres. Development of these technologies will have a significant impact on the clinical relevance of injectable osteogenic scaffolds.

ACKNOWLEDGEMENTS: With thanks to EPSRC for funding this studentship

Synthesis of interpenetrating polymer networks scaffolds of poly (vinyl pyrrolidone) and poly (acrylic acid).

M.V. Flores-Merino,^{1,2} G.C. Reilly¹ and G. Battaglia.²

¹ *The Biomaterials and Tissue Engineering research Group. Department of Engineering Materials University of Sheffield.* ² *Department of Biomedical Science University of Sheffield.*

INTRODUCTION: Interpenetrating polymer Networks (IPNs) are composed by at least two crosslinked networks. Each network is related with the other(s) by non-covalent interactions.^{1, 2} IPNs represent a strategy for combining the properties of several polymeric materials into a single network. The combination of the networks usually comes with certain advantages e.g. improving mechanical properties; increasing resistant to degradation or other improvement in properties.³ In this study, cytotoxicity of IPNs of Poly (vinyl pyrrolidone)-Poly (acrylic acid) (PVP/ PAAc) was investigated.

METHODS:

Synthesis of PVP network: 1-vinyl-2-pyrrolidone (Sigma-Aldrich, UK), di-ethylene glycol bis-allyl carbonate (DEGBAC) (Greyhound Chromatography; UK) and 2,2-azobis (2-methylpropionitrile) (Molekula; UK) in a molar ratio 1:1 with respect to DEGBAC were mixed under nitrogen. Polymerization was carried out for 24h at 50° C and the obtained hydrogels were immersed in an ethanol/water solution (70/30% vol./vol.).

Synthesis of IPNs: dry PVP network was embedded in a solution of acrylic acid, ammonium persulfate and N-N' methyl- Bis-acrylamide (sigma-aldrich, UK) until equilibrium was reached. Polymerization was carried out at 50° C for 24hrs. Samples were sterilized in a solution of ethanol water (70/30% vol/vol). In this work three sequential IPNs of PVP/PAAc denoted as IPN-1 (7.5 % mol PVP), IPN-2 (20.6 % mol PVP) and IPN-3 (34.2 % mol PVP) were synthesized and studied.

Cytotoxicity analysis: primary human fibroblast and a human embryonic stem cell line were used for this work. The quantity of living cells was evaluating by MTT when utilizing an indirect contact method. MTS was used when cells were seeded onto hydrogel surfaces. Cells were also analysed using live/dead assay using Syto 9/ propidium iodide.

RESULTS: The presence of hydrogels did not have noticeable effect on cell growth after 12 days of cell culture in indirect contact with human fibroblast. Moreover, morphology of human fibroblast cells was not affected by IPNs. Microscopy studies show that human fibroblast and human embryonic stem cells were able to attach to all IPNs surfaces. The IPN-3 with 34.2% mol of PVP had higher number of living cells than the other compositions of IPNs in direct and indirect contact experiments.

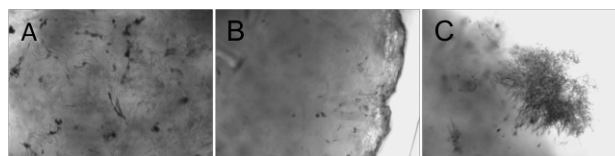


Fig.1 Micrographs showing attachment of human fibroblast onto IPNs surfaces of PVP/PAAC (10x with magnification). A) IPN-1, B)IPN-2 and C)IPN-3.

DISCUSSION & CONCLUSIONS: The results showed that IPNs of PVP/PAAc are biocompatible. IPNs have potential as structural components in vivo for tissue engineering. IPN with higher content of PVP exhibit better biocompatibility properties than IPNs with less PVP content. Differences in the surface roughness of the material and their mechanical properties can be an explanation of the encountered results, however more studies in polymer characterization need to be carry out.

REFERENCES:

1. D. Myung, D. Waters, M. Wiseman, P. E. Duhamel, J. Noolandi, C. N. Ta and C. W. Frank, *Polymers for Advanced Technologies*, 2008, 19, 647-657.
2. L. H. Sperling, in *Interpenetrating Polymer Networks*, American Chemical Society, 1994, pp. 3-38.
3. S. Boileau, B. Boury and F. Ganachaud, *Silicon Based Polymers. Advances in synthesis and Supremolecular organization*, Springer, Montpellier, 2008.

ACKNOWLEDGEMENTS: The authors gratefully acknowledge the financial support provided by CONACyT (to MVF-M).

Efficient Transfection of MG63 Osteoblasts Using Magnetic Nanoparticles And Oscillating Magnetic Fields

A Fouriki¹, MA Clements^{1,2,3}, N Farrow^{1,2}, J Dobson^{1,2}

¹Institute for Science & Technology in Medicine, Guy Hilton Research Centre, University of Keele, Thornburrow Drive, Hartshill, Stoke-on-Trent ST4 7QB United Kingdom ²nanoTherics Limited, Guy Hilton Research Centre, Thornburrow Drive, Hartshill, Stoke-on-Trent ST4 7QB UK, ³Waggoner Center for Alcohol and Addiction Research, University of Texas, Austin, Texas, USA

INTRODUCTION: The human osteoblastic/osteosarcoma cell line, MG63, has been extensively used for *in vitro* research on bone tissue engineering and bone cancers. Often, the production of genetic variants of MG63 are used to examine the role of specific genes in bone oncogenesis and regenerative medicine [1,2]. Most non-viral gene transfection techniques are not particularly effective in transfecting MG63s and/or can be toxic [3]. In this study we have investigated the efficiency of magnetic-nanoparticle based gene transfection using oscillating magnetic fields.

METHODS: MG63 human bone osteosarcoma fibroblasts were transfected with nanoTherics nTMAG nanoparticles (nanoTherics Ltd) and OzBiosciences Polymag particles (OzBiosciences) coated with pEGFP green fluorescent protein reporter construct in response to oscillating magnetic fields of the magnefect-nano system (nanoTherics Ltd). The cationic transfection agent, Lipofectamine 2000TM (LF2000) was used for comparison. MG63 cells were seeded in DMEM culture medium supplemented with 10% foetal calf serum, 100U/ml penicillin, 0.1 mg/ml streptomycin, 0.25ug/ml amphotericin B and 2mM L-glutamine at 9×10^4 cells per well in 24 well plates and allowed to adhere overnight. All transfections were performed in supplemented DMEM medium as follows; nTMAG: 0.1 μ g DNA/0.1 μ l nTMAG per well, Polymag: 0.1 μ g DNA/0.1 μ l Polymag, and LF2000: 0.1 μ g DNA/0.3 μ l LF2000. Following the addition of reagents the plates were transferred to an incubator at 37°C, 5% CO₂ and placed above the oscillating (Frequency 2Hz, amplitude 2 μ m) magnetic field. Magnetic field was produced by pairs of 6x4mm NdFeB magnets per well for 30min. At 30min post-transfection, the magnets were removed and the medium was replaced with fresh supplemented DMEM culture medium. The LF2000 groups were transfected at both 30 min. and 6 hr. At 48hr post-transfection, images of the cells transfected with pEGFP were taken, FACS sorting and cell viability assay (Cyto Tox-ONE, Promega) were performed. The magnefect-nano system was compared to the

cationic lipid transfection agent LF2000, particle and DNA-only controls.

RESULTS: Fluorescence microscope and Fluorescence Activated Cell Sorting (FACS) analysis shows that the magnefect-nano oscillating system enhances overall *in vitro* transfection levels in MG63s in comparison with the leading cationic transfection agent, Lipofectamine 2000TM (p<0.001) tested (Figure 1). Transfection efficiency was up to 54% and cell viability was largely unaffected.

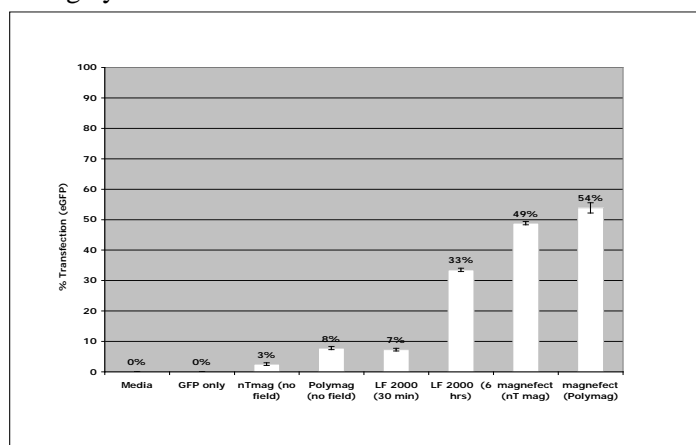


Figure 1: FACS results showing transfection efficiency of the tested groups. N= 3 per group.

DISCUSSION & CONCLUSIONS: The oscillating magnetic field of the magnefect-nano system outperforms the best currently available cationic lipid-based agent. Furthermore, it retains the advantages of magnetic transfection such as short transfection times, lower reagent concentrations than cationic lipid based agents and little or no cytotoxicity. Magnetic nanoparticle-based gene transfection shows promising results for non-viral gene delivery for both *in vitro* and *in vivo* applications.

REFERENCES: ¹Alonso et al (2008) *J Cell Physiol* 217:717-72. ² Hsu et al (2008) *J Bone Miner Res* 23:949-960. ³ Corsi et al (2003) *Biomaterials* 24:1255-64.

ACKNOWLEDGEMENTS: A Fouriki thanks Keele University, nanoTherics Ltd. and EPSRC for funding support.

DEVELOPING SUPPORTIVE CULTURE CONDITIONS FOR A CELLULARISED OSTEOCHONDRAL CONSTRUCT: INFLUENCE OF TRANSIENT SERUM EXPOSURE ON OSTEOGENIC DIFFERENTIATION OF HUMAN MESENCHYMAL STEM CELLS

L. France¹, C. Scotchford¹, V. Sottile², H. Rashidi², D. Grant¹

¹*Bioengineering Group, Division of MMS, Faculty of Engineering, University of Nottingham, Nottingham, UK.* ²*Wolfson Centre for Stem Cells, Tissue Engineering and Modelling (STEM), School of Clinical Sciences, University of Nottingham, Nottingham, UK*

INTRODUCTION: Development of a graded continuous scaffold loaded with a single cell source that has both osteogenic and chondrogenic differentiation potential would have many advantages in the design and use of osteochondral constructs for orthopaedic applications. This approach can be envisaged using human mesenchymal stem cells (hMSCs), which can give rise to both bone and cartilage lineages. To this end, novel culture procedures are required to support hMSC differentiation in the scaffold, which need to satisfy conditions for both osteogenic and chondrogenic differentiation. One main difficulty is that whereas osteogenic treatments comprise the use of serum such as foetal calf serum (FCS), conditions recommended for *in vitro* chondrogenesis are essentially serum-free. In order to address this issue, we evaluated the efficacy and feasibility of osteogenic differentiation in cultures of human mesenchymal stem cells exposed to serum-free conditions.

METHODS: Mesenchymal stem cells (MSCs) were seeded onto Thermanox™ discs at a density of 2×10^4 cells/disc. Osteogenic differentiation was induced using standard culture medium and osteogenic supplement (OS) containing dexamethasone (0.1 μ M), ascorbic acid phosphate (50 μ M), and β -glycerophosphate (10 mM). FCS (10% v/v) was added to the medium for 1,2,3,4 and 5 days. The cells were then cultured in serum-free osteogenic medium for the remainder of the 21 day culture period. Controls used were MSCs cultured in standard media, and MSCs cultured in standard osteogenic media. Metabolic activity and proliferation were assessed by Alamar Blue and DNA assays, whilst the expression of osteogenic markers was detected using RT-PCR, immunohistochemical (IHC) staining, and osteocalcin ELISA. Alizarin red staining, ESEM/EDX, FIB-TEM and Raman spectroscopy were used to confirm and characterise the mineralised matrix.

RESULTS: Alamar blue and DNA assays showed that transient serum exposure supported metabolic activity of MSCs. Successful differentiation was seen in all conditions exposed to OS, with 5 days exposure to FCS showing no statistical difference to the culture exposed to FCS for 21 days. This was confirmed by the detection of osteogenic markers osteocalcin (OCN), osteonectin and alkaline phosphatase using RT-PCR and IHC, and supported by data collected from the OCN ELISA assay. ESEM, EDX and alizarin red detected calcium nodules present in the matrix of all samples, with no significant difference between 5 and 21 days exposure to FCS with FIB-TEM showing that the nodules were present throughout the multilayered structure of the culture. Raman spectroscopy confirmed that the matrix: mineral ratios were similar to that for bone.

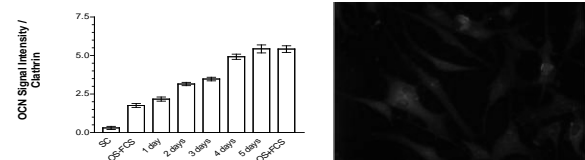


Figure 1: OCN detection in all conditions using RT-PCR and OCN expression in cells after 5 days exposure to OS+FCS

DISCUSSION & CONCLUSIONS: Our data suggests that it is possible to treat the cells with osteogenic supplement and FCS for 5 days, and then remove the serum, producing data that was not significantly different from cells cultured in osteogenic supplement and FCS for the full culture period. These findings provide a foundation for the development of a medium that will support both osteogenic and chondrogenic differentiation due to that fact that the exposure to serum used can now be kept to a minimum without compromising successful osteogenic differentiation.

ACKNOWLEDGEMENTS: Funding from EPSRC for this study is gratefully acknowledged. We also thank Dr. Michael Fay from Nottingham Nanotechnology and Nanoscience Centre for his technical assistance with FIB-TEM.

Self-assembly and gelation properties of novel peptides for biomedical applications

J Gao¹, AF Miller², JE Gough¹, A Saiani¹

¹ School of Materials, The University of Manchester, Grosvenor Street, Manchester, M1 7HS, UK.

² School of Chemical Engineering and Analytical Science, The University of Manchester, Sackville Street, PO Box 88, Manchester, M60 1QD, UK.

INTRODUCTION: Molecular self-assembly is a powerful tool for the preparation of molecular materials with a wide variety of properties. The increasing interest in the self-assembly of peptides is mostly centered on the relationship between their conformation and function. It is now well known that short peptides can self-assemble to form β -sheet rich fibres that become entangled to form hydrogels and these show promise for use in the tissue engineering field [1]. Consequently many studies have focussed on the self-assembly behavior of such peptides and their influence on fibre mechanical and biological properties. Here we will focus on establishing design rules for the effect of ionic complementary peptide primary sequence on hydrogel mechanical properties, and consequently cell behaviour.

METHODS: Two ionic-complementary peptides with alternative hydrophobic/hydrophilic side groups: FEFKFEFK and FEFKFEFK were synthesized using solid phase peptide synthesis and characterised by matrix-assisted laser desorption ionization-time of flight (MALDI-TOF) mass spectroscopy and high performance liquid chromatography (HPLC). Fourier transform infrared spectroscopy (FTIR), small angle X-ray scattering (SAXS) and small angle neutron scattering (SANS) were used to prove the existence of β -sheet rich fibres. Transmission electron microscopy (TEM) and SANS were used to view the fibrillar network formed by all peptides above the critical gel concentration. A stress-controlled rheometer was used to investigate the influences of intrinsic properties, external environment and peptide concentration on the mechanical behavior of peptide hydrogels. Experiments were all undertaken at room temperature. 2D cell culture using chondrocytes, 3T3 fibroblasts and human dermal fibroblasts was performed to prove the potential application of peptide hydrogels as extracellular matrix mimics. Live/dead staining was used to prove the presence of living cells on the gel surface.

RESULTS: Both of the octa-peptides were successfully synthesised with purity $\geq 85\%$. The phase diagram of each peptide has been mapped out as a function of temperature, pH and salt concentration with each forming a transparent hydrogel above a critical peptide concentration through the association of β -sheet rich fibres. Oscillatory rheology confirmed the presence of a gel and showed the elastic modulus can be tuned between 0.001 and 10 kPa depending on peptide concentration, pH and salt type and concentration. By using NaOH to adjust the pH of peptide hydrogels, different cell morphology was observed in 2D cell culture.

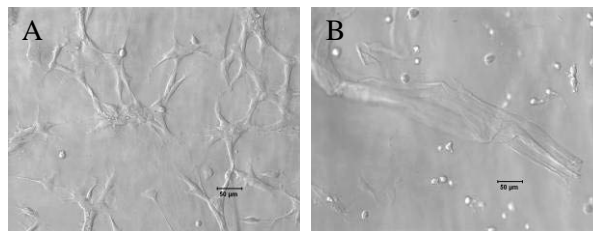


Figure: (A) Optical micrograph of FEFKFEFK gels with spread chondrocytes on the surface. (B) Optical micrograph of NaOH adjusted FEFKFEFK gels with rounded chondrocytes on the surface.

DISCUSSION & CONCLUSIONS: Transparent, self-supporting, temperature stable gels can be produced with fibril network structure and the mechanical properties similar to natural tissue. Furthermore our peptides self-assemble in the presence of cell culture media and the different processing routes and properties of our hydrogel network, influence cell behavior.

REFERENCES: ¹ Y. Nagai, L.D. Unsworth, S. Koutsopoulos et al (2006) *Journal of Controlled Release* **115**:18-25.

ACKNOWLEDGEMENTS: This research was supported by the University of Manchester, School of Materials.

Schwann cells in collagen gels survive plastic compression and maintain their alignment: development of a cellular biomaterial for peripheral nerve repair

Melanie Georgiou, Emma East, Jane Loughlin, Jon P. Golding & James B. Phillips
The Open University, Department of Life Sciences, Milton Keynes, MK7 6AA.

INTRODUCTION: Implantation of a tissue-engineered bridging device into a peripheral nerve injury site would be an attractive alternative to the nerve autograft. Aligned Schwann cells within a tethered collagen gel can promote and guide neuron regeneration *in vitro* and *in vivo*¹. Combining this cellular alignment with plastic compression to stabilise collagen gels² produces a robust cellular biomaterial with improved mechanical handling properties, and the potential to support neuronal growth. The aims of this study were (i) to investigate Schwann cell survival during compression of collagen gels, and (ii) to assess whether cellular alignment, achieved in tethered rectangular collagen gels¹, was retained following compression.

METHODS: The Schwann cell line SCL 4.1/F7 was used throughout. Cells were mixed with neutralised type I rat tail collagen (2 mg/ml), and allowed to set. Cell viability was assessed *in vitro* using propidium iodide exclusion and Hoechst nuclear staining in uncompressed gels, and in plastic compressed gels either 1 hour or 20 hours following compression. To investigate whether alignment was retained following plastic compression, rectangular gels were tethered to permit cellular self-alignment¹ before compression. Alignment was monitored before and after compression using CellTracker dye and image analysis. Confocal microscopy was used to reveal detailed cellular alignment in compressed gels.

RESULTS: There was no significant difference in Schwann cell death between gels that were subjected to 1 or 5 min compression or control gels that received no compression (Fig 1). Compression had no effect on cell death when assessed 1 hour after compression or at 20 h. Image analysis of aligned cells before and after plastic compression showed that cellular alignment was preserved during the compression process. This was confirmed using confocal microscopy (Fig 2).

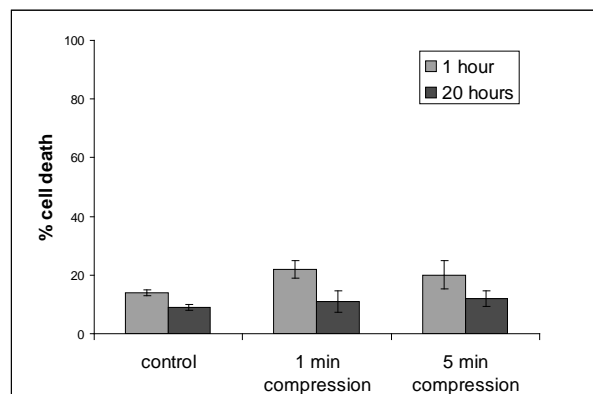


Fig. 1: Schwann cells survive plastic compression. Bars are means \pm SEM.

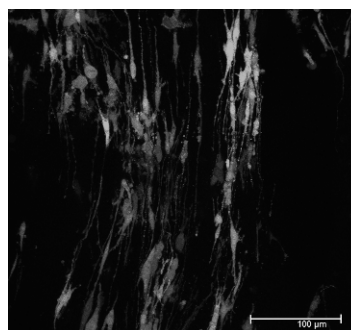


Fig. 2: Confocal micrograph showing Schwann cell alignment after compression of collagen gel.

DISCUSSION & CONCLUSIONS: Schwann cells in collagen gels survive plastic compression, as has been demonstrated previously for other cell types². Here we demonstrate that they also maintain their alignment during the compression process to form an aligned cellular collagen biomaterial that is more mechanically robust than the initial fully hydrated collagen gel. Combining tethered self-alignment with plastic compression technology therefore provides a promising approach for generating nerve repair conduits.

REFERENCES: ¹ Phillips J.B. *et al.* (2005) *Tiss Eng* **11** 1611-7. ² Brown R.A. *et al.* (2005) *Adv Funct Mater* **15** 1762-70.

ACKNOWLEDGEMENTS: This research was funded by an Open University Studentship. Technical support was provided by Chris Elcoate.

Two Photon Polymerisation of Photocurable Biomaterials

A Gill¹ & F Claeysens¹

¹ *Kroto Research Institute, Department of Engineering Materials, University of Sheffield*

INTRODUCTION: Photocurable analogues of the well described biomaterials polylactide (PLA) and polycaprolactone (PCL) have been developed for use in microstereolithography. The biocompatibility of these materials has been assessed, and cellular attachment to these materials has been compared with traditional PLA and PCL with promising preliminary results. Microstereolithography of these materials via two photon polymerisation has produced high resolution microstructures ideal for studying cell-surface interactions, and could be used for the creation of experimental tissue scaffolds and other implantable devices.

METHODS: *Polymer Synthesis:* Polymers were prepared in a two step process. Firstly the desired monomer (ϵ -caprolactone or lactide) were polymerised in the presence of the four armed initiator pentaerythritol. Secondly the products were acrylated with methacrylic anhydride to yield four armed low molecular weight prepolymers with reactive acrylate moieties.

Two Photon Microstereolithography: Firstly the polymer is mixed with Michler's ketone to produce the photosensitive mixture. The sample is prepared in the 'sample sandwich' format according to the literature¹ prior to lithography. Structures are created in a laser direct write fashion, where the sample is moved by a xyz-translation stage and laser radiation (810nm, 150mW, 76MHz, 200fs) focussed to a point within the resin by a high NA objective lens. Once completed the sample is soaked in toluene to remove the uncured polymer. Patterns were produced using the program 'nView' according to the authors design.

RESULTS: NG108-15 cells were culture on flat films of the PCL and PLA-based polymer and MTT assays showed excellent cell metabolic activity on this biomaterial. Additionally, primary Schwann cells showed good proliferation and adhesion on this material. DNA Quantification assay showed a clear difference between NG108-15 cell proliferation on thin films of photocured PLA and PCL and their traditional analogues, with a preference for the former ($p < 0.05$). In a second stage, NG108-15 cells were cultured on 3D structures fabricated by laser microstereolithography. Interestingly, a dependence of cell growth on the particular 2D structure of the

scaffold was observed. The cells attached readily to parallel lines of cured photocurable polylactide, however after 48 hours in culture they did not attach to the bulk surface of the rectangular and square patterns (see figure 1).

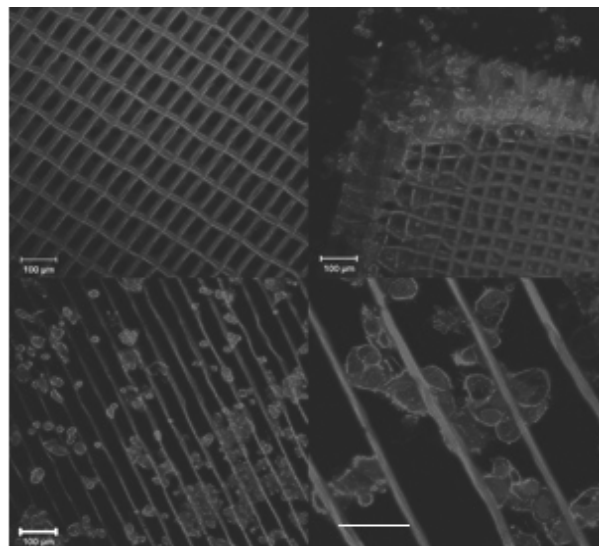


Fig. 1: Photocured PLA microstructures after 48h in culture with NG108-15 cell line. Attachment is observed on lines but rectangular structure remains cell free and attachment to square mesh is observed only on rough edges. (Scale bars: Top and left 100 μ m, bottom right 50 μ m).

DISCUSSION & CONCLUSIONS:

Photocurable biomaterials have been produced and successfully microstructured using two photon polymerisation to create devices for the study of cell-surface interactions. This technique can be further used to create interesting experimental scaffolds for use in tissue engineering and potentially microstructured implantable devices such as nerve guidance channels.

REFERENCES: ¹ J. Serbin, A Ovsianikov, B. Chichkov (2004) Fabrication of Woodpile Structures by Two-Photon Polymerization and Investigation of their Optical Properties, *Optics Express*, 12 (21), 5221-5228.

ACKNOWLEDGEMENTS: Thanks to Celia Murray-Dunning for cell culture and imaging, and to EPSRC and the laser loan pool for funding.

Mechanical Stimulation Inducing Cord-like Structure Forming from Mouse Embryonic Stem Cells

Bin Hu, Ying Yang, Nick R Forsyth, Alicia El Haj

Institute of Technology and Science in Medicine, Keele University

INTRODUCTION: Mechanical stimulation and mechanotransduction have attracted scientists' interest for many years. During embryogenesis, mechanical factors play an important role in cardiovascular system development [1]. A four point bending system providing cyclic strain and shear force stimulation (working mechanism see Fig. 1) was custom made in our lab and was utilized in *in vitro* osteogenesis induction [2]. Here we have tested the mechanical stimulation effect on pre-differentiated vascular progenitor cells via four pointing bending system.

METHODS: mES cell line TG2a (passage 16-28) (a kind gift from Professor Monica Spiteri) were used for the experiment. Undifferentiated mES cells were cultured in gelatinised flasks with DMEM (Biosera) supplemented with 15% FBS, 1% L-glutamin, 1% antibiotic & antimycotic, 1% nonessential amino acid and 10 ng/ml LIF (Millipore). For preinduction of differentiation, cells were cultured in ColIV coated flasks for 4 days fed with α -MEM (Invitrogen) supplemented with 10% FBS, 1% antibiotic & antimycotic but without LIF (differentiation medium) [3]. mES were then passaged onto ColIV coated coverslips followed by 3 days further culture in differentiation medium. Once confluent cells were loaded on the four point bending system for 10 hours at 1 Hz per day for 3 consecutive days; Cells under static culture condition were employed as control group. n=5. Cells were fixed at day 4 and morphology checked under the light microscope. Smooth muscle α actin (SMA) expression was determined by immunostaining.

RESULTS: After 3 days mechanical stimulation, cells formed cord-like structures which exhibited spontaneous contraction in all samples. In static groups, only one similar structure was observed across 5 samples. In our previous result, cells derived from retinoic acid induction only formed spontaneous contract cluster without cord-like structure. SMA-directed immunofluorescence (Figure 2: 5,6) demonstrated the presence of smooth muscle cells in the cord-like structures.

DISCUSSION & CONCLUSIONS: Mechanical stimulation via four point bending system effectively induced the spontaneous cord-like

structure formation and the potential to cohort muscular blood vessels generation *in vitro* requires further investigation.

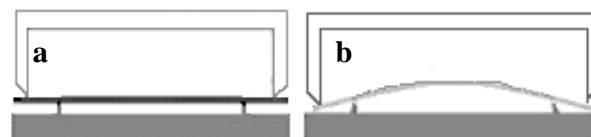


Fig. 1: schematic diagram of one working cycle for four point bending system.

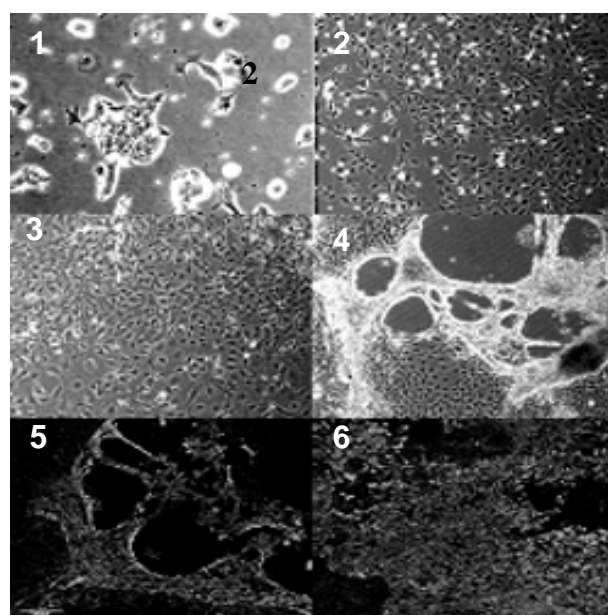


Fig. 2: Cell morphology changes and immunofluorescence staining. 1) undifferentiated mES cells; 2) after 4 days ColIV induction; 3) further culture on ColIV coated cover glass before mechanical stimulation; 4) cells formed cord-like structure after 3 days consecutive mechanical stimulation; 5 & 6) smooth muscle α -actin immunofluorescence staining of mechanical stimulation and static group perspective.

REFERENCES: ¹ K. Yamamoto, et al (2003) Proliferation, differentiation, and tube formation by endothelial progenitor cells in response to shear stress. *Appl Physiol* **95**:2081-88. ² Y. Yang, et al (2002) Development of a 'mechano-active' scaffold for tissue engineering. *Biomaterials* **23**:2119-26. ³ J. Yamashita, et al (2002) *Flk1*-positive cells derived from embryonic stem cells serve as vascular progenitors. *Nature* **408**:92-96.

Monitoring collagen gelling by elastic scattering spectroscopy (ESS)

Hedeer Jawad¹, Martin Austwick², Sandy MacRobert², Alveena Kuraishi¹, Frank Tully³, Tijna Alkseeva¹, Robert Brown¹.

¹UCL, Institute of orthopedics-TREC, Stanmore campus, London, UK, HA7 4LP

²UCL, National Medical Laser Centre, Department of Surgical and Interventional Sciences, Charles Bell House, 67-73 Riding House Street, UK, W1W 7EJ

³The Automation Partnership (Cambridge) Ltd, York way, Royston, Hertfordshire, UK, SG8 5WY

Introduction

Collagen is being used extensively in tissue engineering and on a larger scale in the field of cosmetic surgery. It is either used as a gel or plastically compressed sheet¹. The fundamental science behind collagen gelling has been studied but little is known about the precise timing of gelling and the variables that affect gelling in the first 30 minutes. Critically, before collagen can be engineered as a predictable functional material we must be able to control fibril aggregation and gel formation. Here we report on the use of elastic scattering spectroscopy (ESS) to detect changes in scattering in rat tail and GMP bovine skin collagen during gelling. Effect of cell seeding on gelling is also reported.

Materials and Methods

Rat tail collagen (Firstlink™ UK) and GMP bovine skin collagen (Devro Medical UK) gels were made by neutralizing 1 part 10x MEM and 4 parts collagen solution with NaOH. Collagen solution was poured into a well of a 24 well plate. A fiber optic probe connected to a white light source and spectrometer measured the intensity of backscattered light every 10 seconds over a 60 min, using a standard backscatter monitoring equipment². Scattered intensity was analyzed over 600-770 wavelength and one way ANOVA was used to determine the significant difference in gelling with different collagen types, pH, temperature and cell density. Mechanical strength of the collagen gels was determined from a simple probe test.

Results

As the collagen solution gels, the intensity of the backscattered light decreased. ESS showed a distinctive decrease in the intensity of the backscatter at a particular time during the gelling process (Fig1). The time of this decrease was different in rat tail collagen and the GMP bovine collagen (Table 1). ESS also showed that the presence of cells and pH affected this gelling time and rate. Mechanical probe test indicated gelling was complete at 15 min for rat tail collagen, in agreement with ESS data, the sudden fall in intensity in Fig1. The precise timing of gelling is important for automation purposes, and we hope that this work will contribute significantly for collagen gelling on an industrial scale.

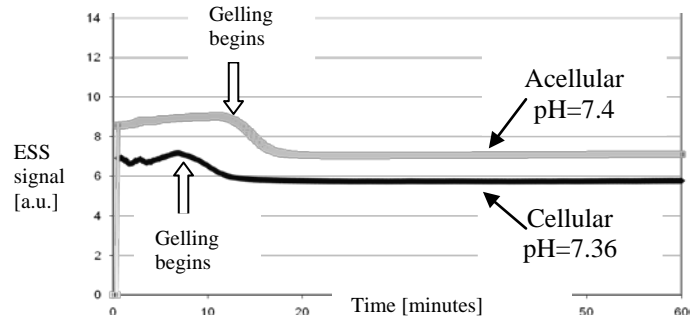


Fig 1 Intensity of backscattered light (a.u) received over a period of 60mins as rat tail collagen solution gels. Measurements taken every 10 seconds.

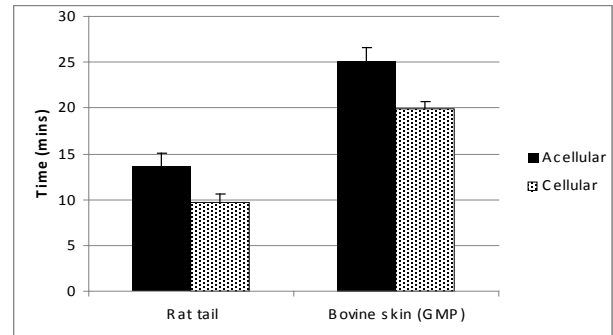


Table 1 Calculated time of maximum gradient of the decreasing intensity of backscattered light indicating the gelling time (s.e.m of n=5)

Discussion and Conclusions

We have shown that there is a need for tight control of the environment when obtaining a collagen gel on an industrial scale. Intensity of backscattered light decreased as the collagen gels, due to increased scattering from the longer fibrils which form. The seeding of cells into the collagen construct affected collagen gelling. Simple mechanical testing of the collagen solution showed the “hardness” of the collagen gel increased with time, due to increase in fibril formation. Creep testing will provide information on the different mechanical properties obtained at different gelling times and how they are affected by factors such as pH and temperature. These properties are relevant for the gels’ suitability for various tissue engineering applications.

References

1. Brown, R.A *Adv. Funct. Mater.* 2005, 15, 1762
2. Kostyuk, O *Proc. Of SPIE* 5486, 198

Acknowledgments TSB-EPSC for funding
Disclosures UCL has patent licensing agreement with TAP

Characterization of Anisotropic and Nonlinear Properties of Fresh and Decellularised Aortic Valves Using Inverse Finite Element

Akram Joda, Sotirios Korossis, Jon Summers, John Fisher, Zhongmin Jin

Institute of Medical and Biological Engineering, University of Leeds, Leeds, UK

INTRODUCTION: Accurate mathematical predictions of soft tissues biomechanics such as heart valves require using constitutive models, which describe their stress-strain relation. Soft tissues properties are known to be highly anisotropic and nonlinear. Fitting experimental stress-strain data of a soft tissue to a constitutive equation requires; first choosing the appropriate mathematical model that can represent the soft tissue behaviour and then finding its parameters. Inverse finite element method has been used successfully for parameters identification of constitutive models of soft tissues¹. The aim of this study was to use the inverse finite element method to identify the parameters of anisotropic nonlinear constitutive models of fresh and decellularised porcine aortic valves, which then can be used in numerical simulations.

METHODS: Experimental uniaxial stress-strain data in circumferential and radial directions of fresh and decellularised porcine aortic valves were obtained from². Two uniaxial finite element models representing circumferential and radial directions for fresh and decellularised aortic valves were created in the explicit finite element software LS-DYNA (LSTC, Livermore) consisting of 400 solid elements each. The measured displacements were used as boundary conditions and the measured cross-sectional forces were used as targets. The constitutive equations used in this study were based on an invariant formulation for soft tissues³ with one fiber family aligned with the circumferential direction. For the inverse finite element method, LS-DYNA was coupled with the optimization software LS-OPT (LSTC, Livermore) to minimize the least square residual of the predicted and measured forces using successive response surface method (SRSM).

RESULTS: Each case was run for ten optimization iterations. The predicted circumferential and radial forces for the fresh and decellularised aortic valves with the optimum parameters were found to be in good agreement with the measured forces as can be seen in Fig. (1 &2).

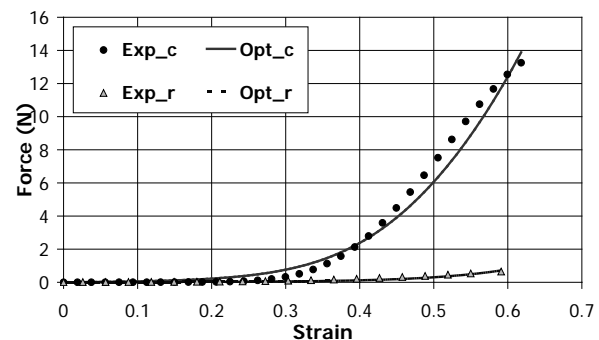
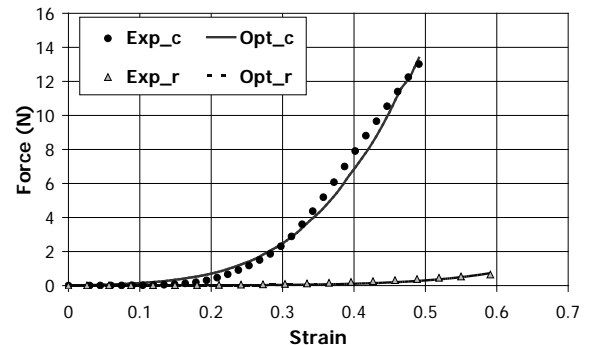


Fig.2 Measured and predicted Forces of decellularised aortic valves

DISCUSSION & CONCLUSIONS: In this work the inverse finite element method was used to characterise the nonlinear and anisotropic properties of fresh and decellularised aortic valves. Good agreement was found between the predicted the measured forces in the two directions using the optimum parameters.

REFERENCES: ¹D. R. Einstein, A.D. Freed, N. Stander, B. Fata, I. Vesely (2005) *Ann. Biomed. Eng.* **33**: 1819-1830.

²S.A. Korossis, C. Booth, H.E. Wilcox, K.G. Watterson, J.N. Kearney, J. Fisher, E. Ingham (2002) *The Journal of Heart Valve Disease* **11**: 463-371.

³A.D. Freed, D. R. Einstein, I. Vesely (2005) *Biomech. Model. Mechanobio.* **4**: 100-117.

ACKNOWLEDGEMENTS: This work was funded by a Marie Curie EST Fellowship, EC Contract Ref.: MEST-CT-2005-020327.

Surface Modified Expanded-polytetrafluoroethylene (ePTFE) Substrates for Retinal Pigment Epithelial Growth and Implantation

V.R.Kearns¹, S.Nian¹, K.Vasilev², C.Sheridan¹ & R.L.Williams¹

¹*School of Clinical Sciences, University of Liverpool, Liverpool, UK*

²*Mawson Institute, University of South Australia, Adelaide, Australia*

INTRODUCTION: Age-Related Macular Degeneration (AMD) is the main cause of irreversible vision loss in older people in the Western World. A potential treatment for AMD could be subretinal transplantation of a functioning retinal pigment epithelium (RPE).

Surface-modified ePTFE can support a functional monolayer of an RPE cell line¹. Plasma polymerisation provides the opportunity to tailor surface chemistry of ePTFE while maintaining substrate porosity and handling properties.

Iris pigment epithelial cells (IPE) have the same embryonic origin and similar properties to RPE cells. They are relatively easy to obtain surgically and may be an alternative cell source for RPE replacement.

The aim of this work was to investigate the ability of ePTFE membranes modified by plasma polymerisation to support the growth of a differentiated monolayer of primary human RPE cells (hRPE) and primary rat IPE (rtIPE).

METHODS: ePTFE membranes were coated with n-heptylamine (HA)². For experiments with rtIPE, substrates were coated with fibronectin, as this was demonstrated in preliminary studies to give optimal cell growth.

hRPE were isolated from cadaver eyes and grown for several passages. rtIPE were isolated from rat eyes and seeded directly onto substrates. Cells were seeded onto HA-ePTFE and tissue culture plastic (TCPS) substrates in a high-serum medium. Medium was replaced at 48h with a low-serum, retinoic acid-containing medium. Substrates were fixed at 7, 14 and 28d. hRPE were stained for F-actin and the markers of tight and adherens junction formation.

RESULTS: With hRPE, actin belts, typical of differentiated epithelial cells, formed around cells on HA-ePTFE by 14d and on TCPS by 28d. Tight junctions were observed on all substrates at 7d and were uniformly distributed over all substrates by 28d. Adherens junctions were observed at 28d (Fig.1).

rtIPE cells attached and spread on the substrates. They were heavily pigmented and exhibited epithelial morphology (Fig. 2). Melanin was distributed around cell nuclei.

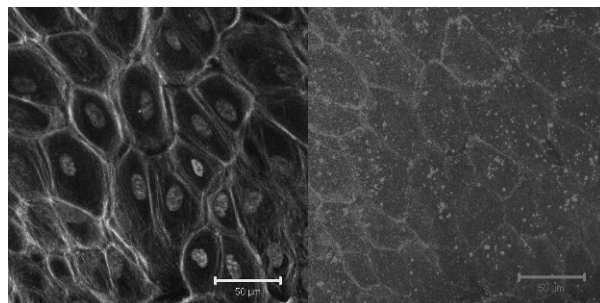


Fig. 1: differentiated hRPE on HA-ePTFE at 28d. Cells demonstrate the formation of actin belts (left) and adherens junctions (right). Scale bars represent 50 µm.

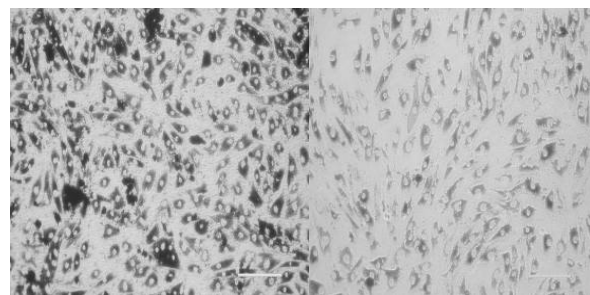


Fig. 2: primary rtIPE cells at 7d on fibronectin coated HA-ePTFE (left) and TCPS (right). Scale bars represent 100 µm.

DISCUSSION & CONCLUSIONS: Surface modification of ePTFE by plasma polymerisation can promote the attachment of IPE and formation of a differentiated layer of RPE cells. This strategy may contribute towards development of a transplantation treatment for AMD.

REFERENCES:

- ¹ Y.Krishna, C.Sheridan, D.Kent, et al. (2010), *BJO In Press* ² K.Vasilev, L.Britcher, A.Casnal and H.J. Griesser (2008), *J Phys. Chem. B* **112**(35):10915-10921

ACKNOWLEDGEMENTS: The authors would like to thank a private local charity and the Foundation for the Prevention of Blindness for their financial support.

Biocompatibility of acellular porcine ureteric scaffold for tissue engineering small diameter vesselsTaha H. Khan^{1,2}, Stacy-Paul Wilshaw¹, Sotiris A. Korossis¹, Eileen Ingham¹, Shervanthi Homer-Vanniasinkam²

1 Institute of Medical and Biological Engineering, University of Leeds, Leeds, LS2 9JT

2 Leeds Vascular Institute, Leeds General Infirmary, Great George Street, Leeds, LS1 3EX

Introduction

The current gold standards for small diameter (<6mm) arterial bypass are autologous vein or artery. However patients may lack suitable conduits and patency rates of synthetic alternatives (e.g. Dacron) are significantly lower. Acellular porcine ureter (AU) may be suitable for use as a scaffold₁. The aim of this study was to investigate the biocompatibility of AU for tissue engineering blood vessels.

Materials and Methods

Porcine ureters were decellularised by sequential incubation in PBS, hypotonic Tris buffer [10mM plus 0.1%(w/v) EDTA, aprotinin (10 KIU.ml⁻¹) pH8.0], 0.1%(w/v) SDS and nuclease (1Uml⁻¹ RNase, 0.5 Uml⁻¹ DNase) solution, and sterilised in 0.1% (v/v) peracetic acid.

Biocompatibility was investigated by contact and extract cytotoxicity tests with porcine smooth muscle (SMC) and endothelial cells (EC). The AU's capacity to support SMC adhesion was initially determined by seeding 5x10mm sections of AU.

Cell seeding of the conduit (8 cm long) was then assessed by (1) seeding SMC and EC simultaneously or (2) seeding SMC first with EC to be seeded at a later stage. (1) SMC and EC were seeded simultaneously, at different cell densities, in 10 ml of culture medium on a rotating AU conduit (1 rpm for 1-2 hours with SMC in the extra-luminal suspension and EC in the luminal suspension) at 37°C. (2) Independent seeding of SMC alone was investigated in a similar fashion on a rotating AU conduit (1rpm for 24 hours with SMC in the extra-luminal suspension) at 37°C.

Results

The AU showed no toxicity to SMC or EC in the in vitro assays, and supported SMC attachment. Simultaneous seeding of AU resulted in EC [luminal] and SMC [advential] adhesion. Adhesion was dependent on cell seeding density and duration. The optimum cell density was 1x10⁶ SMCml with 0.5x10⁶ ECml⁻¹ which resulted in confluency of approximately 60% for SMC and 40% for EC after 2 hours incubation (Fig 1).

Independent seeding with SMC only (Fig 2) with a lower cell density of 2.0x10⁵ SMCml⁻¹ resulted in a confluency of 95%, albeit after 24 hours incubation. Seeding of SMC at a density of 1.5x10⁵ SMCml⁻¹ (Fig 3) gave improved

penetration of cells into the scaffold after 7 days of culture.

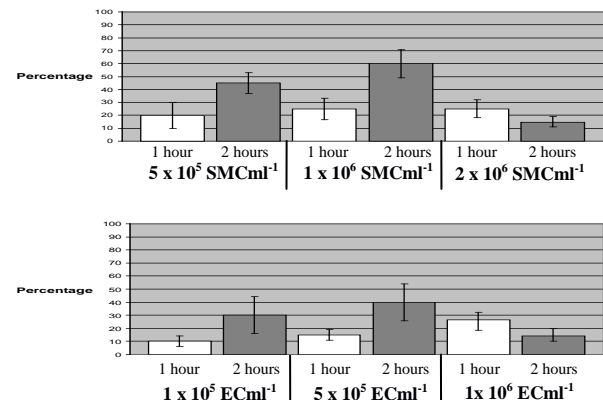


Fig 1. Percentage confluence of SMC (top) and EC (bottom) after 1 and 2 hours adhesion at different cell densities. SMC and EC seeded simultaneously to the adventitial and luminal surface respectively. Data is presented as the mean (n=3; ±95% confidence limits).

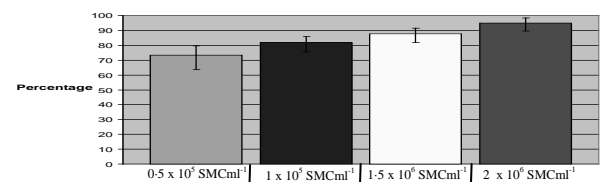


Fig. 2. Percentage confluence of SMC, when the AU was seeded with only SMC at different cell densities on the adventitial surface. Data is presented as the mean (n=3; ±95% confidence limits).

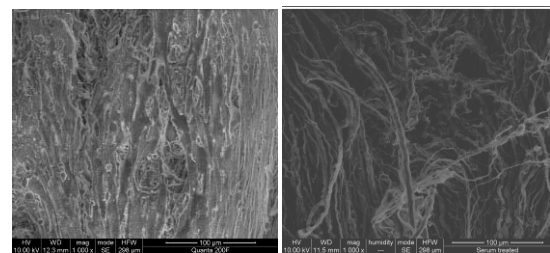


Fig. 3. SEM (x1000) of SMC seeded alone for 24h 1.5x10⁵ SMCml (left) when compared to AU (right)

Discussion and Conclusions

This study demonstrated that the AU was non-toxic. The AU conduit supported adhesion of both SMC and EC simultaneously. When seeded independently, SMC were shown to reach confluency at lower cell densities. Future studies will assess the development of the SMC and EC seeded AU in a physiological pulsatile flow bioreactor.

References

1. Derham et al. (2009) *Tissue Engineering*, **14**, 1871-1882.

Optimisation of Osteogenic and Chondrogenic Differentiation Potential Using Clonal Mesenchymal Stem Cell Populations Derived from Synovial Fat Pad

WS Khan¹, SR Tew¹, AB Adesida¹, JG Andrew¹, TE Hardingham¹

¹ UK Centre for Tissue Engineering, Faculty of Life Sciences, University of Manchester, Oxford Road, Manchester, M13 9PT, UK

INTRODUCTION: Mesenchymal stem cells are a potential source of cells for the repair of bone and articular cartilage defects. We have previously demonstrated that the infrapatellar synovial fat pad is a rich source of mesenchymal stem cells and these cells are able to undergo osteogenic and chondrogenic differentiation^{1,2}. Although synovial fat pad derived mesenchymal stem cells may represent a heterogeneous population, clonal populations derived from the synovial fat pad have not previously been studied.

METHODS: Mesenchymal stem cells were isolated from the infrapatellar synovial fat pad of a patient undergoing total knee arthroplasty and expanded in culture. Six clonal populations were also isolated before initial plating using limiting dilution and expanded. The cells from the mixed parent population and the derived clonal populations were characterised for stem cell surface epitopes, and then cultured in osteogenic medium for 21 days and as cell aggregates in chondrogenic medium for 14 days. Gene expression analyses; alizarin red staining; alkaline phosphatase, glycosaminoglycan and DNA assays; and immunohistochemical staining were determined to assess osteogenic and chondrogenic responses.

RESULTS: Cells from the mixed parent population and the derived clonal populations stained strongly for markers of adult mesenchymal stem cells including CD44, CD90 and CD105, and they were negative for the haematopoietic marker CD34 and for the neural and myogenic marker CD56. A variable number of cells were also positive for the pericyte marker 3G5 both in the mixed parent and clonal populations. The clonal populations exhibited a variable osteogenic and chondrogenic response; two clonal cell populations exhibited a significantly greater osteogenic response, and one clonal cell population exhibited a significantly greater chondrogenic response when compared with the mixed parent population. Results for immunohistochemical staining for collagen I, collagen II, and aggrecan, and Safranin O staining for the six clonal populations and the mixed population are shown in the figure.

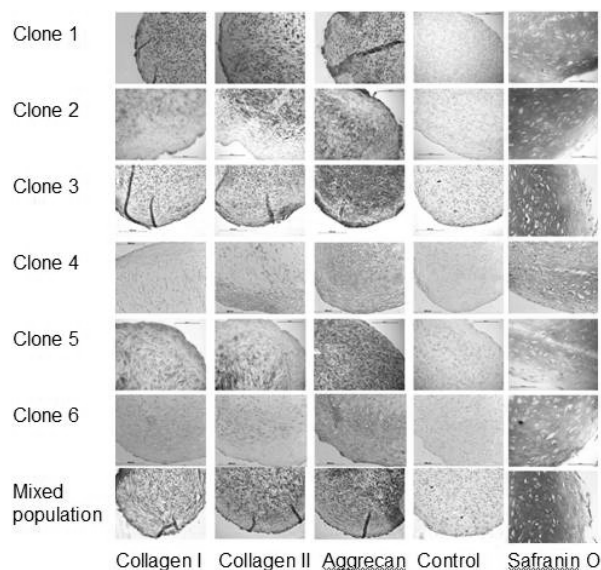


Figure: Immunohistochemical staining for collagen I, collagen II, and aggrecan, and Safranin O staining for the six clonal populations and the mixed population.

DISCUSSION & CONCLUSIONS: Pericytes are a candidate stem cell in many tissue and our results show that all six clonal populations derived from the heterogeneous synovial fat pad population express the pericyte marker 3G5. The variable osteogenic and chondrogenic responses suggest inherent differences between these populations. The osteogenic and chondrogenic potential of the synovial fat pad could be optimised by the identification of clonal populations with a propensity to differentiate down particular differentiation pathways.

REFERENCES: ¹ Khan W.S., Tew S.R., Adesida A.B. & Hardingham T.E. (2007) Human infrapatellar fat pad-derived stem cells express the pericyte marker 3G5 and show enhanced chondrogenesis after expansion in FGF-2. *Arthritis. Res. Ther.* 10, R74. ² Khan W.S., Adesida A.B., Tew S.R. & Hardingham T.E. (2009) The epitope characterisation and the osteogenic differentiation potential of human fat pad-derived stem cells is maintained with ageing in later life. *Injury.* 40, 150-7.

Comparing the Gene Expression of Embryonic and Mesenchymal Stem Cells using Experimental Data and a Novel Mathematical Model

Glen R Kirkham, Anna Lovrics, John King, Virginie Sottile, Kevin Shakesheff, Lee D Buttery

Wolfson Centre for Stem Cells, Tissue Engineering and Modelling (STEM), University of Nottingham, University Park, NG7 2RD

INTRODUCTION: Stem cells have the potential to differentiate into a wide variety of cell types^{1,2}. Biological comparisons between types of stem cells have, to date, been limited to data obtained from distinct studies. With this in mind two stem cell types, mouse embryonic stem cells (mES) and mouse bone marrow mesenchymal stem cells (MSCs), were cultured in the presence of the growth factors TGF β 1 and BMP-2 (separately and in combination). The expression of early osteogenic regulatory genes was tested over a 48 hour time course at established concentrations, and with varying concentrations of growth factors. These data were then used along with previously published data as a basis for a mathematical gene network model. This model has the potential to more effectively determine regulatory interactions, guiding future research more effectively.

METHODS: MSCs and mES were incubated with growth factors in three groups: TGF β 1, BMP-2, TGF β 1 and BMP-2. As well as a control group with no growth factors present. The expression of the genes *Dlx5*, *Msx2* and *Runx2* was monitored at 8, 16, 24 and 48 hours after initial exposure to the growth factors by Real Time RT-PCR analysis. In a second study five concentrations of growth factors were tested between 1-20 for TGF β 1, and 10-400 for BMP-2, both separately and in combination for 24 hours. All expression levels were normalized against GAPDH. Gene expression levels for primary mouse bone cells were also tested using the same conditions.

RESULTS: MSCs and mES cells demonstrated distinct gene expression profiles across the time course (fig 1) and the concentration series (fig 2). The mES showed significant differences compared to the bone cells. The mathematical model was used to accurately visualise and replicate expression profiles and produce predictive interactions for future study (fig 3). Relative expression was measured as fold increase compared to controls (no growth factors).

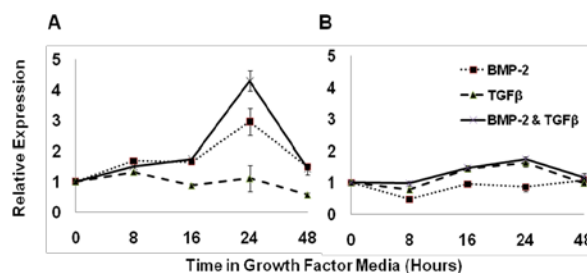


Fig. 1: Expression of *Dlx5* in mES cells (A) and mouse bone cells (B) over 48 hours.

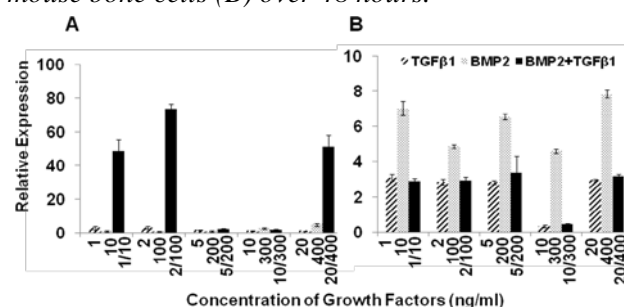


Fig. 2: Gene expression levels of *Msx2* in mES cells (A) and mouse bone cells (B) at 24 hours.

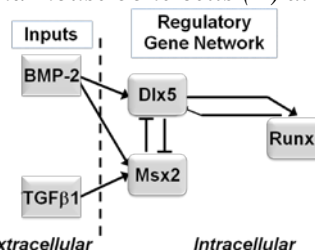


Fig. 3: Simplified mathematical network model of early osteogenic gene expression, used to predict regulatory interactions for future study.

DISCUSSION & CONCLUSIONS: Embryonic and mesenchymal stem cells showed distinct gene expression profiles compared to each other and primary bone. A mathematical model was able to quantify and visualise gene networks and postulate regulatory interactions to more effectively guide future study.

REFERENCES: ¹ Buttery L.D.K *et al* (2001) *Tissue Engineering* 7:1:89-99. ²Kurosawa H *et al* (2003) *J of Biosci and Bioeng* 96:4: 409-411.

ACKNOWLEDGEMENTS: The tissue engineering group at Nottingham University and the BBSRC and EPSRC for funding.

Optimisation of Inkjet printing for the Life Sciences

R Knight, J Gough, C Merry & B Derby

School of Materials, Materials Science Centre, University of Manchester, Manchester, M13 9PL

INTRODUCTION: Biochemical gradients have been shown to be vital in many aspects of developmental biology and tissue repair [1,2], including the differentiation of stem cells, where the local microenvironment is of critical importance in controlling the pathway for differentiation and eventual cell fate. Inkjet printing gives the ability to precisely pattern various biochemicals, such as proteins and sugars, in 2D and has been used to deliver proteins onto substrates with the intention to control cell behaviour [3,4]. Here, we have investigated the inkjet printing of heparin as an important member of the glycosaminoglycan family. Printed gradients could have a direct effect on stem cell differentiation and, due to the interactions of heparin with many growth factors (eg FGFs, BMPs etc) could also be used to create and examine the effects of growth factor gradients on other cell types. The aim here was to establish and optimize a method for printing heparin onto poly-lysine coated slides with a view to assessing the response of mouse embryonic stem cells.

METHODS: Heparin (Iduron, 20 $\mu\text{g}\cdot\text{ml}^{-1}$) containing 0.1 % - 10 % glycerol (v/v) in deionised water was printed using a Fujifilm Dimatix (Santa Clara, California) inkjet printer (10 pl nozzle) onto poly-lysine coated slides (VWR) at 30 v, using a substrate temperature of 60 °C and a spot spacing varying from 50-100 μm . Printed slides were assessed using a combination of interferometry and immunocytochemistry.

RESULTS: Printed heparin in water alone at a drop spacing of 100 μm segregated upon drying to form a ring (Fig 1A.). This phenomenon is well known as “coffee staining” [5]. Glycerol was added to the printing solution in order to increase viscosity so as to prevent the formation of these rings (Fig 1B.). The drop spacing was then reduced to 50 μm and the drops merged into tracks of printed heparin one drop wide whilst successfully maintaining an even distribution of heparin. These tracks were then merged into squares of printed heparin.

DISCUSSION & CONCLUSIONS: It is thought that rapid evaporation at the thin edges of printed drops encourages fluid flow from the thicker central areas of the drops to the outer edges of the drop. This flow drags dissolved molecules to the

edge of the drop where they become pinned to the substrate to leave a ring of solute at the edge of the drop and comparatively less towards the central area upon drying. The addition of glycerol here is likely to have disrupted the flow of liquid by altering the evaporation rate at the edge of the drops, thereby disrupting the formation of the typical coffee staining to leave a more even distribution of printed heparin.

By over-printing heparin, it is possible to create a concentration gradient that seeded cells will respond to differentially. Furthermore, owing to the interactions of heparin with many growth factors, it may subsequently be possible to make gradients of these biochemicals and study their effects on cultured cells. Development of a method to accurately print biochemicals into gradients and other patterns holds great potential for studying cell responses to varying microenvironments by mimicking some of the conditions found in the body, in particular for investigating the conditions found during development and wound repair.

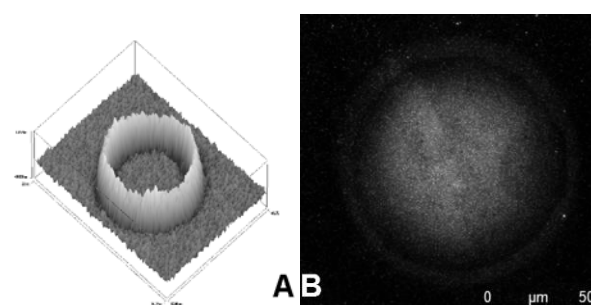


Fig.1. Heparin (20 $\mu\text{g}\cdot\text{ml}^{-1}$) in deionised water with and without glycerol. A. Water-only printed drop showing coffee stain effect by interferometry, B. 10% glycerol in water printed drop showing even distribution of heparin by immunofluorescence.

REFERENCES: ¹L. Wolpert (1996) *Trends Gen.* **12**: 359. ²L.C. Gerstenfeld, D.M. Cullinane, G.L. Barner, et al, (2003) *J. Cell. Biochem.* **88**: 873. ³ K. Watanabe, T. Miyazaki & R. Matsuda (2003) *Zool Sci* **20**: 429. ⁴E.A. Roth, T. Xu, M. Da et al, (2004) *Biomaterials.* **25**: 3707. ⁵R. D. Deegan, O. Bakajin, T. F. Dupont et al. (1997) *Nature.* **389**: 827.

ACKNOWLEDGEMENTS: This work was funded by the BBSRC (ref: BB/G024332).

Aligned neurite outgrowth on electrospun PLGA nanofibres

M. Krämer¹, J.B. Chaudhuri¹, P.A. De Bank², M.J. Ellis¹

¹ Department of Chemical Engineering, University of Bath, UK

² Department of Pharmacy and Pharmacology, University of Bath, UK

INTRODUCTION: Injuries to the central nervous system (CNS) have traumatic consequences such as irreparable disability due to the inability of the CNS to regenerate injured nerve fibres. The development of novel scaffolds is important to facilitate axonal growth through injured environments of the CNS¹. Poly(lactic-co-glycolic acid) (PLGA) is one of the most widely used synthetic polymeric materials for scaffold fabrication in tissue engineering. It is biodegradable, biocompatible and FDA approved², but so far with little application in nerve tissue engineering. This study explores the potential use of PLGA scaffolds for nerve tissue engineering, acting as a potential carrier for nerve cells and guide for directional nerve cell differentiation.

METHODS: Scaffolds were produced by electrospinning, a process for obtaining fibres in the nanometre scale³, using 10% w/w polymer (75:25 PLA:PGA) in chloroform:methanol (3:1). Aluminium foil (for random fibres) or two aligned aluminium electrodes (for aligned fibres) were used as collectors. The polymer solution was pumped at 3ml/h flow rate and voltage of 15kV was applied. Alignment of fibres was verified by Fast Fourier Transform and Oval Profile plug-ins in ImageJ. PC12 cells were used as a model neuronal cell to analyse the polymer's ability to support cell attachment, proliferation and neurite extension. Cells were cultured in RPMI 1640 medium with 10% FCS, 1mM sodium pyruvate, and 1% antibiotic/antimycotic. For differentiation, cells were exposed to 40 ng/ml nerve growth factor (NGF) in medium containing 1% FCS only. The percentage of neurite-bearing cells, number of neurites per cell, length of neurites and alignment of neurites along nanofibres were analysed.

RESULTS: PC12 cells attached along electrospun fibres. When exposed to NGF these cells stopped dividing and extended neurites. On random fibres, neurite orientation was random (Fig 1A), whereas on aligned fibres 63% of neurites extended grew along the fibre orientation $\pm 10^\circ$ (Fig 1B+2). After 7 days of exposure to NGF, cells had 1-4 neurites on random fibres, reaching a maximum length of 188 μm , whereas on aligned fibres, cells had predominantly 1-2 neurites reaching lengths of up to 900 μm .

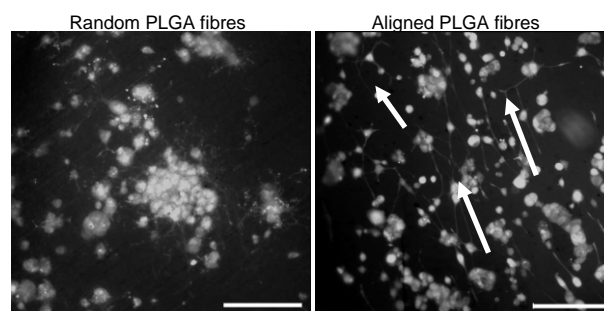


Fig. 1: Effect of fibre alignment on direction of PC12 cells' neurite outgrowth induced by 40 ng/ml NGF after 4 days. Arrows indicate alignment (Bar=200 μm).

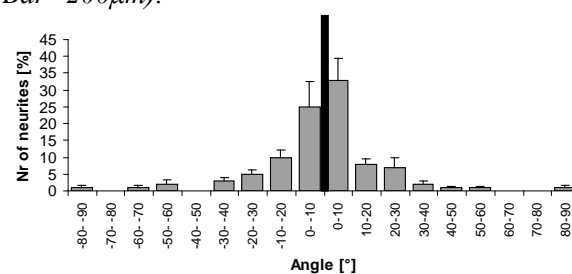


Fig 2: Alignment of neurites along electrospun fibres. Bar indicates fibre orientation (set at 0°).

DISCUSSION & CONCLUSIONS: Previously published studies have not investigated the effect of aligned nanofibres on guidance of neurite outgrowth from PC12 cells. Here, electrospun aligned PLGA nanofibres were shown to be suitable in supporting attachment and differentiation of PC12s. Aligned fibres reduced the number of neurites per cell, directed neurite outgrowth along fibre orientation and increased the length of neurites. This work suggests that the PLGA scaffold strongly influences neurite organisation, which is potentially useful for future therapeutic approaches.

REFERENCES: ¹S. Thuret, L.D.F. Moon, F.H. Gage (2006) *Nature Reviews Neuroscience* 7:628-643. ²L. Lu, S.J. Peter, et al (2000) *Biomaterials* 21:1837-45. ³A. Martins, R.L. Reis (2008) *International Materials Reviews* 53:257-274.

ACKNOWLEDGEMENTS: The authors would like to thank the University of Bath for funding this project.

Investigating the Relationship between Surface Properties of Polymers and Protein Adsorption

D. Kumar¹, S.L. Wilson¹, N.R. Forsyth¹ & Y. Yang¹

¹Institute of Science and Technology in Medicine, Keele University, UK

INTRODUCTION: Electrospun synthetic, biodegradable nanofibrous materials have the ability to mimic the topographical architecture and surface chemistry of native extracellular matrix (ECM)¹. The aim of this study is to investigate different polymer surfaces regarding wettability and protein adsorption. Protein attachment is an indicator of cell biocompatibility and can be used to determine preferential scaffold materials for maximum cell adhesion².

METHODS:

Electrospinning: Poly lactic acid (PLA); and poly- ϵ -caprolactone (PCL) were dissolved in a mixture of ratio 7:3 of chloroform and dimethylformamide. Polymer solutions were electrospun to coverslips at a low fiber density using the parameters detailed in Table 1. A static ground collector was used to fabricate random nanofiber scaffolds and a rotating mandrel was used to attain aligned nanofiber scaffolds. Additionally; PLA and PCL films were also produced from a solution where the polymer was dissolved in chloroform only.

Table 1. Parameters used to fabricate aligned/random PCL & PLA nanofiber scaffolds.

Parameter	PCL		PLA	
	Aligned	Random	Aligned	Random
Working Distance	20cm	15cm	20cm	15cm
Voltage	4.5kV	4kV	6kV	6kV
Flow Rate (ml/min)	0.01	0.01	0.025	0.025
Volume: ml	0.018	0.018	0.025	0.025

BSA Model Protein & Staining: 50 μ l of Bovine Serum Albumin (BSA) [500 μ g] was added to each polymer surface and incubated at 37°C for 2 hours. After removing BSA solution and rinsing, 400 μ l of 0.1% (wt/v) Coomassie Dye was added to samples for 10 minutes.

Contact Angle: 10 μ l of ultra pure H₂O was applied to coverslips using a Hamilton syringe. Images were taken using a CCD camera. Images were assessed using the Image J plug-in.

RESULTS:

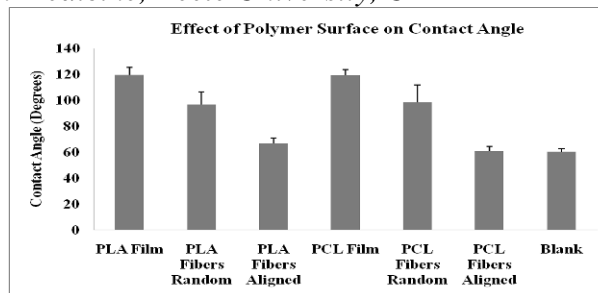


Figure 1. Contact Angles of droplets on different polymer surfaces (n=4)

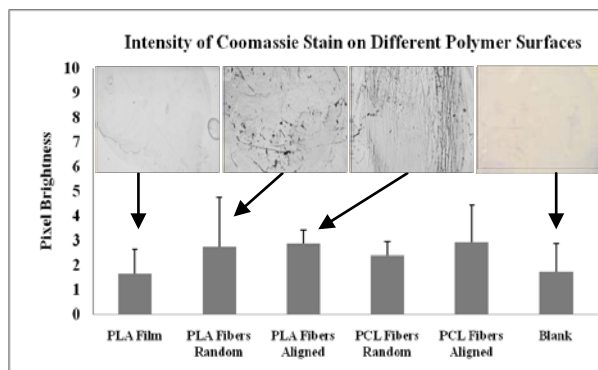


Figure 2. Protein adsorption on different polymer surfaces (n=3). Evaluated using Image J software; where 10=black, 1=white.

Low density of aligned nanofibers does not change much wettability when compared to blank coverslips as shown in Fig 1. However; nanofibres encourage qualitatively greater protein adsorption than films and blank coverslips (Fig 2).

DISCUSSION & CONCLUSIONS:

Aligned topography and high surface area to volume ratio of nanofibers can influence greater protein adsorption despite having similar wettability to blank coverslips. Thus greater protein deposition is expressed on fiber surfaces compared to films and blanks and so are preferable for cell attachment in tissue engineering applications.

REFERENCES:

- ¹ S. Heydarkhan-Hagvall et al (2008). Three-dimensional electrospun ECM-based hybrid scaffolds for cardiovascular tissue engineering *Biomaterials* **29**: 2907-2914.
- ² Laurencin C. et al (2005) *Biomaterials* **26**: 7530-36.

ACKNOWLEDGEMENTS: I. Wimpenny & M. Ahearne

DESIGN OF NANOPARTICLES RESPONSIVE TO INFLAMMATORY STIMULI AND THEIR USE IN TRANSDERMAL

J. Laliturai¹ & N Tirelli²

Laboratory of Polymers and Biomaterials, School of Pharmacy and Pharmaceutical Sciences, University of Manchester. ^{1,2}

INTRODUCTION: In recent years, nanoparticles have been widely researched for applications in pharmaceuticals, computing technologies, textiles, agriculture, etc. The nanoparticles investigated in the present study are based on poly(propylene sulfide) (PPS). This polymer is sensitive to oxidation; it is known that inflammatory cells use a number of approaches to destroy their target and oxidative species (e.g. reactive oxygen species) are one of these weapons. The oxidation of PPS turns it into the more hydrophilic poly(propylene sulfoxide); therefore, an anti-inflammatory drug encapsulated in PPS can be released in response to the presence of inflammation-borne oxidants. A fundamental problem to overcome with nanocarriers is that their recognition as foreign objects, which leads them to be rapidly internalized and destroyed by immune cells such as macrophages, neutrophils, etc. To overcome this obstacle, poly(ethylene glycol)-containing polymers are employed to coat colloidal objects and hide them from sentinel cells ("stealth" character).

METHODS: To study the uptake of nanoparticles, the fluorescently labeled PPS nanoparticles concentrations of 0.5, 1, 2, and 4 mg/ml were incubated for 30 mins, 2, 4, and 24 hrs with non-activated and activated macrophage J774.2 in a 96 well plate. For the activated condition, cells were incubated with 500 ng/ml of lipopolysaccharide for 24 h before being tested. The fluorescence intensity after lysing the cells was measured to calculate the amount of nanoparticles that were taken up by macrophages with a 96-well plate reader. After measuring nanoparticles uptake, lysed cell were used in order to analyze the protein content of cells in each well.

To study the mechanism of the uptake, cells were pretreated with inhibitors to inhibit each mechanism of endocytosis for 30 min. Then cells were incubated with 4 mg/ml of PPS nanoparticles in the presence of an inhibitor for 2 h. The uptake of nanoparticles and the protein content were also measured to calculate the ratio of the uptake of the inhibitor to the control.

RESULTS:

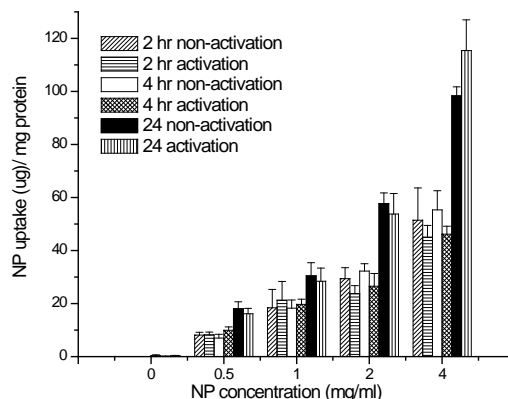


Fig. 1: The amount of PPS nanoparticles uptake by non-activated and activated macrophage J774.2 in various incubation periods.

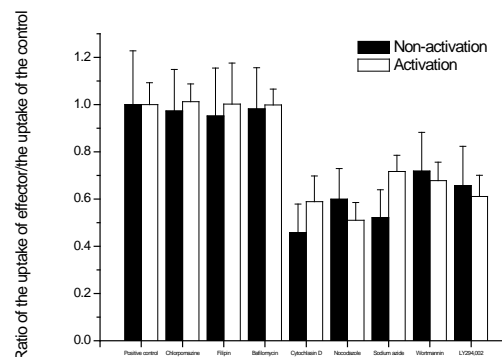


Fig. 2: The ratios of the uptake with the inhibitor to the uptake of the control by non-activated and activated macrophage J774.2

DISCUSSION & CONCLUSIONS: The nanoparticles were internalized very slowly and in very small amounts by both activated and non-activated cells, and the uptake was proven to follow an endocytic mechanism prevalently based on macropinocytosis. This finding suggests that the nanoparticles have a generally "stealth" behaviour and their internalization in cells follows a simple uptake of the extracellular fluid phase.

The behavior of PPS nanoparticles in the presence of neutrophils, that are capable of generating large amounts of extracellular oxidative species, will be studied to prove the possibility of extracellular oxidation of PPS nanoparticles.

pH-Responsive Microgel Dispersions: from Restoring Intervertebral Disc Height to Microgel Design for Soft-Tissue Repair

Sarah Lally¹, Tony J. Freemont² and Brian R. Saunders¹

1. Biomaterials Research Group, School of Materials, University of Manchester, Manchester, UK.
2. Tissue Injury and Repair Group, School of Medicine, University of Manchester, Manchester, UK.

INTRODUCTION: At least 40% of lower back pain is attributed to intervertebral disc (IVD) degeneration. This is where the gel-like nucleus pulposus begins to dehydrate causing pores cracks to form, compressing the vertebrae.

In this work, we have looked at using microgels which are crosslinked polymer particles with the ability to swell when their pH gets close to the pKa. The microgel can be injected into the IVD as a fluid and will swell to form a gel in situ, forming a similar form of support as the original tissue.

METHODS: The microgels were synthesised using emulsion polymerisation. They were polymerised using different monomers in different ratios, so that it is possible to compare and predict the characteristics of the microgel dependant on its constituents.

The microgels are then characterised in a number of ways, firstly looking at the particles size at increasing pH. This can give us an indication of the pH at fluid-gel transition point. This is further backed up with gel phase diagrams where the points at which the fluid becomes a gel; at what pH and what concentration of microgel particles (Fig. 1). Furthermore, these gels are tested using rheology to ascertain their biomechanical strength, which allows us to see that the gels are appropriate for the application.

RESULTS: The monomers can make a big difference to the characteristics of the polymers. The amount of the acidic monomer can change the degree by which the microgel swells, with a higher concentration causing the particles to swell more. It also alters the pKa of the system, which enables us to move the fluid-gel point dependant on the composition.

The glass transition temperatures and molecule flexibility also have an effect on the swelling, pKa and biomechanical strength of the gels. More flexible structural molecules show higher degrees of swelling, showing the particles opening up more. The less flexible molecules are unable to swell as much, and also show higher mechanical moduli than those that are more flexible.

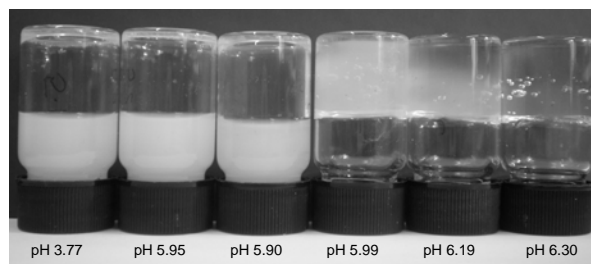


Fig. 1: Image of poly(BMA/MAA/BDDA) gel phase diagram, all 10 wt% and increasing pH. It is possible to see that the particles are not fully swollen until pH 6.3, where the gel becomes clear.

DISCUSSION & CONCLUSIONS: It has been possible for us to compare the different compositions of monomers in order to understand this system. It is possible to draw conclusions and alter the compositions dependant on the outcome that would be optimal for the patient. Whether the system requires a low pKa due to particularly degenerated tissue, or a high modulus due to the biomechanical strain on the IVD, it could be possible to have variations on the microgel composition for different degrees of degeneration. With further cell related research, it will be possible to see whether it is a viable idea for a medical device.

REFERENCES: Saunders, J.M., Tong, T., LeMaitre, C.L., Freemont, T.J., Saunders, B.R., *Soft Matter* (2007) 3: 486-494, Lally, S., MacKenzie, P., LeMaitre C.L., Freemont, T.J., Saunders, B.R., *Journal of Colloid and Interface Science*, (2007), 316: 367-375, Lally, S., Bird, R., Freemont, T. J., Saunders, B. R., *Colloid Polym Sci*, 2009, 287: 335-343

ACKNOWLEDGEMENTS: The University of Manchester School of Enterprise department for funding, and also the EPSRC through the School of Medicine.

Biomechanical Testing of Low-Concentration SDS Decellularised Porcine Pulmonary Valves

J Luo, John Fisher, Zhongmin Jin, Eileen Ingham, Sotirios Korossis

Institute of Medical and Biological Engineering, University of Leeds, Leeds, UK

INTRODUCTION: A decellularisation treatment method incorporating low-concentration SDS was developed for producing acellular pulmonary valve conduits. The aims of this study were to assess the effectiveness of the protocol and to investigate the biomechanics of the acellular scaffold.

METHODS: Porcine pulmonary roots (n=6) were disinfected using an antibiotic wash solution, and the pulmonary artery walls were peeled of an outer layer. The conduits were then washed sequentially in: hypotonic Tris buffer (HTB; 10mM Tris pH 8.0, 0.1% (v/v) EDTA, 10KIU aprotinin); 0.1% (v/v) SDS in HTB, DNase and RNase solutions, and PBS. Following treatment, the valves were sterilized using 0.1% (v/v) peracetic acid¹.

Histological stains, including H&E, Hoechst and Miller's elastin, were used to assess the effectiveness of the decellularisation method.

Uniaxial tensile tests to failure² were used to compare the tensile properties of fresh (FL) and decellularized leaflets (DL; n=6~9) and pulmonary artery walls (FW; DW n=6) in the circumferential [C] and radial [R] directions for the leaflets, and the circumferential [C] and axial [A] directions for the pulmonary artery wall.

RESULTS: Histology confirmed that the decellularisation was complete and the pulmonary root histoarchitecture was well retained. The biomechanical tensile properties of the fresh and treated samples are presented in Table 1 and Table 2 (* P<0.05 ANOVA). There were no significant differences in the biomechanical parameters between treated and native valvular tissues, with the exception of the leaflet failure stress in the radial direction and the wall failure stress in the circumferential direction.

Table 1. Biomechanical properties at the transition point of fresh and decellularised pulmonary leaflets and artery wall

	Transition stress (MPa)	Transition strain (%)
--	----------------------------	--------------------------

FL[C]	0.72±0.25	16.1±5.1
DL[C]	1.11±0.33	17.3±2.8
FL[R]	0.20±0.06	15.1±6.1
DL[R]	0.14±0.04	16.1±3.7
FW[C]	0.18±0.04	120.8±8.5
DW[C]	0.16±0.03	109.0±8.1
FW[A]	0.12±0.01	96.5±13.1
DW[A]	0.13±0.03	92.8±13.7

Table 2. Biomechanical properties at the failure point of fresh and decellularised pulmonary leaflets and artery wall

	Failure stress (MPa)	Failure strain (%)
FL[C]	7.3±0.8	59±11.6
DL[C]	9.9±2.3	44±4.1
FL[R]	1.8±0.4	66±15.4
DL[R]	0.8±0.2*	56±9.0
FW[C]	1.1±0.3	195±13.1
DW[C]	0.7±0.1*	188±18.3
FW[A]	0.6±0.1	156±18.5
DW[A]	0.6±0.1	167±14.6

DISCUSSION & CONCLUSIONS: Successful decellularisation of porcine pulmonary roots was achieved using low concentration SDS. Although significant differences were observed between the treated and native tissues in terms of the biomechanical properties in the extra-physiological stress range, the acellular valvular scaffolds have the potential to be used, either seeded or non-seeded with cells, as valve replacements in the pulmonary position.

REFERENCES: ¹ C. Booth, S.A. Korossis, H.E. Wilcox, K.G. Watterson, J.N. Kearney, J. Fisher, E. Ingham (2002) *The Journal of Heart Valve Disease* **11**: 457-462. ² S.A. Korossis, C. Booth, H.E. Wilcox, K.G. Watterson, J.N. Kearney, J. Fisher, E. Ingham (2002) *The Journal of Heart Valve Disease* **11**: 463-371.

ACKNOWLEDGEMENTS: This work was funded by the Engineering and Physical Sciences Research Council (EPSRC).

Type II collagen Expression in Tendon: a new look at tendon development and repair

Marissa L. Maciej, Gareth D. Hyde, Raymond P. Boot-Handford, Gillian A. Wallis and Karl E. Kadler
Wellcome Trust Centre for Cell-Matrix Research, Faculty of Life Sciences, University of Manchester, Oxford Road, Manchester M13 9PT UK

INTRODUCTION: More than 32 million traumatic and repetitive motion injuries to tendons and ligament occur annually in the USA¹. No treatment exists for repetitive motion injuries whilst surgery is the best option for reconnecting torn tissue. However, the injury site is permanently weakened leaving patients with impaired function and long-term physiotherapy needs. The slow rate of healing and poor outcome is partly explained by the paucity of cells in tendons and ligaments and to the inability of adult cells to re-establish the rich extracellular matrix (ECM) of the tissues. There is an urgent need to understand tendon development as a prerequisite to devising new therapies to promote tendon regeneration.

We provide evidence here that tendons and cartilage have a common embryological origin and that mesenchymal precursor cells expressing the *col2a1* gene (which encodes type II collagen) form the cellular origin for tendon. Q-PCR, Western blot analysis and mass spectrometry (not shown here) show that adult tendon contains type II collagen. A full understanding of the function of type II collagen in tendon, perhaps in stabilising a stem-progenitor niche, might lead to new therapeutic opportunities for the treatment of tendon and ligament injuries.

METHODS: Semi-quantitative RT-PCR, mass spectrometry and Western Blotting techniques were used to investigate the presence of type II collagen in tendon. Histology, Xgal staining, sectioning and paraffin wax embedding was performed on the *Col2a1LacZROSA26* lineage tracer mouse.

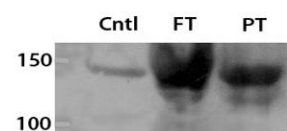
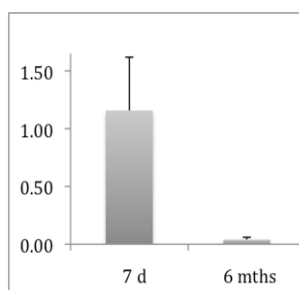


Fig 1: Collagen II is present in tendon.

(L) q-PCR expression of *Col2a1* in 7 day and

6 month-old tendon. (R) Western blot showing collagen II protein in flexor (FT) and patellar (PT) tendons. Control shows xiphoid cartilage.

RESULTS: qPCR showed that *col2a1* was expressed in 1-week-old and 6-month-old mouse

flexor tendon. Western blotting and mass spectrometry (not shown) confirmed the presence of type II collagen protein. Xgal-stained sections from the hindlimb of *Col2a1LacZROSA26* 7 day old mice showed the presence of LacZ-positive cells throughout the tendon, which showed that the majority of the cells had expressed *col2a1* during embryonic development.

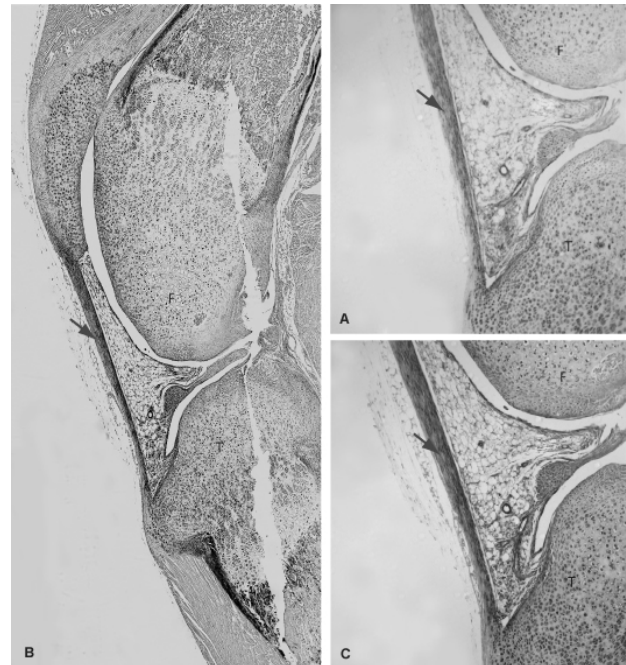


Fig 2: Postnatal patellar tendon (red arrow) contains cells that had expressed *Col2a1*. F, femur; T, Tibia. (A) Xgal stained cells (blue) indicates *Col2a1* expression. (B,C) Xgal and H&E stained.

CONCLUSIONS: Future work will isolate tendon stem-precursor cells for studies of *col2a1* expression and tendon induction. Characterisation of the genes expressed during tendon development may lead to the production of novel treatments for tendon injury.

REFERENCE: Schoen, D. C. (2005) Injuries of the wrist. *Orthop. Nurs.* 24: 304-307

ACKNOWLEDGEMENTS: The authors would like to thank Dr. S. Taylor and Ms. C-Y. C. Yeung for help and guidance during this project.

Creating a tissue engineered autologous prosthesis for use in stress urinary incontinence (SUI) and pelvic organ prolapse (POP) repair

A Mangera¹, AJ Bullock², CR Chapple¹ & S MacNeil²

¹ Sheffield teaching Hospitals NHS trust, Sheffield. ² Kroto Research Institute, University of Sheffield, Sheffield.

INTRODUCTION: SUI and POP affect almost 40% of women causing significant disturbance in quality of life. Decline in collagen is postulated to have aetiological significance. A woman has an 11% chance of requiring surgery for these conditions by the age of 80. A range of synthetic and biological substitutes have been used to improve results of surgical repair, but none have been found to be ideal. Synthetic materials cause a foreign body reaction and lead to risk of erosion whereas biological materials are often resorbed leading to failure. We propose the use of tissue engineering to overcome the problems seen with current prostheses.

METHODS: We isolated and cultured fibroblasts obtained from buccal mucosal biopsies. 1.3 million fibroblasts were attached to 2.5cm² of an electrospun fabric of Poly(L)lactic co-glycolic acid (PLGA) polymer and cultured for two weeks in 10%DMEM medium.

Using AlamarBlue (a vital stain) & DAPI (a nuclear stain) we observed cell attachment to the PLGA polymer. We assessed the effect of fibroblast addition on polymer contraction using serial photographs over 2 weeks. We also assessed the biomechanical properties of the tissue engineered prostheses (TEP) involving ultimate tensile strength, strain & Young's modulus of elasticity using a Bose electroforce instrument. Finally we assessed the amount of collagen produced by our TEP using Sirius red staining.

RESULTS: We have produced TEP with good cellular attachment (AlamarBlue & DAPI). The addition of fibroblasts to the PLGA polymer led to contraction of up to 50%. The cells in these prostheses have the intrinsic ability to produce collagen as shown by Sirius red staining (Figure 1). The ultimate tensile strength, strain and Young's modulus of the TEP are currently less than the ideal identified for paravaginal tissue [1] (Table 1).

Fig. 1: Collagen staining on scaffolds at 14 days culture, (n=9 ±SEM)

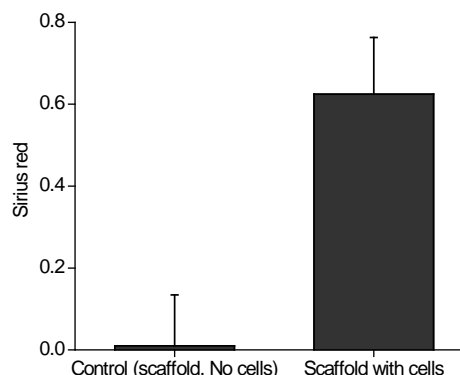


Table 1. Mechanical properties of TEP

Mechanical Properties (±SEM)	TEP	Ideal for paravaginal tissue [1]
Ultimate tensile strength (MPa)	0.22±0.03	0.42-0.79
Ultimate strain	0.13±0.02	0.37-0.68
Young's Modulus/ Elasticity (MPa)	3.23±0.69	6.65-10.26

DISCUSSION & CONCLUSIONS: We have developed a prosthesis which allows ingrowth of cells and has the ability to contract and intrinsically produce collagen. We suggest these prostheses will stimulate fibrosis in vivo & therefore reinforce already weakened tissues. Current work is now focused on developing prostheses with better mechanical properties.

REFERENCES: ¹Lei L, Song Y, Chen R. Biomechanical properties of prolapsed vaginal tissue in pre- and postmenopausal women. Int Urogynecol J Pelvic Floor Dysfunct 2007; 18:603-607.

ACKNOWLEDGEMENTS: Research grants were awarded by the Urology Foundation and Robert Luff Foundation

DEVELOPMENT OF AN IN VITRO CO-CULTURE MODEL TO INVESTIGATE PERIPHERAL MYELIN FORMATION WITH HUMAN MESENCHYMAL STEM CELL

C. Mantovani¹, D. Mahay¹, M. Brohlin², M. Wiberg², S. Shawcross¹ & G. Terenghi¹

¹Blond McIndoe Research Laboratories, University of Manchester, UK, ²Department of Surgical & Perioperative Science, University Hospital, Umea, Sweden

INTRODUCTION: Peripheral nervous system myelin is formed by Schwann cells (SC), and wraps around one axon by a dynamic process of extensions and spiralling of the SC plasma membranes. In this study we have used an *in vitro* model for myelin formation involving glia-neuronal interactions, using human adult dMSC and dissociated adult dorsal root ganglia neurons in co-culture to obtain the myelination of growing neurites.

METHODS: Co-culture with neuronal cells was also carried out with human adipose mesenchymal stem cells (ASC) differentiated into SC-like cells. The cells were co-cultured in the presence of NGF, BDNF and ascorbate for 14 days. Semi-quantitative RT-PCR and Western Blotting techniques were used to investigate the presence of the myelin proteins that establish myelination.

RESULTS: The gene transcripts and protein expression for protein zero (P0), peripheral myelin protein-22 (PMP-22), myelin basic protein (MBP) and myelin-associated glycoprotein (MAG), were detected following the co-culture of both differentiated stem cells types with the dissociated neurons, but not in the control cultures of differentiated human MSC and ASC or DRG cultured alone.

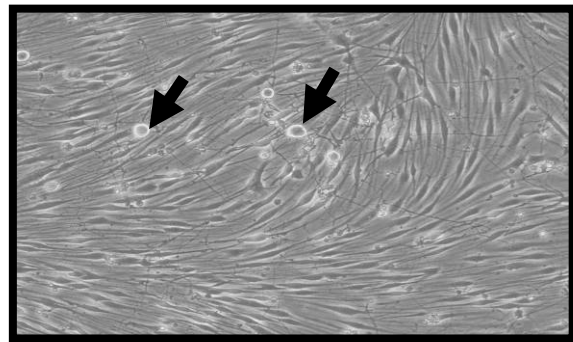


Fig 1: DRG/dMSC and DRG/dASC were grown in direct contact for 2 weeks using a medium composed of 50% (v/v) BS medium and 50% (v/v) α -MEM differentiation medium plus neurotrophic factor and ascorbate to stimulate myelin formation (arrow neuronal cells).

DISCUSSION & CONCLUSIONS: The results suggest myelination is established *in vitro* when the two cells are in contact under these conditions. This co-culture strategy will be a useful tool to investigate the myelination and de-myelination phenomenon for both glia and stem cells under controlled micro-environmental conditions.

REFERENCES: D. Mahay, G. Terenghi, Shawcross S.G.(2008) *Exp Cell Res.* 314:2692-701. P.J. Kingham, D.F. Kalbermatten, D. Mahay et al (2007) *Exp Neurol.* 207:267-74.

ACKNOWLEDGEMENTS: The authors would like to thank Acorda Therapeutics (USA) for the generous supply of GGF-2 for the continuation of this work. This work was supported by the Rosetrees Trust.

Characterisation of Schwann Cells and Stem Cells Of Different Age Origins

J Marshall, MC Mantovani, MS Haneef, G Terenghi and SG Shawcross

Blond McIndoe Research Laboratories, University of Manchester, Manchester UK

INTRODUCTION: Annually, 300,000 peripheral nerve injuries occur in Europe alone¹. This results in a large socio-economic burden. Current surgical methods for repair of peripheral nerve axotomy-type injuries are autologous nerve graft or microsurgical joining of the severed nerve fibres. Both of these treatments are far from ideal due to donor site morbidity and low success rates². A fundamental part of being able to successfully and productively treat peripheral nerve injuries would involve understanding how nerve regeneration is affected by age. In addition, if stem cell-based therapies are to be applied to nerve repair then it would be useful to know if donor age affects the differentiation capacity and function of the stem cells. Bone marrow-derived mesenchymal stem cells (MSCs) are an easily accessible source of stem cells and thus candidates for use in nerve repair.

METHODS: Schwann cells (SCs) from the sciatic nerves and MSCs were harvested from neonatal, young and aged adult Wistar rats. The MSCs were differentiated along osteogenic, adipogenic, chondrogenic and SC-like (dMSCs) lineages. To compare the uMSCs, dMSCs and SCs from the three age groups, their proliferation rates were measured using an alamar blue assay. The SCs, uMSCs and dMSCs from the three age groups were co-cultured with dorsal root ganglia neurons (DRG) in a non-contact culture system³ to investigate the secretion of Nerve Growth Factor (NGF) and Brain-derived Neurotrophic Factor (BDNF) and their effects on DRG neurite outgrowth; the secreted growth factors were quantified using an ELISA method.

RESULTS: The three different ages of uMSCs were able to successfully differentiate into adipogenic, osteogenic, chondrogenic and SC-like lineages (Figure 1). The proliferation rates of the three different aged uMSCs showed no significant difference.

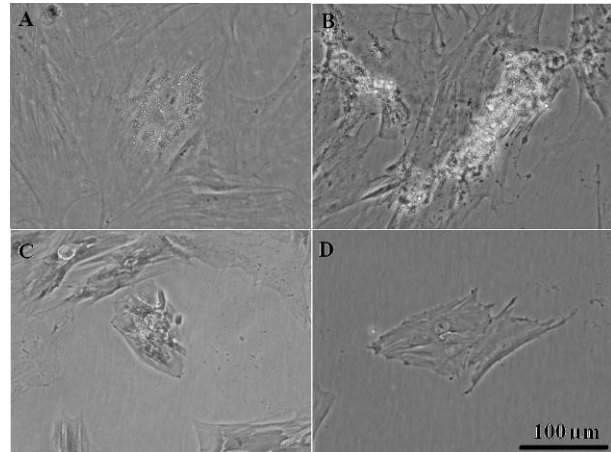


Fig 1: Differentiated (Young) MSCs A– adipogenic (oil red O) B– osteogenic (alizarin red) C– chondrogenic (toluidin blue) D– undifferentiated.

CONCLUSIONS: The differences between the various age lineages of MSCs is very difficult to assess. All three different ages were able to successfully differentiate into osteogenic, adipogenic, chondrogenic and SC-like lineages within the same period of time. However, the percentage of differentiation is difficult to accurately calculate. The proliferation rates assessed using alamar blue also showed no difference between the three different ages of uMSCs.

REFERENCES: 1. Belkas J.S, Shoichet M.S and Midha R (2004) Operative Techniques in Orthopaedics **14**(3) 190-198. 2. Parabi A., Yang S.Y., Seifalian M. *et al.* (2010) Plastic Reconstructive and Aesthetic Surgery **XX**. 3. Caddick J., Kingham P.J, Gardiner N.J *et al.* (2006) *Glia* **54**(8) 840-849.

ACKNOWLEDGEMENTS: The authors would like to thank Acorda Therapeutics (USA) for the generous supply of GGF-2 for the continuation of this work and Prof. Stefano Geuna and Dr Stefania Raimondo, University of Turin, Italy, for the supply of aged Wistar rat cells.

Culture and delivery of autologous keratinocytes on microcarriers for cutaneous repair

M Eldardiri¹, Y Martin¹ & J Sharpe¹

¹ *Blond McIndoe Research Foundation, Queen Victoria Hospital, East Grinstead, West Sussex.*

INTRODUCTION: Burns and scalds are common and often devastating forms of trauma and continue to present a significant clinical problem. Sprayed autologous keratinocytes (AK) are well established as a therapy for treating such injuries. Microcarriers have been developed for the culture and delivery of AK cells and may allow cells to be more rapidly delivered to the wound bed without the use of proteolytic enzymes or murine feeder cells (1). We have investigated growing AK cells on microcarriers *in vitro* with the aim to optimise growth conditions and cell delivery and performed an *in vivo* study to examine transplanted cell fate and the quality of wound repair in a pig model.

METHODS: Human AK were grown on microcarriers, SphereCol (collagen, Advanced BioMatrix) and CultiSpher G (gelatin, Percell Biolytica), in a stirred bioreactor to examine the effect of culture conditions on cell proliferation and differentiation (1). In a separate *in vivo* study, twelve full thickness wounds were created in two large white pigs and isolated from the surrounding epidermis by PTFE chambers. Wounds were treated with green fluorescent protein (GFP)-labeled AK cultured on CultiSpher G microcarriers and compared with sprayed AK alone, microcarriers only and untreated wounds.

RESULTS: AK proliferated well on microcarriers in a range of conditions. To date AK have predominantly been grown on microcarriers after initial expansion. However our results showed that primary isolated cells can also be cultured on gelatin and collagen beads (Fig 1).

Histological analysis of the wounds showed a thin layer of flattened cells with an epithelial-like morphology on the surface of the wounds treated with AK + microcarriers and AK alone after 14 days. Immuno-staining against cytokeratin 14 (K14) indicated a greater quantity of cells exhibiting an epithelial phenotype in wounds treated with AK + microcarriers (Fig 2, A and B) when compared with control wounds. The surface of these wounds was similar in appearance to AK alone. GFP was detected in wounds treated with AK + microcarriers and AK alone (Fig 2, C).

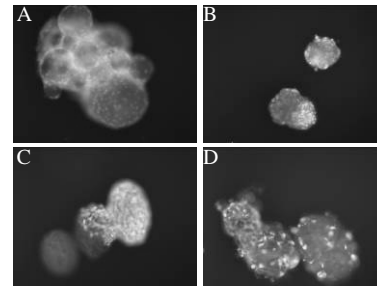


Fig. 1: Acridine Orange stain shows cells growing on microcarriers, SphereCol with (A) AK (B) AK with irradiated 3T3 and on CultiSpher G with (C) AK (D) AK with irradiated 3T3

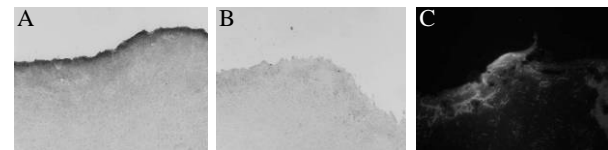


Fig. 2 K14 staining showing an increase in the formation of a 'neo-epidermal' layer after 14 days following treatment with (A) AK + microcarriers when compared with (B) control wounds. (C) Expression of GFP indicates the presence of transplanted AK in wounds treated with AK + microcarriers (shown) and AK alone.

DISCUSSION & CONCLUSIONS: Our findings demonstrate the potential for using microcarriers to culture keratinocytes for the clinical treatment of skin loss. Optimised culture conditions may allow cells to be expanded upon primary isolation from skin biopsies, reducing the risk of contamination through handling. The use of this technique could reduce costs, culture time and improve the quality of wound healing.

REFERENCES: (1) Borg DJ, et al. (2009) *J Biomed Mater Res A*; 88(1):184-194.

ACKNOWLEDGEMENTS: This work was supported by Sparks and the Charles Wolfson Foundation.

Investigating the Role of Collagen in the Biomechanical Behaviour of Peripheral Nerves.

S.Mason^{1,2} & J.B.Phillips¹

¹Department of Life Sciences, ²Department of Physics and Astronomy, The Open University, Milton Keynes, MK7 6AA, UK

INTRODUCTION: Restoration of the tensile properties of nerves, in particular their ability to bend and stretch during limb movement, is an important consideration in the design of tissue engineered repair conduits and other repair approaches. An understanding of the mechanical architecture of peripheral nerves is therefore desirable. Previous research has identified that the stiffness of rat peripheral nerves varies longitudinally according to where they traverse joints¹. This study examines collagen fibril diameter and fibril number in specific regions of rat median and sciatic nerve.

METHODS: Joint and non-joint regions of median and sciatic nerves were resected *post mortem* from 250-350g rats. These samples were maintained at their *in situ* tension and fixed and stained for transmission electron microscopy. Ultrathin sections were prepared and stained with uranyl acetate and Reynolds lead citrate. Collagen fibril diameter and number of fibrils per 580x380 nm region of interest (ROI) in the epineurium and the endoneurium (*Fig 1*) were measured using ImageJ, and joint and non joint regions of each nerve compared.

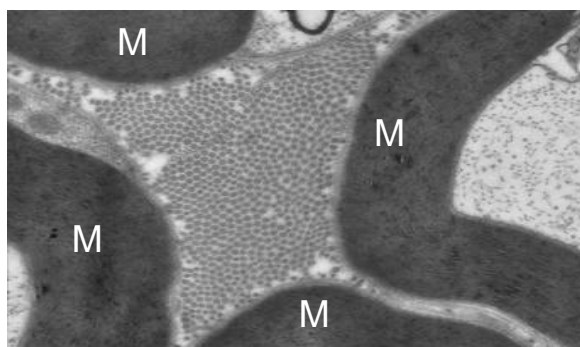


Fig 1: Collagen fibrils in the endoneurium of rat median nerve. (M = myelin sheath)

RESULTS: In the median nerve, mean collagen fibril diameter was significantly smaller in the joint region compared to the non joint region (*Table 1*). Number of fibrils per region of interest was significantly greater in the joint than the non joint regions in the endoneurium and epineurium of the median nerve (*Table 1*). These trends were not observed in the sciatic nerve.

Region	Mean fibril diameter (nm)	Mean number of fibrils per ROI
Endoneurium		
Joint	42.1 ± 2.86 *	59.2 ± 3.24 *
Non Joint	47.1 ± 2.87	48.0 ± 1.18
Epineurium		
Joint	66.1 ± 5.74 *	32.6 ± 2.97 *
Non Joint	77.9 ± 6.61	24.6 ± 1.86

Table 1: Collagen fibril diameter and fibril number in the median nerve. Mean collagen fibril diameter was significantly smaller and fibril number significantly greater in the epineurium and endoneurium in the joint regions of the median nerve. Data are means ± S.E.M, from at least 5 nerves, $p < 0.05$ (paired *t* test).

DISCUSSION & CONCLUSIONS: Collagen plays an important role in tissue biomechanics, and studies in tendons report smaller collagen fibril diameters at sites which are compressed during movement^{2,3}. In this study, collagen fibrils in the epineurium and endoneurium of rat nerves exhibited a range of diameters, the distribution of which varied between joint and non joint regions in the median nerve. Although fibrils were smaller in the joint area compared to the non joint, they were greater in number, which may suggest that localised variation in nerve stiffness may be due to differences in the size and number of collagen fibrils per unit cross sectional area, rather than the total amount of collagen present.

REFERENCES: ¹Phillips JB, Smit X, De Zoysa N, Afoke A, Brown RA (2004). *J. Physiol*, 557 (3): 879-87.

²Lavagnino M, Arnoczky SP, Frank K, Tian T (2005) *J Biomech*, 38(1):69-75

³Parry DAD, Barnes GRG, Craig AS (1978). *Proc R Soc Lond*, 203, 305-321

ACKNOWLEDGEMENTS: With thanks to F.M Colyer, H.A. Davies, S.Walters, K.A.Evans and A.K.Stramek.

Nanotopography as a Means to Control Skeletal Stem Cell Differentiation

RJ McMurray¹, N Gadegaard², ROC Oreffo & MJ Dalby¹

¹ Centre for Cell Engineering, Joseph Black Building, University of Glasgow G12 8QQ

² Dept of Electronic and Electrical Engineering, Rankine Building, University of Glasgow G12 8QQ

³ Bone and Joint Research Group, University of Southampton, Southampton, SO16 6YD, UK

INTRODUCTION: Skeletal stem cells (SSCs) derived from the bone marrow are known to be multipotent, and under the right conditions have been shown to differentiate down several cell lineages to form tissues such as bone, fat and cartilage. The ability to control how and when SSCs differentiate using nanotopography holds great potential not only for producing in vitro substrates capable of directing stem cell differentiation without the need for chemical supplements whilst also allowing for cell expansion but could also be used in vivo, e.g. patterning of hip implants to produce a more osseointegrative substrate. In the current study, osteogenic differentiation was examined following culture of skeletal stem cells on substrates with controlled disordered nanopits; for the first time this was done over a time-course study.

METHODS: Primary human skeletal stem cells enriched for STRO-1 were used at passages 1-2. Throughout the cells were maintained in basal medium (10% FBS/ α MEM, Life Technologies) at 37°C with 5% CO₂ in humid conditions. Cells were cultured for 7, 14, 21 and 28 days. At each time point STRO-1 and ALCAM antibodies were used to detect the stem cell phenotype, combined with osteopontin and osteocalcin, both bone cell markers to indicate progression from a stem cell down an osteogenic lineage. Silicon shims were used to emboss the disordered nanopits (100 nm deep, 120 nm diameter, and 300 nm pitch \pm 50 nm disorder) into polycaprolactone (PCL). Planar PCL was used as a negative control while planar PCL combined with osteogenic medium to induce osteogenic differentiation was used as a positive control. No osteogenic supplements were used in combination with the nanotopography.

RESULTS: By using a combination of skeletal stem cell markers in conjunction with bone cell markers over successive time points it was possible to assess the effect of the disordered nanopit topography on the osteogenic differentiation of SSCs over time when compared to those cultured on positive and negative controls. Results showed that SSCs cultured on the disordered nanopit

topography underwent osteogenic differentiation without the need for any osteogenic supplements.

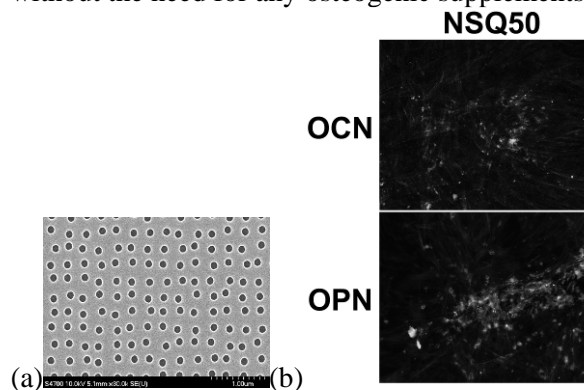


Fig 1. (a) SEM image of NSQ50 topography, (b) OCN and OPN immunofluorescent staining of skeletal stem cells after 28 days of culture on NSQ50 nanopit substrate in the absence of osteogenic media. Red=actin, Blue=nucleus, Green=OCN/OPN.

DISCUSSION & CONCLUSIONS: The results presented here show the first temporal profile of skeletal stem cell differentiation when cultured on nanopit substrates and provide further evidence that nanotopography alone may offer a valuable new approach for stimulating the osteogenic differentiation of skeletal stem cells over that of defined media.¹

REFERENCES: ¹ Dalby M.J., Gadegaard N., Tare R., Andar A., Riehle M.O., Herzyk P., Wilkinson C.D.W., Oreffo R.O.C. The Control of Mesenchymal Stem Cell Differentiation Using Nanoscale Symmetry and Disorder. (2007) *Nature Mat.*

ACKNOWLEDGEMENTS: RJM is funded by a Lord Kelvin/Adam Smith Scholarship. MJD, ROCO and NG are funded by the BBSRC, EPSRC and EU. We also thank Dr Rahul Tare for providing the skeletal stem cells.

Mechanical and Biochemical Contributions to Topography-Induced Mechanotransduction

LE McNamara^{1,2*}, R Burchmore², MO Riehle¹, and MJ Dalby¹

¹ Centre for Cell Engineering, Faculty of Biomedical and Life Sciences, University of Glasgow, UK

² Sir Henry Wellcome Functional Genomics Facility, Faculty of Biomedical and Life Sciences, University of Glasgow, UK.

INTRODUCTION: Mechanotransduction is the process by which cells respond to mechanical stimuli (e.g. stretching, surface topography) via signalling cascades or tensile forces from the cytoskeleton acting on the nucleus. This results in downstream gene- and protein-level changes that mediate the overall cellular response to the mechanostimulus. Appropriate mechanosignalling is also crucial for tissue development and function. Topographic substrata, such as microgrooves, are valuable non-invasive tools to investigate mechanotransduction, and increase knowledge of cell-material interactions.

METHODS: RNA and protein was extracted from human fibroblasts cultured for 24h on quartz microgrooved substrates (2.5 μm depth x 25 μm pitch) or planar controls, for microarray and proteomic studies. Fluorescence 2D-Difference Gel Electrophoresis (DiGE, discussed in [1]) was used to examine differential protein abundance. Functional interactions between differentially abundant transcripts and proteins were analysed by Ingenuity Pathways Analysis (IPA). Chromosome territories were examined with Fluorescence *In situ* Hybridisation (FISH), and cellular architecture was visualised using 3D confocal microscopy.

RESULTS: IPA analysis highlighted transcript-level changes in the abundance of components of important canonical pathways, including ERK/MAPK and actin-related signalling, and permitted the integration of transcriptomic and proteomic data. In addition to altered levels of particular proteins and protein-coding transcripts, many small RNAs (including small nucleolar RNAs and a microRNA) were differentially abundant. Such untranslated small RNAs are functional effectors, with roles in RNA editing, or modulation of mRNA translation. Nuclear and chromosomal organisation was altered on the topography. Lamin B tubule-like structures (Fig. 1), with a probable role in nucleocytoplasmic transport, were rearranged or dramatically reduced in frequency in cells on the topography, concordant with effects on nucleolar morphology. FISH results suggest that chromosomal repositioning contributed to direct

mechanotransduction, apparently on a continuum with chromosome size.

This was corroborated by a disparity in spatial arrangement of the differentially expressed genes across a small (Ch19) and large (Ch1) chromosome.

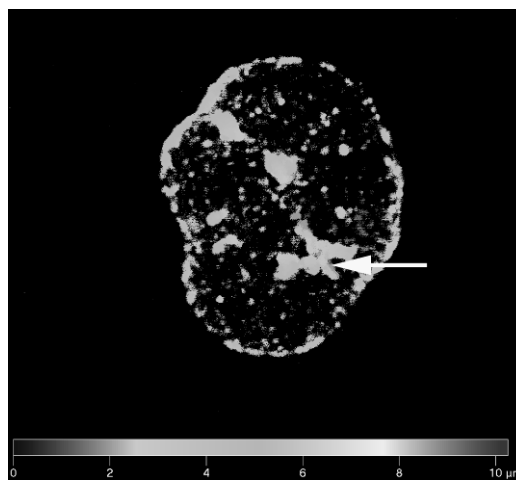


Fig. 1: Depth-coded image of a 3D reconstructed lamin B-immunostained nucleus, showing a transnuclear tubule traversing the nucleus (arrow).

DISCUSSION & CONCLUSIONS: These results illustrate the involvement of direct mechanical effects and biochemical signalling pathways in topography-induced mechanotransduction. Modulated levels of protein and small RNA direct effectors are suggestive of the induction of rapid-response mechanisms downstream of the mechanostimulus. This research should increase our knowledge of mechanotransduction, and thus stimulate rational advancements in development of future biomaterials tailored to the direction of favourable cell responses.

REFERENCES: ¹ L.E. McNamara *et al.* (2010) *J. R. Soc. Interface*, **7**:S107-118.

ACKNOWLEDGEMENTS: LEM was funded by BBSRC DTG BB/D526329/1. The authors thank Ms. F. Kantawong, Dr. K. Jayawardena, Dr. N. Klauke, Ms. S. McFarlane, Ms. J. Wang, Dr. P. Herzyk, and all in CCE, SHWFGF and MBSU for their assistance and helpful discussion.

Development Of An *Ex Vivo* Intervertebral Disc Model System To Test Novel Cell Based Tissue Engineering Therapies

E.A.Mitchell¹, A.M. White¹, S.Richardson¹, J.A.Hoyland¹

¹ School of Biomedicine, University of Manchester, Manchester, England.

INTRODUCTION: Currently there is a substantial amount of interest in developing novel cell based / tissue engineering therapies for intervertebral disc (IVD) degeneration¹. Such therapies need to be tested *in vitro* or *in vivo* before translation to clinic. However, current animal models do not accurately mimic the human IVD or disease pathophysiology and thus a more appropriate model system for efficacy testing is required. We have previously described a unique bioreactor which can mimic the load and humoral environment of the human IVD and shown that IVD explants can be maintained in this system for 2 weeks with maintenance of cell viability and tissue integrity². This study advances this previous work and details a whole disc model system for testing therapies in a mechanical environment pertaining to that of the human IVD.

METHODS: Bovine caudal IVDs (ages 9-18 months) were isolated in the presence of heparin, and either excised as discs and subsequently enclosed within an apparatus to mimic endplates (constrained discs) or as motion segments with intact endplates (intact discs).

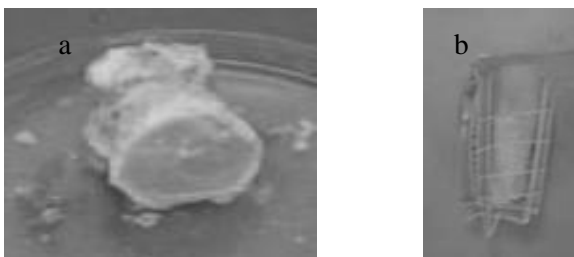


Figure 1: (a) intact discs; (b) constrained discs artificial endplates to prevent swelling of IVD.

Samples were subjected to a daily hydrostatic loading regime (as detailed previously²) for set time points up to 5 weeks. Unloaded control discs were cultured for the same period. Following loading 6mm punch biopsies were taken from the nucleus pulposus (NP) and the outer annulus fibrosis (AF) and assessed to determine cell viability, glycosaminoglycans and collagen content. Atomic force microscopy was used to assess ultrastructural changes

RESULTS: Cell viability: In constrained IVDs cell number and viability was substantially decreased in both the loaded and unloaded samples. Cell viability in intact discs was maintained throughout the culture period with no significant differences between loaded or unloaded samples.

Tissue integrity: Alcian blue staining confirmed that loading helped to maintain GAG content in constrained discs. GAG content was maintained up to 35 days in intact discs and staining was similar in both loaded and unloaded intact discs. Immunohistochemistry demonstrated strong immunopositivity for type I collagen in the AF of loaded constrained discs and intact discs which was corroborated by AFM data demonstrating that the collagen fibril bundles were more orientated in these samples. Likewise there was strong type II collagen immunopositivity in the NP of constrained and intact discs with more intense staining (cellular and pericellular) in loaded intact discs. AFM showed that collagen fibrils were orientated while in unloaded samples collagen fibrils were less orientated and not as well demarcated.

CONCLUSION: Cell viability and tissue integrity was maintained both in loaded isolated and intact discs throughout extended culture, although the data suggests that intact discs are a more optimal model. Importantly our data shows that mechanical load is critical in maintaining the ECM structure and cell function in the IVD model. Therefore, when regenerating new tissues it is essential to consider the native environment and mimic it as closely as possible in both *ex vivo* and *in vitro* settings.

REFERENCES: ¹ Richardson *et al*, Biomaterials, 2006, 27: 4069-4078 ² Le Maitre *et al*, J Tissue Eng Regen Med, 2009, 3: 461-469

ACKNOWLEDGEMENTS: Thanks to Arthritis research UK for funding this study

The Importance of Mechanical Load in Modifying Collagen Architecture as Identified by Atomic Force Microscopy

E.A.Mitchell¹, A.M. White¹, S.Richardson¹, N. W. Hodson¹, M.J. Sherratt¹, J.A.Hoyland¹

¹ School of Biomedicine, University of Manchester, Manchester, England.

INTRODUCTION: Collagen architecture and fibre formation is critical to the function of tissues. In regenerative medicine it is essential to create tissues which behave like native tissue. In load bearing tissues such as the intervertebral disc (IVD) mechanical load is thought to play a major role in regulating the formation and functionality of the ECM and thus must be factored in to model systems. . To date changes in ECM structure have been qualitatively assessed by histological, immunohistochemical or ultrastructural (electron microscopy (EM)) techniques. However, one of the primary limitations of EM is the modification required for effective visualisation of small features. Here, we have employed a newly developed tissue section atomic force microscopy (AFM) approach ⁽¹⁾ to characterise collagen fibril architecture in mechanically loaded and unloaded intervertebral discs *in vitro*.

METHODS: Bovine caudal discs were isolated with intact endplates. Discs were hydrostatically loaded with a regime designed to mimic normal human IVD loading (encompassing both static and dynamic loads) ⁽²⁾ for a period of 6 weeks. Unloaded discs were maintained in culture media for the same time period. Samples of AF and NP were frozen and cryosectioned at 5µm, and imaged by intermittent contact mode in air using a Veeco Multimode AFM with a Nanoscope IIIa controller.

RESULTS (Figure 1): AFM of these cryosections clearly identified well preserved structural features within the IVD tissue, including variable diameter collagen fibrils embedded in the ECM. In addition to the well characterised 67 nm collagen banding pattern, molecular structures, including telopeptide ridges were evident on many of the component collagen fibrils. Freshly isolated AF contained well defined individual fibres, which were woven into different layers giving a “basket-weave” appearance. Although the ECM architecture of loaded AF samples was similar to freshly isolated disc, fibril bundles appeared more closely packed with a pronounced

orientation. Two dimensional fast fourier transform (2D FFT) analysis of the AFM images confirmed that the fibres were highly orientated and periodic. In contrast, collagen fibril structure in unloaded cultured discs was less well defined, fibrils appeared shorter and periodic structures were absent from 2D FFT images.

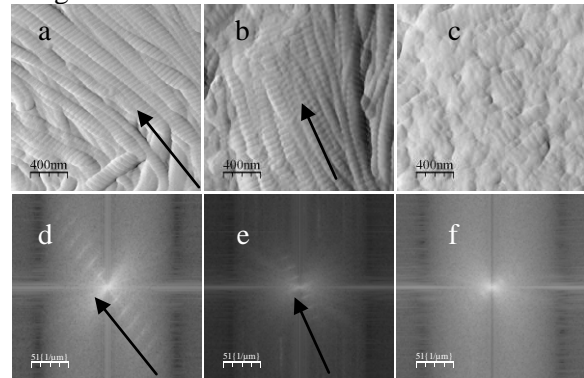


Figure 1: AFM images and their respective 2D FFT. (a) The T=0 sample (b) 6 week loaded IVD AF section (c) unloaded IVD AF sample. (d-f) 2D FFT analyses of AFM images.

Conclusion: Load has been shown to play an essential role in the maintenance and orientation of collagen fibers in the IVD. The use of AFM has enabled ultra-structural imaging of collagen fibrils within the AF and has effectively demonstrated that loading of whole discs induces changes in ECM structure/assemblies. Imaging at the nanoscale level thus provides information on changes in ECM structure. Importantly this study has highlighted the use of AFM as an analytical tool to define ECM structure in tissue engineering/ regeneration studies.

REFERENCES ¹ Graham et al Matrix Biol., 2010, in press ² Le Maitre et al, J Tissue Eng Regen Med, 2009, 3: 461–469

ACKNOWLEDGEMENTS: This work was funded by the Arthritis research UK and Research into Ageing.

Homogeneity study of biodegradable polymer films applied in peripheral nerve injury

S. A. Mobasseri, S. Downes

Materials Science Centre, Department of Engineering and Physical Sciences,
The University of Manchester

INTRODUCTION: Peripheral nerve injury is common expression illustrated nerves damage outside the spinal cord and the brain. Nerve repair is usually unsuccessful; however, under surgical implantation of guidance conduit, axon extension can reconnect and regenerate functional contacts. Biodegradable polymer films represent profound results by eliminating the complications of autograft and allograft. However, there are still requirements for synthetic nerve guide conduit including batch to batch variation reduction of manufacturing process. The aim of this study is to characterise the effect of environmental factors on fabrication of PCL/PLA solvent casted films.

METHODS: In this study, Polycaprolactone (PCL) and Polylactic acid (PLA) blend films (80/20) were produced by solvent casting. It is believed that environmental parameters such as temperature, humidity and air flow are having the major effect on the surface structure.

PCL/PLA blends films preparation: PCL and PLA pellets were dissolve in chloroform to make (3% w/v) solution and casted onto the glass cover slip (18x18 mm). The films were dried out in three different environments; 1) general laboratory environment without any control on temperature, humidity and air flow, 2) controlled temperature/humidity environment with constant $T = 23 \pm 1^\circ\text{C}$, $H\% = 50 \pm 2\%$ without any control on air flow 3) controlled T/H environment under the glass cover.

RESULTS: Nine batches of specimens were fabricated in each mentioned environment. The visual examination revealed the significant distinction in surface topology (figure1). Group1 has the considerably non-consistent surface structure according to the SEM images. The surface structure was varied with the T/H alteration in laboratory environment. However, samples in group 2 have the comparable surface morphology. Surprisingly, group3 has the smoothest surface structure with low porosity (figure2). Group3 is the thinner films with the thickness 0.1218 mm and the thickness of group1 and group2 is 0.1316 mm and 0.1443 mm respectively. The pores size of group1 and group2 are in range of Depth= 1-3 μm ,

Width= 3-4 μm and Depth=1-3 μm and Width= 1-6 μm , respectively.

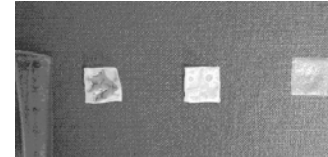


Figure 1: Left to right samples of; group1, group2 and group3.

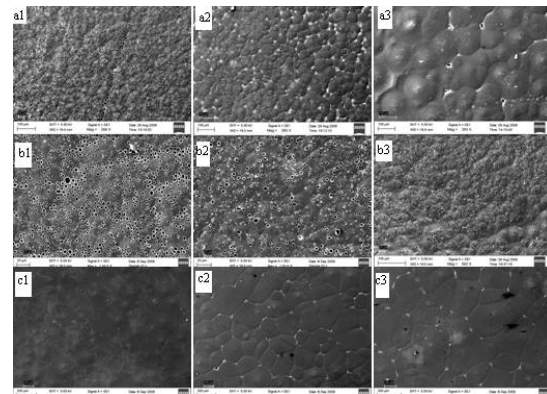


Figure 2: SEM images of a) group1 b) group2 c) group3.

DISCUSSION & CONCLUSIONS: The characteristic analysis well explained the vital rule of the T/H condition on the production of the solvent casted films. The films made in laboratory have considerably different surface texture. The formation of pores and also the size of them are changed with variation of these factors. The constant parameters in controlled room make the films more consistent in surface morphology, surface roughness, and pores size. High temperature and constant humidity produce films with bigger pores and higher surface roughness. However, the porosity decreased as a result of increasing solvent evaporation rate in group3. In conclusion, it is believed that the dominant factor on the polymer film fabrication is the solvent evaporation rate which is dependent on the environmental temperature and humidity condition, air flow, solvent and solution concentration.

REFERENCES: ¹ M. Sun and S. Downes, (2009) *J Mater Sci Mater Med* 20(5):1181-92. ² Z.G. Tang *et al*, (2004) *Biomaterials*20: 4741-4748. ³ S. Ichihara, Y. Inada, T. Nakamura (2008) *Injury, Int. J. Care Injured* 39S4, S29-S39.

Physico-chemical Characterisation of Functional Electrospun Scaffolds for Bone and Cartilage Tissue Engineering

P-A Mouthuy, H Ye*, G Oommen, Z Cui

Institute of Biomedical Engineering, Department of Engineering Science, University of Oxford, UK

INTRODUCTION: Electrospun fibres have received much attention for their potential application in Tissue Engineering [1]. These are similar to native collagen fibrils in the extracellular matrix both in scale and 3D arrangement.

This study investigates the potential of the electrospinning technique to build a three-dimensional construct recapitulating the zonal matrix of the bone-cartilage interface. Mimicking the zonal organisation of this interface will help the production of functional osteochondral grafts for regeneration of skeletal joint defects [2,3].

METHODS: Polymer solutions were prepared by dissolving poly(lactic-co-glycolic acid) (PLGA) without or with collagen type I (at ratio 7:3, 8:2 and 9:1) at 15% (w/v) in hexafluoroisopropanol. Hydroxyapatite nanoparticles (nHAp) were also added at concentrations up to 50% (w/v). Homogenised polymer solutions were then electrospun on a thin layer of phosphate buffer saline solution spread on the collector in order to facilitate the membrane detachment and recovery.

RESULTS AND DISCUSSION:

Results have shown that electrospun membranes containing different amounts of nHAp could easily be obtained after a proper homogenisation of the initial solutions. Incorporation of increasing amounts of nHAp in PLGA solutions were not affecting significantly the average diameter of the fibres, generally of about 700nm. However, in presence of collagen, fibres with diameters below 100nm were generally observed and the number of these fibres was inversely proportional to the ratio PLGA:collagen and proportional to the content of nHAp.

In absence of collagen, the membranes were rather hydrophobic, although the contact angles were progressively dropping from 125° to 110° when the content of nHAp was increased from 0% to 50%. Membranes containing collagen were much more hydrophilic: the contact angles were between 60° and 110°, the values being proportional to the ratio PLGA:collagen and the content of nHAp.

With regards to the mechanical properties, the addition of nHAp from 0% to 50% in absence of

collagen resulted in decreasing dramatically both the Young modulus (Y_m), from 34.3 ± 1.8 MPa to 0.10 ± 0.06 MPa, and the ultimate tensile strain (ϵ_{max}), from a value higher than 40% to 5%. However, the presence of collagen together with nHAp allowed the creation of membranes much stiffer, although more brittle, as shown for membranes made with a ratio 8:2 and 10% of nHAp, for which $Y_m = 70.0 \pm 6.6$ MPa and $\epsilon_{max} = 7\%$.

CONCLUSIONS:

This work shows the potential of electrospinning as a technique to produce a wide range of membranes from which some can be selected in order to create, thanks to a multilayered arrangement, a 3D scaffold with a gradient of properties mimicking the zonal matrix of the bone-cartilage interface.

REFERENCES:

[1] Li, W.-L., R. M. Shanti, and R. S. Tuan. In C.S.S.R. Kumar (Ed.). *Tissue, Cell and Organ Engineering* 2006; 9: 135-187. [2] Woodfield T. B., Van Blitterswijk C. A., De Wijn J., Sims T. J., Hollander A. P., Riesle J. *Tissue Engineering* 2005; 11:1297-1311. [3] Sharma B., Williams C. G., Kim T. K., Sun D., Malik A., Khan M., Leong K., Elisseeff J. H. *Tissue Engineering* 2007; 13: 405-414.

ACKNOWLEDGEMENTS: This work is supported by EPSRC.

Electrospinning Photocrosslinkable Methacrylate Monomers for Tissue Engineering

Farina Muhamad^{1,2}, Yixiang Dong^{1,2}, Joachim H.G.S Steinke³, Molly M. Stevens,^{1,2}

¹Department of Materials, Imperial College London, London, U.K.

²Institute for Biomedical Engineering, Imperial College London, London, U.K.

³Department of Chemistry, Imperial College London, London, U.K.

INTRODUCTION: Nanofibers produced from electrospinning are promising for tissue engineering because of the similarity in fibre diameter to elements of the native extracellular matrix.¹ Fibres can be aligned within the scaffold to control and direct cellular interaction and matrix deposition.² Here we report the development of a new processing technology for electrospinning low molecular weight photocrosslinkable methacrylate monomers/ oligomers to produce topologically and functionally diverse nanofibre scaffold materials with tunable properties. Cysteine-containing RGD peptides conjugates were introduced through their addition during photo-polymerization to increase bioactivity of the scaffold.

METHODS: Nanofibre scaffolds were produced by electrospinning varying ratios of methyl methacrylate (MMA) and diethyl glycol dimethacrylate (DEGDMA) with ethanol as solvent. Poly(ethylene oxide) (PEO) was introduced as a carrier polymer to facilitate fibre formation during electrospinning.³ After electrospinning, the nanofibres were immediately photocrosslinked by exposure to UVB light. A range of techniques were applied to characterise the nanofibres including scanning electron microscopy (SEM), fourier transform infrared spectroscopy (ATR-FTIR), nuclear magnetic resonance (NMR) and mass-loss analysis. In addition, the effect of the nanofibres on cell viability of Saos-2 osteosarcoma cells was assessed by cell metabolic assay (MTS), live-dead viability assay and immunostaining for actin and nuclei.

RESULTS: Photocrosslinkable nanofibers were successfully developed using electrospinning and UV post-crosslinking. PEO was extracted by immersing the nanofibers in deionized water overnight. SEM imaging of the photocrosslinked fibres (Fig. 1) demonstrates that the fibres maintained a fibrous structure in water with slight swelling and fibre diameters of approximately 850 nm. The proliferation of Saos-2 cells was significantly increased on the MMA:DEGDMA photocrosslinked nanofibres in comparison to flat surfaces formed from same ratio of monomers (Fig. 2).

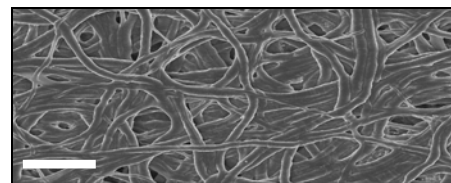


Fig. 1: SEM micrographs of PEO/MMA: DEGDMA nanofibres produced by electrospinning post-overnight incubation in water. Scale bar: 5µm

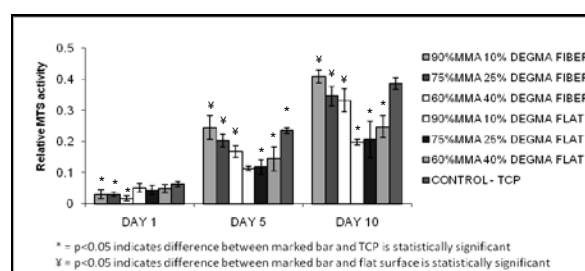


Fig. 2: Metabolic activity of Saos-2 cells cultured on MMA-DEGDMA photocrosslinkable nanofibres with varying ratios of MMA to DEGDMA, MMA-DEGDMA flat surfaces and TCP are included as controls.

DISCUSSION & CONCLUSIONS:

Photocrosslinked nanofibres were produced via reactive electrospinning. Their ability to support cell viability effectively was demonstrated. These materials hold considerable promise for designing highly functional scaffolds with nanometer-sized features.

REFERENCES: ¹Stevens, M. M.; George, J. H., (2005) *Exploring and Engineering the Cell Surface Interface*. Science **310** (5751), 1135-1138.

²Pham, Q. P., (2006) *Electrospinning of polymeric nanofibers for tissue engineering applications: a review*. Tissue Engineering **12** (5), 1197.³Tan, A. R.; Ifkovits, J. L.; Baker, et al, *Electrospinning of photocrosslinked and degradable fibrous scaffolds*. Journal of Biomedical Materials Research Part A **2008**, 87A (4), 1034-1043.

ACKNOWLEDGEMENTS: Malaysian Government Fellowship and ERC grant "Naturale".

Two-dimensional/three-dimensional cell culture of chondrocytes on self-assembled octapeptide scaffolds

A Mujeeb, JE Gough & A Saiani

Materials Science Centre, University of Manchester, Grosvenor Street, Manchester, M1 7HS, UK

INTRODUCTION: Tissue engineering is an exciting blend of materials science and technology focusing on the fabrication of *de novo* structural design at an atomic level with the aim to create artificial tissues [1]. Here we will exploit the concept of self-assembly to construct well-defined peptide based hydrogels at room temperature. We have recently investigated the self-assembling and gelation properties of a series of ion-complementary peptides based on the alternation of non-polar hydrophobic and polar hydrophilic residues [2]. In this work we focus on two specific octapeptides: FEFEFKFK and FEFKFEFK (F: phenylalanine, E: glutamic acid, K: lysine) (Figure: 1A). By varying peptide concentration and type we aim to tailor hydrogel stiffness, porosity, viscosity, fibre density and other mechanical properties to control cell interactions and subsequent tissue growth for cartilage repair.

METHODS: The octapeptides were synthesised using a solid phase peptide synthesiser (a ChemTech ACT 90 peptide synthesiser). The fibre morphology of the hydrogels was analysed using TEM and Cryo-SEM. The mechanical properties of the hydrogels were determined using oscillatory rheology. Bovine chondrocytes were used to assess the biocompatibility of the scaffolds under 2D/3D cell culture conditions, particularly looking into cell morphology and proliferation using light microscopy, live-dead and immunohistochemical staining, MTS ([3-(4,5-dimethylthiazol-2-yl)-5-(3-carboxymethoxyphenyl)-2-(4-sulfophenyl)-2H-tetrazolium), LDH (lactate dehydrogenase), Alamarblue and DNA assays.

RESULTS: The purity of the peptide was found to be >87%. Fibre morphology examined by TEM revealed nanofibres present in the gel matrix with a diameter of 4.5nm. Cryo-SEM confirmed the presence of dense interconnecting fibres (Figure: 1C). Oscillatory rheology showed that above a critical concentration, the hydrogels exhibited solid-like behaviour. An elastic modulus (G') within the 0.01-100 KPa range was observed for these hydrogels. Protocols for the preparation of scaffolds for 2D and 3D (homogeneous

incorporation of cells) cell culture have been developed using the cell culture medium properties (pH and ionic strength) to trigger the gelation. The hydrogel developed were subsequently used to culture bovine chondrocytes over 21 days (Figure: 1D). The cell proliferation results demonstrated the scaffolds to be cytocompatible with the cells showing varying metabolic activity.

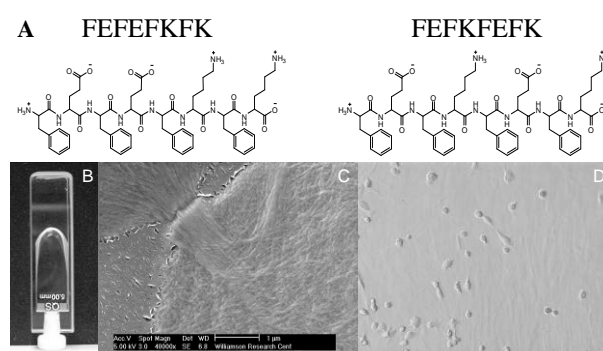


Figure: 1. (A) Chemical structure of octapeptides; (B) FEFEFKFK hydrogels formed at 20 mg ml^{-1} ; (C) Cryo-SEM micrographs of hydrogel showing a dense fibrillar network (scale bar = $1 \mu\text{m}$); (D) Optical micrograph of cell-seeded hydrogel FEFEFKFK (scale bar = $50 \mu\text{m}$).

DISCUSSION & CONCLUSIONS: We demonstrated that the spontaneous self-association of peptides into well-defined fibrous networks formed stable hydrogels supporting 2D and 3D cell culture conditions *in vitro*. The research is now focusing on functionalising these gels using biological signals to trigger specific cell behaviours.

REFERENCES:

1. S.G. Zhang Nature Biotechnology 21, 1171 (2003).
2. A. Saiani et al. Soft Matter, 5, 193 (2009)

Novel bioactive glass/gelatin composite scaffold for bone tissue engineering

D Nadeem & B Su

BioMEG, School of Oral & Dental Sciences, University of Bristol, UK

INTRODUCTION: Although a variety of bone scaffolds have been produced using bioactive glasses, many share similar shortcomings. One of the more prevalent issues is the use of toxic or harsh chemicals in the fabrication process, often present as organic solvents for the polymeric phase. Another issue, often encountered *in-vivo*, is the hydrolytic degradation of the polymer matrices (e.g. PLLA, PLGA). The majority of these bio-resorbable polymers tend to undergo bulk degradation *in-vivo*, causing a massive influx of acid and acute inflammation, due to acidosis, of the host tissue^[1]. Bearing this in mind a natural, enzymatically degradable, polymer such as gelatin, would be better suited as a matrix polymer for a bone scaffold.

METHODS: Bioactive glass and gelatin were used to produce a wet foam that was stabilised by either forced gelation or freezing, followed by freeze drying. The fabricated scaffolds were then characterised through light microscopy and resin infiltration to assess pore morphology, porosity and interconnectivity. A Micro-CT scanner was also used to produce 3D models of the scaffolds. The stability of the fabricated scaffolds, as well as samples crosslinked by dehydrothermal (DHT) treatments, was evaluated by aqueous submersion over a period of 6 days. Bioactivity was also assessed by quantifying the rate of apatite formation in simulated body fluid.

RESULTS: A model (Figure 1) of the fabricated scaffold was produced using images acquired by a Micro-CT scanner. Characterisation by light microscopy and resin infiltration demonstrated a morphology matching the physical criteria of an ideal scaffold^[2], namely the presence of a three dimensionally porous and interconnected network, with pore windows at least 100µm in diameter to aid the growth of bone tissue and vasculature. Aqueous submersion of the scaffold samples showed significant degradation in porous structure and loss of mass dependant on the crosslinking treatment used. Samples crosslinked by DHT treatment, at 160°C, showed only a 17% loss in mass after submersion (Table 1) as well as preservation of the scaffold's original morphology.

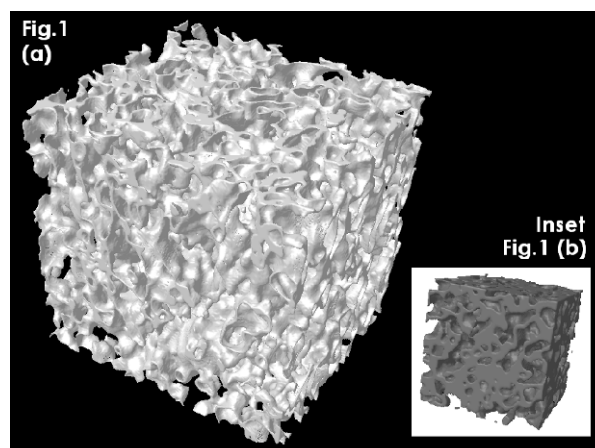


Fig. 1:(a)3D model of fabricated scaffold. Note the highly interconnected appearance in contrast to (b)model of scaffold with low interconnectivity

Table 1. Percentage weight loss after aqueous submersion of scaffolds crosslinked by DHT.

Non crosslinked	DHT treatment at 120°C	DHT treatment at 160°C
22%	36%	17%

DISCUSSION & CONCLUSIONS: Ceramic foams with open porosity typically present a spherical pore morphology with multiple pore windows. However, through the optimisation of several processing parameters, it was possible to fabricate a composite scaffold with an atypical, sponge-like morphology that provided a fully interconnected, 3-dimensional, porous network exhibiting a pore-size range of 100-300µm. The aqueous stability of the gelatin polymer matrix presents a similar problem to the bulk degradation of the synthetic polymer matrices that are used in many tissue engineering scaffolds. However, as illustrated by Table 1, the stability of gelatin can be modified through the degree of crosslinking. Optimisation of the temperature and exposure period of DHT treatment can be used to vary the degree of crosslinking induced and thereby control the *in-vivo* stability of the gelatin polymer matrix.

REFERENCES: ¹K. Rezwan, Q. Z. Chen et al. (2006) *Biomaterials* **27(18)**: 3413-3431 ²J. R. Jones, (2009) *Journal of the European Ceramic Society* **29(7)**:1275-1281.

Photopolymerised Hyaluronic acid-based hydrogels

S.Ouasti, N.Tirelli

School of Pharmacy, University of Manchester, Manchester, UK.

Contact: sihem.ouasti@manchester.ac.uk

INTRODUCTION

Hyaluronic acid (HA) is a natural extracellular polysaccharide that has been extensively used for the design of cell matrices. It contains hydroxy and carboxylic groups through which modifications are possible that allow chemical cross-linking of the material and that can modulate the adhesion and proliferation of cells

METHODS

Hyaluronic acid of various molecular weights [MW: 64KDa, 234KDa] was functionalized with thiol groups in order to prepare hydrogels by photopolymerisation. Hydrogels contained 5 to 20mg/ml of native or 10% thiolated HA (SH-HA). Poly (ethylene glycol) diacrylate (peg-DA) was added as a comonomer in order to optimize elastic modulus and swelling behavior. Rheology measurements and degradability study were performed on the resulting gels. Also, murine fibroblasts were cultured for 9 days on top of the hydrogels. Microscopy analysis and proliferation assay were conducted every 3 days in order to assess both change in the phenotype of the cells and their proliferation on the hydrogels.

RESULTS & DISCUSSION

Rheology data revealed that the elastic modulus of the hydrogels were in the range of kPa which physiologically correspond to the thickness or consistency of the brain or liver tissue. Moreover when hyaluronidase was added (100U/mL) before photopolymerisation, the elastic modulus decreased by a third.

Mouse fibroblasts seeded on thiolated HA gels, showed a round shape and proliferated in clusters, which is typical of a non-cell adhesive material. But relevant changes in phenotype and proliferation were observed when the adhesive peptide GCGRGDS was incorporated at 1:100 thiol/acrylate into the hydrogels. The fibroblasts started spreading after only two days of culture and their proliferation rate was comparable to the one on TCPS. They were cultured for up to 9 days and reached 100% confluency.

Fig 1: Viscous and elastic modulus evolution during photopolymerisation with initial solution containing 2% SH-HA and 5% peg-DA w/v.

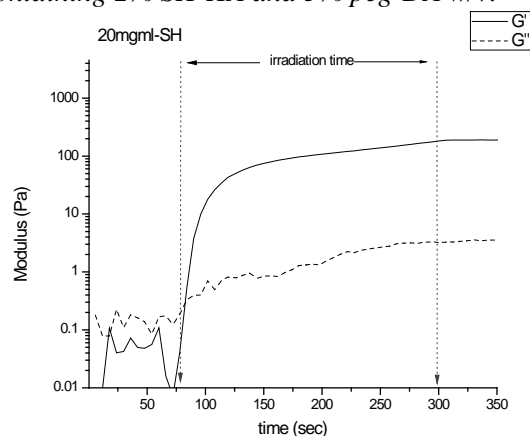
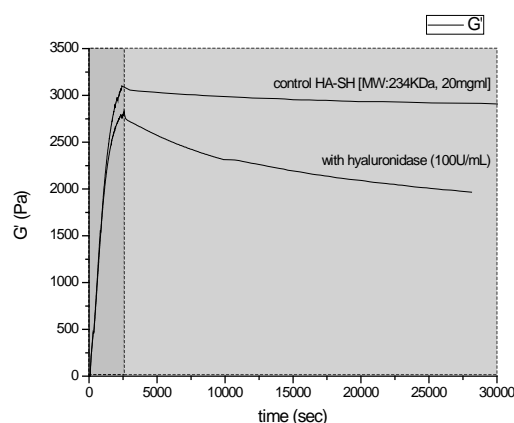


Fig 2: Elastic modulus evolution during photopolymerisation with initial solution containing 2% SH-HA, 5% peg-DA w/v and 100u/mL Hyaluronidase.



CONCLUSIONS

Here the data suggest that thiolated HA hydrogels of soft consistency can be enzymatically biodegraded and that by incorporating and adhesive peptide it can support fibroblast adhesion and proliferation.

REFERENCES

- 1) Park YD, Tirelli N, Hubbell JA. **Photopolymerized hyaluronic acid-based hydrogels and interpenetrating networks.** Biomaterials. 2003 Mar;24(6):893-900.

ACKNOWLEDGEMENTS

BBSRC for funding this project.

Surface Modification of an Elastomeric Membrane for Cardiac Tissue Engineering

Isha Paik¹, James E. Dixon¹, Peter Rivett², Kevin M. Shakesheff^{1,§}

¹Wolfson Centre for Stem Cells, Tissue Engineering and Modelling (STEM), School of Pharmacy, University of Nottingham,

NG7 2RD, UK., ²Tannlin Ltd. Irvine, Ayrshire, KA11 4HP, UK.

[§]To whom correspondence should be addressed: Kevin.Shakesheff@nottingham.ac.uk

INTRODUCTION: Cardiovascular disease is the leading cause of death and disability worldwide. However current therapies including cardiac myoplasty and donor transplantation provide outcomes with limited success¹. Cardiac tissue engineering (CTE) using mechanically compatible materials, such as elastomers, may provide cells with a physical support *in vivo* and improve clinical outcomes. Recently, significant findings were published where ‘muscular thin films,’ consisting of micro-patterned polydimethylsiloxane (PDMS) were manufactured, cultured with synchronously contracting neonatal rat cardiomyocytes (CMs) and used to produce fully active CM-driven devices². Below we describe two separate techniques, plasma polymer deposition and micropatterning with fibronectin, to encourage cell attachment. The long term aim being to develop an *in vitro* pump that is driven by human embryonic stem cell-derived CMs which will efficiently deform PDMS tubes to produce fluid flow.

METHODS: PDMS (Sylgard 184, Dow Corning, Midlands) was spin coated on to glass slides pre-coated with PVA, using a 400 Lite Spinner (Laurell Technologies, North Wales) at 2000rpm. Freely suspended membranes were oxygen etched and plasma coated with allylamine monomer, this method has been previously described³. Seven different surface types were investigated, (see Figure 1). Static water contact angle (WCA) was measured with a CAM 200 Optical Contact Angle Meter (KSV Instruments LTD) to investigate surface wettability over 15 days.

PDMS membranes were micro-patterned by airbrushing labelled fibronectin, (Alexa Fluor 488, Invitrogen, UK) through a micro-stencil (Tannlin, Irvine, UK) at 20 psi. The fibronectin band width was 25 μm , with a gap of 90 μm between each band. A total of 0.5×10^6 GFP-labelled 3T3 cells were seeded. Images were taken using the Nikon Eclipse TS100 Microscope at x 10 magnification.

RESULTS: PDMS shows consistent hydrophobic behaviour ($<90^\circ$). Oxygen etched and allylamine treated surfaces are initially hydrophilic

(approximately 71°), but recover their hydrophobicity over time for all deposition thicknesses tested. Clearly defined fibronectin lanes were visible on the PDMS surface following airbrushing through micro-stencils (Figure 2a) with successful attachment of 3T3 cells to these regions, (Figure 2b).

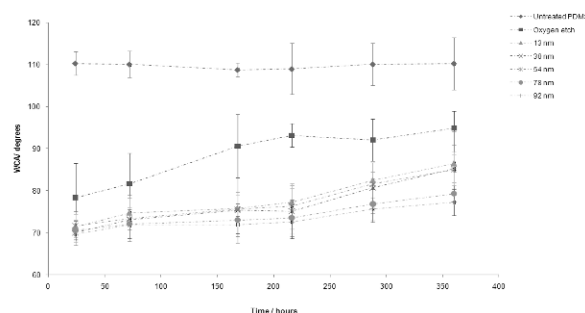


Figure 1. WCA of plasma coated surfaces as a function of time post plasma treatment. **Note:** Each thickness in (nm) represents the allylamine deposition thickness.

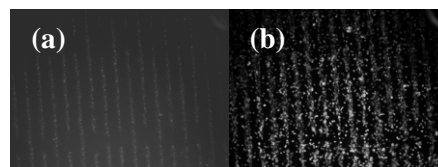


Figure 2. (a): Fibronectin micro-patterned (red) PDMS and (b): adhered 3T3 cells (green).

DISCUSSION & CONCLUSIONS: PDMS surfaces treated with plasma polymerised allylamine proved unstable over a period of 15 days and therefore were not taken forward for cell attachment experiments. Controlled cell growth through fibronectin micropatterning was more promising with respect to 3T3 cell attachment. Future studies will investigate human embryonic stem cell-derived CMs attachment to these modified membranes and whether they exhibit synchronous contraction on these membranes.

REFERENCES: ¹ Hidalgo-Bastida, L.A., et al., (2007) *J Act Bio* **3**:457-467. ² Feinberg, A.W., et al., (2007) *Science* **317**: 1366, ³ Zelzer, M., et al., (2008) *Biomater*, **29**:172-184.

ACKNOWLEDGEMENTS: BBSRC/RegenTec.

Automated Computation of 3D Histomorphometry within implanted hydroxyapatite porous scaffolds

A.J.B Parish^{1,2}, G. R Davis² & K.A Hing¹

¹ School of Engineering and Material Sciences & IRC Queen Mary & Westfield University of London E1 4NS, ² Institute of Dentistry at Barts and The London, University of London E1 2AD UK.

INTRODUCTION: Methods for quantifying bone associated with removed implants has classically been done manually, with help from staining and microscopy. These methods are generally destructive, time consuming, and operator dependant. These problems can be overcome by the use of digitised data and computational algorithms. In this case the method of digitisation is via X-ray micro-tomography and the computation via high level computer languages such as python.

METHODS The imaging technique utilised in this process is X-ray micro-tomography² used for its high resolution and non destructive qualities (Fig.1). The system studied was a porous hydroxyapatite, implanted in the femoral condyle of New Zealand white rabbits with the internal bone growth being the sought-after data.

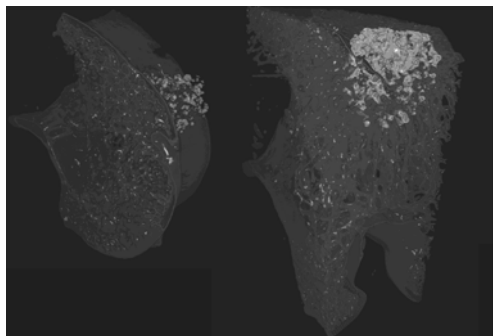


Fig. 1: 3D renders of bone with implant virtually cut in different ways, with data produced from XMT and displayed in Drishti

The computation of the data comprised a multi-step approach. Each of the voxels in the sample was given an eight bit value to denote its intensity and then processed in the form of strings. The data was processed using a collection of simple boundary conditions combined with area averaged conditions, in this system the voxels can be designated various identities including but not limited to bone, hydroxyapatite and mounting resin (Fig.2). Once the definition has been completed, more advance processing can be carried out, giving such data as contact and total surface area, the size and number of bone islands, and pore interconnection sizes.

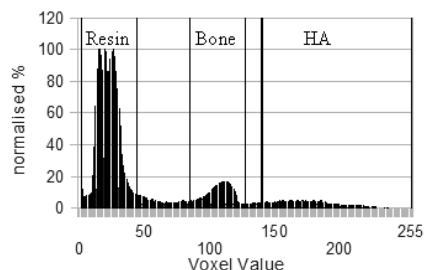


Fig. 2: Material justified 8 bit histogram of the XMT samples normalised to the highest intensity.

RESULTS: Data was produced at a much faster rate and was compared with that produced manually and found to be within reasonable error¹ (Fig.3). However this process was found to produce false positives on samples without bone growth, due to semi filled voxels of HA.

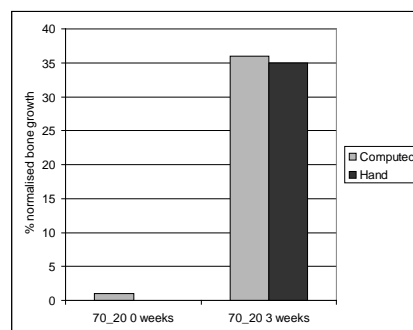


Fig. 3: Normalised bone growth processed by hand and by linear computation scanning.

DISCUSSION & CONCLUSIONS: With the processing power of computers constantly increasing, it is now possible to do high level image processing on a consumer PC. It is therefore possible for small scale groups to produce results from a mass of data in an automated way with an acceptable and measurable error. Finally with the continuous properties of programs more processes can be bolted on to the existing algorithms to perform more and more in-depth analysis.

REFERENCES: ¹ K.A Hing *et. al.* (2005) *Journal of Materials Science-Materials in Medicine* **16**: 467-475. ² G.R Davis *et. al.* (2003) *Journal De Physique IV* **104**:131-134

ACKNOWLEDGEMENTS: The EPSRC and ApaTech Ltd for AJBP's CASE award, M.-K. Mafina and V. Castagna.

Use of an *in vitro* muscle model to investigate cellular and molecular aspects of exercise physiology: answering the key questions

D.J. Player¹, N.R.W. Martin¹, P. Davies¹, N. Sculthorpe¹, P.C. Castle¹, S. Passey¹, V. Mudera³, R. Ferguson⁴ & M.P. Lewis^{1,2}

¹Muscle Cellular and Molecular Physiology Group, Institute of Sport and Physical Activity Research, University of Bedfordshire, Bedford, ²UCL Eastman Dental Institute, London, ³UCL Institute of Orthopaedics and Musculoskeletal Science, and ⁴School of Sport, Exercise and Health Sciences, Loughborough University.

INTRODUCTION: Research within exercise physiology has traditionally focused upon measurements of gross physiological function of skeletal muscle. However, in order to develop a greater understanding of the exact mechanisms that contribute to skeletal muscle in response to exercise, the cellular and molecular determinants need to be investigated. There is a growing body of *in vivo* research utilising methods of molecular biology, which has led to the establishment of proposed genes and proteins involved in the adaptation of skeletal muscle to exercise stimuli. *In vivo* exercise testing poses problems with regards to experimental control; accounting for inter-individual differences and methods relating to tissue sampling are common flaws of such research. *In vitro* models of skeletal muscle for investigating adaptation to exercise are in their infancy and generally lack biomimicry. It is therefore necessary to develop a model which has greater physiological relevance with respect to exercise, which encompasses the nature of the investigations currently underway in our laboratory.

METHODS: An established protocol was used for this experiment (Brady et al, 2008). Briefly, muscle derived cells (MDCs) were seeded in neutralised type-1 rat tail collagen and plated into a custom made multi-array 3D well system, containing five chambers. Each chamber held a custom built floatation bar ("A-frame") at either end. The collagen was allowed to gel in a standard incubator (37°C, 5% CO₂). Once set the collagen construct was cut away from the sides of the chamber and suspended in growth medium (20% foetal calf serum in high glucose DMEM). The "A-frames" provided two attachment points within the culture so that, as the cells attached and contracted, lines of longitudinal principle isometric strain developed. This tension provided sufficient mechanical stimulus to promote the realignment of the MDCs in a single plane. The result was a 3D tissue possessing uniaxially aligned and differentiated myotubes capable of performing

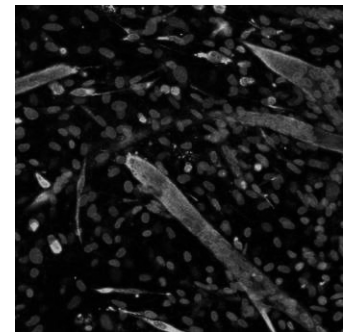
directed contraction. These models can be used for testing in their own right, or can be tethered to a

culture force monitor, which allows real time analysis of force generation within the construct. An attachment of a stepper motor can also be made to the CFM (tensioning culture force monitor; t-CFM) to allow programmable regimes of mechanical strain to be applied to the construct. Once experimentation is complete the gels can be used for staining, protein analysis or PCR.

Fig. 1: 25 µm section through the 3D collagen construct, stained for desmin (green) and nuclei (blue).

STUDY DESIGN:

This methodology is currently being used to investigate the following questions; (i). is an individual's ability to respond to a resistance exercise stimulus predetermined by the number of muscle precursor cells one possesses? (ii). Do distinct signalling pathways exhibit a degree of 'cross talk' during adaptation to specific forms of exercise? (iii). Does the extracellular matrix impede the regenerative potential of aging skeletal muscle?



RESULTS: Immunohistochemical analysis confirmed the formation of primary myotubes (Fig 1). Preliminary PCR and CFM data suggests that the myotubes present in these 3D cultures is representative of *in vivo* muscle development and regeneration.

DISCUSSION & CONCLUSIONS: The components of the *in vitro* muscle model are in place to investigate cellular and molecular questions which remain to be elucidated in the field of exercise physiology.

REFERENCES: Brady et al., (2008), Synergy between myogenic and non-myogenic cells in a 3D tissue-engineered craniofacial skeletal muscle construct. *J Tiss Eng Regen Med*, 2(7) 408-417.

MODULATION OF PROTEIN RELEASE FROM PLGA MICROSPHERES

R Qodratnama¹ FRAJ Rose¹ & KM Shakesheff^{1§}

¹ Wolfson Centre for Stem Cell, Tissue Engineering and Modelling (STEM), Centre for Biomolecular Sciences, School of Pharmacy, University of Nottingham, NG7 2RD, UK.

[§] To whom correspondence should be addressed: Kevin.Shakesheff@nottingham.ac.uk

INTRODUCTION: There are two main characteristics associated with controlled drug release from PLGA matrices: an initial burst release and often incomplete release of drug¹. The burst release phase provides a rapid and sharp increase of drug concentration at potentially toxic levels. Incomplete release of the drug can result in below-therapeutic-window concentrations being sustained. Blending PLGA with other polymers has been shown to facilitate degradation-mediated drug release. Hydrophilicity of polymer matrices can be enhanced by co-polymerisation with poly ethylene glycol (PEG)². The aim of this study was to modulate the release kinetics of a model protein, lysozyme, from microspheres fabricated from PLGA (85:15) alone in comparison to PLGA microspheres fabricated from PLGA blended with PEG-containing polymer triblocks.

METHODS: PLGA-PEG-PLGA triblocks were synthesised via ring opening polymerisation using either PEG 1000 or PEG 1500 and designated 'triblock II' (TBII) and 'triblock IV' (TBIV), respectively. Both triblocks were characterised using NMR, GPC, and rheology on 20, 25, 30, and 35% (w/v) solutions of triblocks. PLGA 85:15 (118 MW) was heat-blended with either TBII (PLGA-PEG-PLGA; Mn: 2015-1500-2015) or TBIV (PLGA-PEG-PLGA; Mn: 1450-1000-1450) in two different compositions- triblock/PLGA 10:90 or 30:70 - resulting in four formulations: TB2/PLGA 30:70, TB2/PLGA 10:90, TB4/PLGA 30:70, TB4/PLGA 10:90.

Lysozyme-loaded microspheres were fabricated using a solid-in-oil-in-water (S/O/W) emulsion method followed by protein release profiling using an infusion pump over a 30-day period and a BCA assay (for total protein)³.

RESULTS: Rheological studies showed that sol-gel and gel-sol transition temperatures were dependent on triblock composition and not on the wt% of the individual triblocks. The sol-gel transition temperatures were determined as 33°C and 10°C and the gel-sol transition temperatures were determined as 41°C and 16°C for TB-II and TB-IV, respectively. The microparticles fabricated were in the size range of 100-200 µm and

entrapment efficiencies were over 60% in all cases. The release study showed that 50% of the incorporated protein was released in first 26 days of the study in case of TB/PLGA 30:70 formulations whilst this amount is approximately 12% for 10:90 formulations. The initial release (first day) were not significantly different amongst formulations and on day 26 formulations containing higher amount of PEG, i.e. TB/PLGA 30:70, had highest percentage of release, 49.64% and 48.65% from TB2/PLGA 30:70 and TB4/PLGA 30:70, respectively.

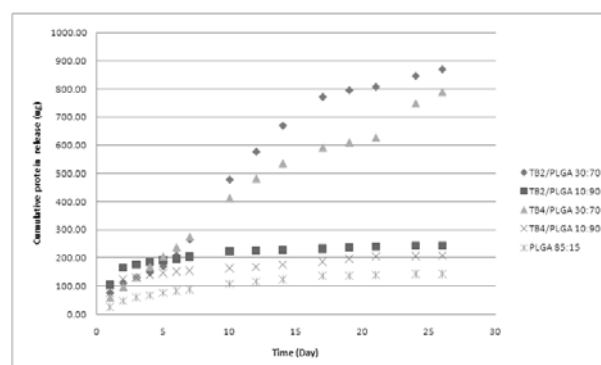


Fig. 1: Cumulative release profile of lysozyme from five different PLGA or triblock/PLGA microspheres.

DISCUSSION & CONCLUSIONS: In conclusion, fabricating microparticles from heat-blended PLGA (85:15 118 MW) with PLGA-PEG-PLGA triblocks altered protein release kinetics in comparison to microparticles made from PLGA alone. Protein release from the triblock/PLGA microparticles shifted the typical tri-phasic release profile to one with a constant protein release, in the first month of the study.

SELECTED REFERENCES:

¹Kim HK, Park TG. 1999. *Biotechnology and Bioengineering* 65(6):659-667. ²Chen SB, Pieper R, Webster DC, Singh J. 2005. *International Journal of Pharmaceutics* 288(2):207-218. ³Morita T, Sakamura Y, Horikiri Y, Suzuki T, Yoshino H. 2000. *Journal of Controlled Release* 69(3):435-444.

ACKNOWLEDGEMENTS: Special thanks to Drs. Andrew Olaye, Lloyd Hamilton and Cheryl Rahman for their guidance and demonstrations.

3D CULTURE MODEL FOR AGGREGATION AND DIFFERENTIATION OF EMBRYONIC STEM CELLS USING POLY (lactide-co-glycolide) MICROPARTICLES

O.Qutachi, K.M. Shakesheff, L.D. Buttery

Wolfson Centre for Stem Cells Tissue Engineering and Modelling, Centre of Biomolecular Sciences, School of Pharmacy, University of Nottingham, Nottingham, U.K

INTRODUCTION: Stem cells provide a valuable tool in regenerative medicine, which aims to repair damaged tissues and organs. Embryoid bodies (EBs) formed during the process of embryonic stem cell (ESC) differentiation are considered as a 3D model that provides direct cell to cell interactions and in some aspect mimics the early stages of embryogenesis¹ One of the problems of this approach is variability in the size and numbers of EBs and heterogeneity in differentiation. The aim of this study was to provide a 3D model that aim to direct the differentiation of EBs by using Poly (lactide-co-glycolide) microparticles (MPs) that could be loaded with biochemical factors and provide a controlled release 3-D ESC culture model

METHODS: PLGA MPs were fabricated using single emulsion method in which 14% w/v PLGA polymer (42 kDa) in DCM is homogenized in 200ml of 0.3% PVA at 19000 RPM. The created MPs are vortexed overnight. The particles were collected via centrifugation washed 3 times with distilled water and freeze dried before storing at -20°C. Mouse ESC cells and MPs were labeled with Cell tracker Red coumarin-6 respectively. The ESC-MPs aggregation was performed by three different methods. With static and centrifugation methods, cell densities were 10×10^4 /well in v-shaped 96-well plate and the ratio between the cells and the MPs were 1:1, 2:1 and 3:1. In the static method ESC-MPs suspensions were cultured for 5 days under standard conditions while with forced aggregation the cells were spun at 750g for 5 minutes. The third aggregation method was via biotin-labeling of cells and avidin cross linking² Cells were biotinylated by incubation in 1mM sodium periodate at 4°C for 10 minutes then incubated in biotin solution at 37°C for 30 minutes on 3D roller at 15rpm. The cells were re-suspended with the aggregation medium containing avidin 80µg/ml. The cell density was 50×10^4 /ml and the ratios to the MPs were 3:1, 10:1 and 20:1.

RESULTS: Up to 80 % of the fabricated PLGA MPs ranged between 5 to 18 µm in diameter with a mean of 10µm Fig1. The three different cell-MPs

aggregation methods were successful Fig 2; and the most promising one was the biotin avidin cross linking at 3:1 ratio.

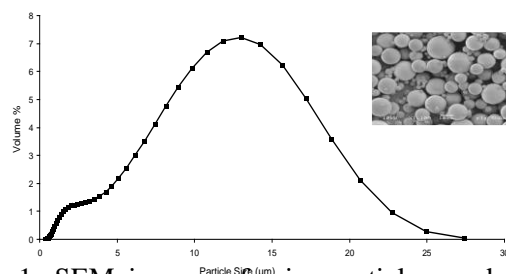


Fig.1: SEM images of microparticles made from PLGA 50:50 with particle size distribution of as measured by laser light scattering size analyser.

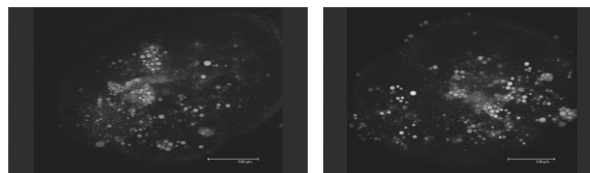


Figure 2: Confocal images (20X) revealing the distribution of PLGA MPs (green) within mouse ESC aggregates.

DISCUSSION & CONCLUSIONS: The size range of MPs fabricated provided a suitable and reproducible approach for mixing MPs into cell aggregates. Work is in progress to exert further control over cell to MP ratio and testing MPs loaded with biochemical factors and controlled within aggregates to control cell activity and differentiation

REFERENCES: ¹Desbaillets, I., U. Ziegler, et al., *Embryoid bodies: an in vitro model of mouse embryogenesis*. *Experimental physiology* (2000). 85(6): 645-51. ²De Bank PA, Hou QP, Warner R M, Wood IV, Ali BE, MacNeil S, Kendall DA, Kellam B, Shakesheff KM and Buttery LD. *Accelerated formation of multicellular 3D structures by cell-to-cell cross-linking* (2007). *Biotechnology and Bioengineering*, 97:1617-1625.

ACKNOWLEDGEMENTS: I would like to thank my family, the tissue engineering group and the University of Nottingham.

Injectable poly(α -hydroxy acid)-hydrogel composites with controlled mechanical properties for bone regeneration applications

C Rahman¹, F Rose¹ and K Shakesheff¹

¹ Wolfson Centre for Stem Cells, Tissue Engineering and Modelling, Division of Drug Delivery & Tissue Engineering, The University of Nottingham, UK.

INTRODUCTION: Three-dimensional polymer scaffolds have emerged as a potential treatment for bone regeneration applications. The design criteria for a successful injectable scaffold are challenging. Physically, the material must flow through a needle and then an *in vivo* trigger must restrict flow at the site of regeneration. For bone regeneration applications, it is crucial that scaffolds exhibit adequate mechanical strength.

We have previously developed an injectable scaffold formed by liquid sintering of PLGA/PEG microparticles¹. Liquid sintering is a process in which the polymer particles lose a plasticizer (PEG) and hence experience an increase in their glass transition temperature over time. Our scaffold undergoes this glass transition temperature within the body such that material hardens at 37°C.

We describe here the production of novel composite matrices by combining our PLGA/PEG scaffolds with hydrogels (hyaluronic acid, fibrin or Pluronic F127).

METHODS: PLGA/PEG particles were fabricated by high temperature blending of PLGA and PEG polymers. The PLGA/PEG particles were mixed with the hydrogel component manually and the mixture was packed into PTFE moulds. The mould was placed at 37°C for 2 hours to allow scaffold formation.

Compressive strength of composite scaffolds was tested using a TA.HD+ texture analyser (Stable Microsystems). The Young's Modulus of Elasticity was computed by determining the slope of the stress-strain curve along the elastic portion of deformation. The structural morphology of the scaffolds was examined in a scanning electron microscope (SEM) (JEOL JSM-6060LV). The samples were mounted on aluminium stubs with and were sputter-coated with gold.

RESULTS: Following 2 hours sintering at 37°C, PLGA/PEG-scaffolds prepared without gel had maximum compressive strength of 2MPa, with a Young's Modulus of 38 (Figure 1). PLGA/PEG-Pluronic F127 and PLGA/PEG-fibrin composites had maximum compressive strength of 1.2MPa and 0.6MPa respectively, with Young's Modulus

values of 18 and 20 respectively. PLGA/PEG-hyaluronic acid composites had higher maximum compressive strength of 2.5MPa, with a Young's Modulus value of 45. These compressive strength values are comparable with human trabecular bone, which ranges from 0.22 to 10.44MPa².

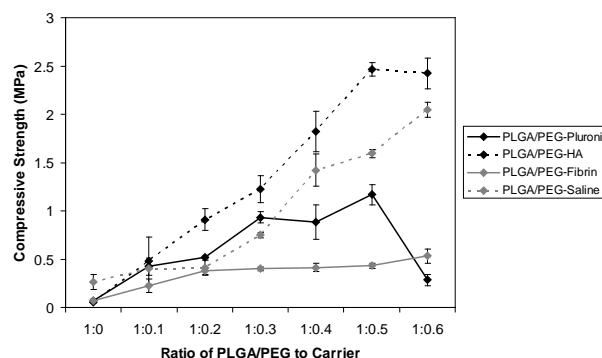


Figure 1. Compressive strength of PLGA/PEG-hydrogel composite scaffolds sintered at 37°C for 2 hours.

DISCUSSION & CONCLUSIONS: The PLGA/PEG-hydrogel composites effectively combine the desirable qualities of both the particulate and gel materials to produce a unique scaffold for use in regenerative medicine. Future work will assess growth factor delivery from these composite scaffolds for bone regeneration applications.

REFERENCES: ¹ L. Hamilton, R.M. France, K.M. Shakesheff (2006) *Pharm Pharmacol* **58**:A52-53. ² M.J. Mondrinos, R. Dembzyński, L. Lu (2006) *Biomaterials* **27**:4399-408

ACKNOWLEDGEMENTS: Financial support was provided by the FP7 project 'Angioscaff'. Hyaluronic acid was provided by BioHyos (Sweden).

Collagen gel as a 3D *in vitro* tissue model for ameloblastoma studies

C. Raison, S. Porter, S. Fedele, M. P. Lewis¹, V. Salih

Division of Biomaterials & Tissue Engineering, UCL Eastman Dental Institute and ¹University of Bedfordshire, 256 Gray's Inn Road, London, WC1X 8LD, UK

INTRODUCTION: Ameloblastoma is a rare locally invasive epithelial odontogenic tumour of the jaw which can cause significant and debilitating bone destruction. *In vitro* studies of ameloblastoma are sparse in the literature, and little is known regarding patterns of ameloblastoma cell growth and invasion, as well as relevant gene and protein expression. This study aims to (i) use plastic-compressed collagen gels as a robust and relevant biomimetic to culture ameloblastoma cells in a 3D *in vitro* tissue model [1] and (ii) perform histology, immunohistochemistry (IHC) and gene expression assays to characterise tissue remodelling, cell growth and invasiveness.

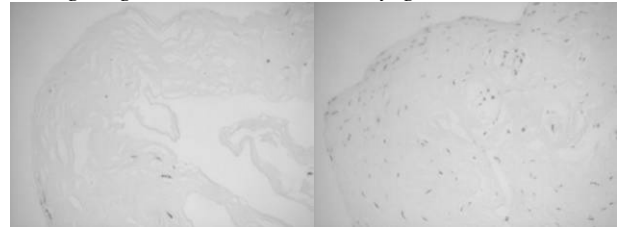
METHODS: Collagen type I, isolated from rat tails (First Link UK), was used to make hydrated gels suitable for seeding cells. Ameloblastoma AM-1 cell line [2] and HOS and MG-63 osteoblast-like cells were added to the gel. Plastic compression was then used to expel the water content, rapidly increasing the gel's mechanical strength without compromising cell viability [1]. Compressed gels were rolled into spirals to provide easy handling and provide a multi-layered 3D environment to observe tissue remodelling and cell distribution. Gels were incubated at 37°C with 5% CO₂, in the medium appropriate to the cell line (Gibco).

Gels were bathed in either mineralising or normal media, for up to 4 weeks in culture, to observe the extent of collagen remodelling and differences in gene expression at different time points. Each gel was halved at the end of its culture period. One half was processed for histology and the other used for TRIzol-based RNA extraction (Invitrogen) and subsequent reverse transcription and qPCR (Applied Biosystems). H&E staining was performed to histologically assess tissue remodelling and cell migration (histology was carried out at the Royal London Hospital Pathology laboratory). IHC will be performed to visualise the expression of bone- and cancer-associated proteins.

RESULTS: Expression of bone-associated proteins osteonectin and alkaline phosphatase, and ameloblastoma-associated proteins bcl-2 and

MMP-2 will be detected by qPCR. Antibodies against bone-related and cancer-related proteins will be used in IHC visualisation. Pending results will help to characterise growth patterns across the different cell types, media types and culture times.

Fig. 1: Sample H&E-stained transverse sections of collagen gel rolls. These 20 day gels contain HOS



cells and were cultured in normal (left) or mineralising (right) medium, producing different patterns of collagen disruption, cell viability and cell distribution.

DISCUSSION & CONCLUSIONS: Compressed collagen gel is an appropriate tissue model for research into ameloblastoma, due to its biological relevance; its ultrarapid and reproducible construction; tolerance of changing the experimental variables; and its support of cell viability and migration. Histology of processed gels and qPCR of extracted RNA will characterise cell growth and migration, collagen remodelling and gene expression in AM-1, HOS and MG-63 cell-seeded collagen gels under different culture conditions.

REFERENCES: ¹ R.A. Brown, M. Wiseman, C. Chuo, U. Cheema, S.N. Nazhat (2005) *Adv. Funct. Mater.* **15**: 1762-1770. ² H. Harada, T. Mitsuyasu, N. Nakamura, Y. Higuchi, K. Toyoshima, A. Taniguchi (1998) *J. Oral Pathol. Med.* **27**: 207-212.

ACKNOWLEDGEMENTS: This work was funded by Ms. Adele Biss. Laboratory instruction was provided by Pauline Levey, Nicky Mordan and Dr Ivan Wall. The AM-1 human ameloblastoma cell line was a kind gift from Professor Harada, Iwate Medical University, Japan.

The influence of scaffold architecture on interconnectivity and permeability

Y Reinwald¹, G Lemon², C.Rahman¹, KM Shakesheff¹

¹ Division of Drug Delivery and Tissue Engineering, School of Pharmacy, Wolfson Centre for Stem Cells, Tissue Engineering, and Modelling (STEM), Centre for Biomolecular Sciences, University of Nottingham, University Park, NG7 2RD, UK

² Division of Applied Mathematics and Theoretical Mathematics, School of Mathematical Sciences, University of Nottingham, University Park, Nottingham, NG7 2RD, UK

INTRODUCTION: For physical characterisation of tissue engineering scaffolds, important parameters include interconnectivity (IC) and permeability as they influence nutrient diffusion [1], circulation of extracellular material [2], cell adhesion [3] and ingrowth of blood vessels and bone tissue [4, 5]. To date, mostly qualitative attempts were described for the determination of IC. This study presents a novel approach to quantify scaffold interconnectivity in 3D and aims to describe scaffold permeability in combination with pore size, pore distribution, porosity, window size and distribution and IC [6].

METHODS: Supercritical carbon dioxide (scCO₂)-foamed scaffolds were fabricated from poly (lactic-co-glycolic acid) (PLGA) of different weight average molecular weights (Mw). Pore size and distribution, porosity and interconnectivity were obtained from micro computed tomography (MicroCT). Window size and distribution were measured by scanning electron microscopy (SEM). Scaffold permeability was determined from pressure measurements across the scaffolds and subsequent calculations using Darcy's Law.

RESULTS: Scaffolds were fabricated from 37, 53 and 109 kDa PLGA (85:15; Figure 1). Scaffolds from lower Mw PLGA resulted in higher average pore sizes and porosities as shown in Table 1. IC was defined as the ratio of pore volume accessible from the scaffold exterior by a sphere of known diameter, to the total pore volume.

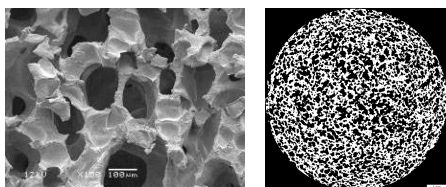


Figure 1: Representative images illustrating the structure of scCO₂-foamed PLGA scaffolds. SEM micrograph (left) and MicroCT image (right).

Increase in sphere diameter and PLGA Mw lead to a decrease in IC. For example, at a sphere diameter of 102 μ m the interconnectivities (IC₁₀₂) were 40%

17% and 5% for 37, 53, and 109 kDa respectively. Moreover, scaffold permeability decreased with increasing PLGA Mw.

Table 1: Summary of scaffold average pore size, porosity, interconnectivity

Mw [kDa]	Pore size [μ m]	Porosity [%]	IC ₁₀₂ [%]
37	142 (\pm 3)	53 (\pm 9)	40
53	127 (\pm 4)	49 (\pm 3)	17
109	98 (\pm 4)	39 (\pm 4)	5

DISCUSSION & CONCLUSIONS: Polymer molecular weight influenced the physical properties of scCO₂ foamed scaffold [7] including pore interconnectivity and permeability. Further investigations are necessary to examine the effect of process conditions on scaffold interconnectivity.

REFERENCES:

- ¹Hui, P. W. Journal of Biomechanics 1996, 29, 123-132.
- ²Gross, K. A.; Rodriguez-Lorenzo, L. M. Biomaterials 2004, 25, 4955-4962.
- ³Hou, Q. P.; Grijpma, D. W.; Feijen, J. Journal of Biomedical Materials Research Part B-Applied Biomaterials 2003, 67B, 732-740.
- ⁴Kuboki, Y.; Takita, H.; Kobayashi, D.; Tsuruga, E.; Inoue, M.; Murata, M.; Nagai, N.; Dohi, Y.; Ohgushi, H. Journal of Biomedical Materials Research 1998, 39, 190-199.
- ⁵Otsuki, B.; Takemoto, M.; Fujibayashi, S.; Neo, M.; Kokubo, T.; Nakamura, T. Biomaterials 2006, 27, 5892-5900.
- ⁶Karande, T. S.; Ong, J. L.; Agrawal, C. M. Annals of Biomedical Engineering 2004, 32, 1728-1743.
- ⁷Tai, H. European Cells & Materials 2007, 14: 76-77.

ACKNOWLEDGEMENTS: The author would like to thank Dr. Daniel Howard and Dr. Lisa White for their support throughout this study.

Identification of the Human Nucleus Pulposus Cell Phenotype and Its Application in characterising Adult Stem Cell Differentiation for Tissue Engineering Therapies for the Intervertebral Disc

S Richardson¹, B Minogue¹ & J Hoyland¹

¹ *Regenerative Medicine, School of Biomedicine, Faculty of Medical and Human Sciences, The University of Manchester, UK*

INTRODUCTION: Low back pain presents a significant clinical problem, affecting up to 80% of the population at some point in their lives. In a significant number of cases the underlying cause in intervertebral disc (IVD) degeneration, for which there is currently no successful long-term treatment. However, adult stem cell-based tissue engineering offers potential for future therapeutic intervention. For these tissue engineering therapies to be successful it is essential that the correct cell phenotype is produced, although the cells of the central nucleus pulposus (NP) region of the human IVD are poorly characterised. Therefore we used Affymetrix microarrays and quantitative real-time PCR (qRT-PCR) to identify potential phenotypic markers to distinguish NP cells from their closely related articular chondrocyte (AC) cells. These gene signatures were then used to identify the differentiation of adult stem cells in type I collagen gels towards an NP rather than an AC cell phenotype.

METHODS: Affymetrix microarray analysis was performed on normal human NP and AC cells to identify novel differentially expressed genes. Genes identified from microarray analyses were then validated using qRT-PCR analysis. Human bone marrow-derived mesenchymal stem cells (MSCs) and adipose-derived mesenchymal stem cells (ASCs) were expanded in monolayer and seeded in triplicate into type I collagen gels (Arthro-Kinetics Plc) at a final density of 4×10^6 cells/ml and cultured in differentiating medium (DM) under standard conditions for 14 days. Following culture, RNA was extracted, cDNA reverse transcribed and qRT-PCR performed to quantify changes in expression of standard marker genes and our novel NP phenotypic marker genes. Immunohistochemical analysis was also conducted to localise expression of the phenotypic markers with gels.

RESULTS: Affymetrix microarray analyses identified a panel of NP positive and NP negative (AC positive) marker genes, which were validated by qRT-PCR. Both ASCs and MSCs cultured in type I collagen gels demonstrated significant

increases in the conventional marker genes COL2A1 and ACAN, as well as the novel NP marker genes PAX1 and FOXF1 compared to monolayer controls (figure 1). While both ASCs and MSCs in type I collagen gels lacked expression of the AC marker genes IBSP and FBLN1, MSCs demonstrated large and significant increases in FBLN1 following differentiation in type I collagen gels, while ASCs lacked expression of this gene. When protein expression levels were studied, ASCs appeared to express higher levels of the NP markers PAX1 and FOXF1 while MSCs expressed higher levels of the AC markers IBSP and FBLN1.

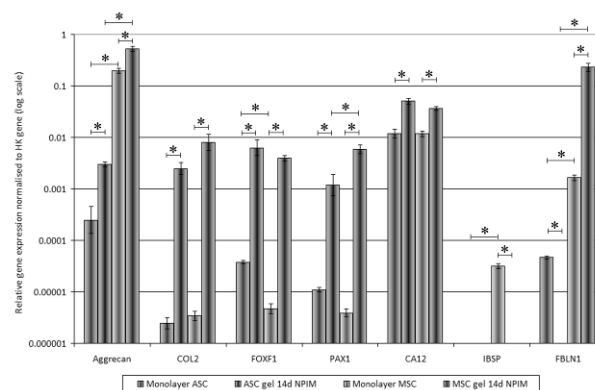


Fig. 1. qRT-PCR analysis of NP positive and negative markers in human ASCs and MSCs during differentiation in collagen hydrogels. * $P < 0.05$.

DISCUSSION & CONCLUSIONS: This study identifies, for the first time, the human NP cell phenotype. It also demonstrates that these phenotypic marker genes can be used to determine differentiation of MSCs and ASCs to an NP-like rather than an AC-like phenotype. Interestingly, these results suggest that ASCs may be a more appropriate cell type than MSCs for repairing the human IVD.

ACKNOWLEDGEMENTS: This project was funded by Arthritis Research UK (ARUK). Dr Richardson is funded by Research Councils UK (RCUK).

Development of an Acellular Dermis

P. Hogg¹, P. Rooney¹, S. Wilshaw², E. Ingham² & J. Kearney¹.

¹ NHS Blood and Transplant, Tissue Services, Liverpool UK. ² Institute of Medical and Biological Engineering, University of Leeds, UK

INTRODUCTION: The use of tissue engineered acellular matrices is increasing in the field of regenerative medicine and NHSBT Tissue Services are establishing a programme to introduce a range of acellular allografts. In this study we have adapted a patented decellularisation protocol such that acellular dermis could be produced under Good Manufacturing Practice (GMP) conditions. The decellularisation protocol does not affect structural strength, biochemical properties or *in vitro* and *in vivo* biocompatibility.

METHODS: Skin from 20 human donors was used in this study (with full R&D consent). Briefly, the epidermis was removed and the dermis was decellularised and decontaminated using sequential treatments with hypotonic Tris buffer, sodium dodecyl sulphate, (with protease inhibitors), nuclease solution (DNase and RNase) and peracetic acid. The acellular dermis was compared with cellular dermis and assessed histologically; biochemical analysis was performed by measuring residual levels of DNA and levels of collagen denaturation, biomechanical analysis was performed by measuring ultimate tensile stress and strain and biocompatibility was assessed by *in vitro* cytotoxicity and by implantation into a mouse model. The protocol was scaled up to demonstrate that an entire batch of skin from one donor (~ 2500 cm²) could be decellularised under GMP conditions

RESULTS: Histological examination showed that the epidermis had been removed cleanly from the dermis and there was no evidence of cells in the dermis (Figure 1). The decellularisation protocol was capable of removing 92 – 98% of DNA depending on the batch size of the tissue. There were no significant changes in structural strength when the tissue was pulled to break (Figure 2) or in levels of collagen denaturation. The acellular dermis did not exhibit any *in vitro* cytotoxicity. When implanted into the backs of hairless mice, whole skin elicited a foreign body/immune response and was encapsulated by a thick cellular capsule; cellular dermis was also surrounded by a capsule but it was less pronounced and some tissue resorption could be observed. In contrast, implanted acellular dermis did not elicit any major response, there was evidence of recipient cellular

migration into the depth of the tissue and these cells were occasionally accompanied by vascular tissue. At the periphery of the implant, there was clear evidence of integration of the acellular dermis with recipient tissue and it was often difficult to distinguish the tissues.

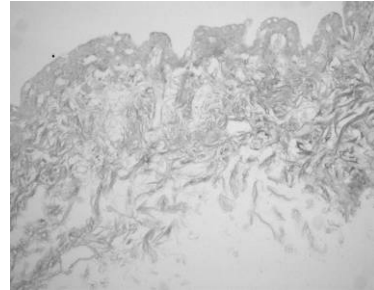


Figure 1. Decellularised human dermis showing lack of cells and no alteration to morphology

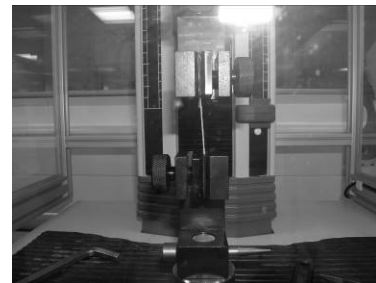


Figure 2. Dumbbell shaped piece of acellular dermis being pulled to break in a tensile tester.

DISCUSSION & CONCLUSIONS: This study has adapted a patented decellularisation protocol and scaled it up such that an entire donation of human skin can be decellularised under GMP conditions. The decellularised dermis is free of cells and biochemical and biomechanical properties have not been affected. The tissue is not cytotoxic either *in vitro* or *in vivo* and the data suggests that the acellular tissue becomes incorporated into a recipient following transplantation. Acellular dermis is currently produced outside the UK and is used in a range of surgical procedures; this is the first report of GMP decellularisation of human dermis in the UK. This acellular dermis will be available as an allograft to surgeons towards the end of 2010.

P62: Development of a reproducible wound to create an *in vitro* model of spinal cord injury

L Ross¹, S Boomkamp², S Barnett², N Gadegaard¹, M Riehle¹

¹ Centre for Cell Engineering, ² Glasgow Biomedical Research Centre, University of Glasgow, G12 8QQ, UK

INTRODUCTION: Damage to the central nervous system (CNS) causes highly debilitating injuries to victims due to the loss of motor control and sensory data from, potentially, large areas of the body. The lack of growth factors and the formation of a scar consisting of densely packed glial cells prevents severed spinal axons, whose cell bodies survive, from re-growing past the site of injury thus almost always making the damage permanent.

One factor critical to producing an *in vitro* model of spinal cord injury (SCI) is the creation of a reproducible wound. Excessive damage caused to substrates during wounding could lead to distortion of topography and irregular wounds and re-growth. To this effect, cuts made by various scalpel blades in PDMS devices were analysed using a scanning electron microscope (SEM).

METHODS: Polydimethylsiloxane (PDMS) devices were cast (ratio of base to curing agent 10:1) against a master fabricated with SU-8 on silicon, then these were cut into 13 mm disks with 50% of the surface covered by pattern. For testing the devices were cut with either a Feather No. 11 blade or a Fine Science Tools ultra fine micro knife. The cuts were made as follows: by dragging the blade across the surface (slash), by vertically inserting the blade into the device (stab) or slicing off sections of the device (cut). The devices were then sputter coated with an 18 nm layer of gold and analysed with a Hitachi S-3000H SEM.

RESULTS: The Feather No. 11 blade caused extensive damage to the devices; see *figure 1 (a)*. Significant distortion of the topography was observed along the slash, with a large number of ridges pulled out of alignment. Pieces of PDMS debris up to 20 µm in size littered the wound site and the blade created a fissure between 1 and 10 µm wide. Similar damage can be observed when stabbing. The cut left a ragged surface and generated large amounts of debris.

The Fine Science Tools ultra fine micro knife caused less damage to the devices; see *figure 1(b)*. The only major damage was observed around the area where the blade was first inserted. In this

small region distortions to the alignment of the topography could be seen for ~ 100 µm. Debris and the fissure created by the slash were < 5 µm in size. The stab left a barely detectable scar << 1µm wide with only minor debris. The cut left a relatively smooth surface with debris < 10 µm in size.

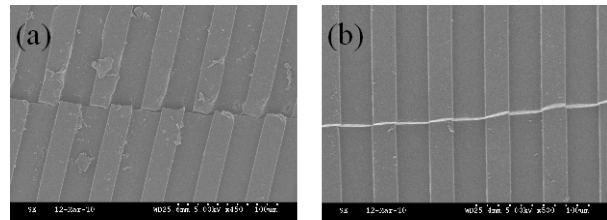


Fig. 1: (a) SEM image of a slash wound caused by a Feather No. 11 scalpel blade in PDMS. Substantial damage has been caused to the topography. (b) A slash wound caused by a Fine Science Tools ultra fine micro knife. Only minor damage is visible.

DISCUSSION & CONCLUSIONS: To minimise damage to the topography and debris created, a fine bladed scalpel should be used in a stab type wound. A method of creating the same depth of wound and eliminating variability caused by users still need to be established. Mixed spinal cord cultures (as shown in *figure 2*) will be wounded in various ways to see how wound shape, size and the substrate used effect healing.

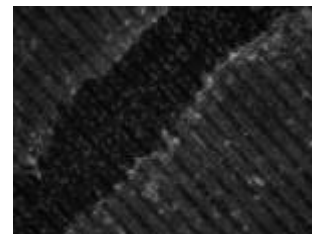


Fig. 2: Mixed spinal cord culture grown on PDMS and wounded with a Feather No. 11 blade. Stained for SMI31 (red), PLP (green) and DAPI (blue).

ACKNOWLEDGEMENTS: L Ross is a member of the Doctoral Training Centre in Cell and Proteomic Technologies and is funded by the EPSRC. We also thank the NC3Rs for their support of this work.

The in vivo assessment of Adipogenic Derived Stem Cells in combination with micro-carriers to provide a novel method for soft tissue reconstruction.

J Roxburgh¹ & JR Sharpe¹

¹ *Blond McIndoe Research Foundation, Queen Victoria Hospital, East Grinstead, RH19 3DZ*

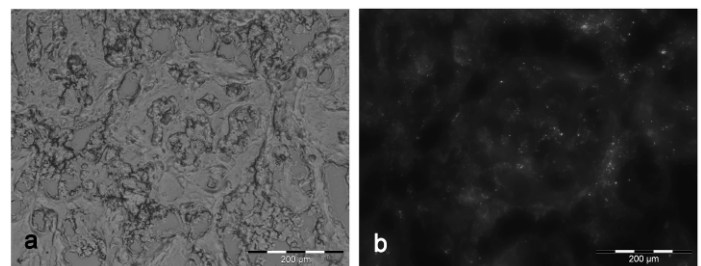
INTRODUCTION: When subcutaneous soft tissue is lost due to trauma such as severe burns, reconstructive surgery is required to restore the function and contour of the body. Current approaches are generally limited to surgical intervention and there has been little progress in the development of advanced therapies. Transplantation of autologous adipogenic derived stem cells (ADSCs) to the burn site may provide a regenerative strategy. ADSCs can be harvested from subcutaneous adipose tissue, cultured on gelatin micro-carrier beads and delivered to the trauma site (1). ADSCs may be differentiated into mature adipocytes before or after implantation (2). These studies assess the suitability of gelatin micro-carriers for this application by investigating the attachment, proliferation and differentiation of ADSCs on micro-carrier beads in vitro and their survival and contribution to tissue bulk in a pig model.

METHODS: Human ADSCs were isolated from discarded tissue following surgery with patient consent, seeded onto Cultispher G gelatin micro-carrier beads (Sigma Aldrich), and incubated in rotating culture for 14 days. Cell attachment and proliferation was assessed by acridine orange and cell differentiation by Oil Red O to detect for the presence of triglyceride lipid. Adipogenic markers adiponectin and adipisin were measured by quantitative PCR. Following initial in vitro assessment ADSCs were isolated from subcutaneous fat from 3x large white pigs. ADSCs were retro-virally transduced to express green fluorescent protein (GFP) to allow the survival and contribution of the cells to tissue bulk to be assessed in vivo. GFP labeled ADSCs cultured on beads were injected subcutaneously into 6 sites on the paravertebral region of the pigs. After 12 days wounds were excised and frozen sections taken to examine for the presence of GFP positive cells.

RESULTS: In the in vitro studies Acridine orange staining showed cells attaching and proliferating on the surface of beads after 14 days. After 21 days in differentiation medium, lipid droplets were present in cells stained with Oil Red O. Increased expression of adipisin and adiponectin in response to exposure to differentiation medium was detected

by qPCR. Preliminary in vivo findings have showed that a large number of GFP positive cells could be detected in areas injected with gelatin micro-carriers seeded with ADSCs (figure 1). GFP positive ADSCs were located in discrete areas and had not diffused from the injection site. The gelatin microcarrier beads had not been resorbed during the 12 days in vivo and no inflammatory or foreign body reaction was observed.

Fig. 1. a) Section through sub-dermal layer



presence of micro-carrier bead after 10 days. b). the same area viewed under fluorescent light showing fluorescent GFP +ve ADSCs.

DISCUSSION & CONCLUSIONS: Our findings demonstrate that gelatin micro-carriers provide a suitable culture and delivery substrate for ADSCs and may have the potential to deliver these cells for the restoration of soft tissue bulk. The presence of triglyceride lipids and the up-regulation of adipisin and adiponectin confirmed the presence of mature adipocyte cells following exposure to differentiation medium. To further investigate the potential for clinical application of ADSCs on micro-carrier beads in vivo animal studies will investigate the fate of ADSCs delivered subcutaneously in a pig model.

REFERENCES:

- (1) Rubin et al. PRS 2007; 120(2):414-424.
- (2) Cho et al. Biochem Biophys Res Commun 2006; 345(2):588-594.

HIGHLY CONTROLLED NANOTOPOGRAPHY ON TI FOR PRECISE CONTROL OF CELL BEHAVIOUR

T Sjöström¹ & B Su¹

¹*Department of Oral & Dental Science, University of Bristol, UK*

INTRODUCTION: The next generation of biomaterial surfaces will require characteristics that can specifically control cell and gene behaviour. A promising technique for triggering specific cell behaviour is the use of nanotopography with well defined and tuneable dimensions. One major challenge will be to translate topographies from model surfaces used in the lab to clinically relevant surfaces. In our work we aim to provide advanced surface patterning techniques directly onto Ti surfaces which are widely used as orthopaedic and dental implant materials. We use electrochemical techniques which allow for fast and reliable oxide patterning of large surface areas of Ti with arbitrary shapes. In this particular work we have utilized block copolymers (bcp) to create a mask on Ti surfaces for through-mask anodization.

METHODS: 0.5 wt% PS-P4VP was dissolved in toluene solution, spin- or dipcoated onto mechanically polished Ti substrates and finally subjected to a solvent vapour for 3 h. The Ti samples were then immersed in a 0.3 M oxalic acid and anodized at varying voltages at 17 °C. O₂ plasma treatment was used to remove the polymer masks and reveal the titania structures. The surfaces were imaged using atomic force microscopy (AFM).

RESULTS: Figure 1 shows AFM images of Ti surfaces with nanopatterns of titania after anodization and removal of the polymer mask. The oxide patterns have inherited the typical arrangement of bcp films. Without solvent annealing of the bcp masks a disordered nanodot oxide array was achieved. Solvent annealing in THF vapour resulted in a relatively well ordered nanodot array while a chloroform vapour caused a lamellar bcp arrangement resulting in a ridge-type oxide pattern after anodization. The height of the oxide structures was dependent on the voltage/current conditions during anodization with the oxide structures in Figure 1 having a height of 10 nm after anodization at 3 V.

DISCUSSION & CONCLUSIONS: Our previous work has shown that changing Ti oxide structure height from 15 to 100 nm influences the differentiation pathway of hMSC's with lower

nanotopographies stimulating an osteospecific lineage [1]. Also the degree of ordering of nanotopography has been shown to be highly significant for cell behaviour [2]. The through-mask anodization technique used here allowed for precise control of both degree of order and of oxide height. Furthermore, different types of oxide nanopatterns were achieved and centre-centre distances in between structures could be tuned by varying the bcp molecular weight. The anodizations were performed without any prior surface reconstruction or selective removal of one of the polymer blocks, further simplifying the patterning procedure.

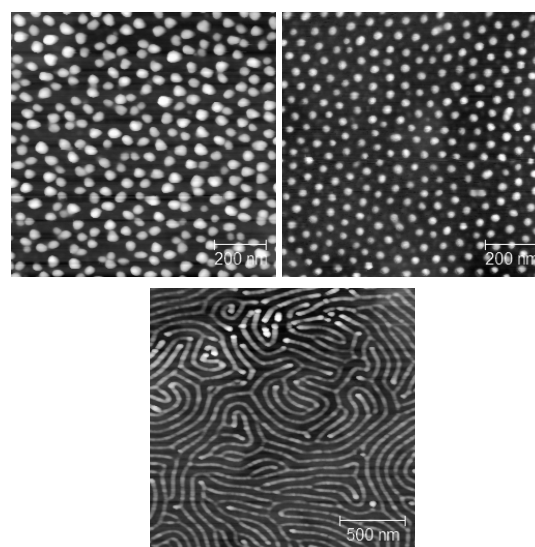


Fig. 1: Titania nanopatterns on Ti surfaces after through-mask anodization and removal of the bcp mask. Disordered nanodot surface (top left), ordered nanodot surface (top right) and fingerprint-like ridge pattern (bottom).

In conclusion, through-mask anodization using bcp masks was shown to be a highly efficient method for oxide nanopatterning of Ti surfaces with high flexibility of nanopatterns and dimensions. In vitro work on these surfaces are currently ongoing using mesenchymal stem cells.

REFERENCES: ¹ T. Sjöström, M. Dalby, A. Hart et al (2009) *Acta Biomaterialia* **5**:1433-41. ² M. Dalby, N. Gadegaard, R. Tare et al (2007) *Nature Materials* **6**:997-1003.

Atomistic Simulations of Collagen Fibrils

I Streeter^{1,2} & N H de Leeuw^{1,2}

¹ *Institute of Orthopaedics and Musculoskeletal Science, University College London, UK*

² *Department of Chemistry, University College London, UK*

INTRODUCTION: Collagen is a highly complex material in terms of its structure and its behaviour. Its material and behavioural properties are ultimately determined by the amino acid sequence of the tropocollagen, as this controls the self-assembly of collagen fibrils, and their interaction with other molecules and with cells. In order to better understand collagen as a material, we have performed molecular dynamics (MD) simulations of a fibril whilst retaining atomistic resolution. MD simulations are commonly used to investigate the behaviour of proteins by calculating their motion and interactions on an atom by atom basis. However, extending this concept to investigate something as large as a fibril was not trivial.

METHODS: An atomistic model of a fibril was built, in which each type I collagen protein was represented by over 39,000 atoms, connected in the correct arrangement for its amino acid sequence. For each tropocollagen there were also 11980 intrafibrillar water molecules. The supramolecular arrangement of the fibril was based on an x-ray diffraction experiment [1].

The simulations used the MD software Amber 9 [2]. Our simulations are novel in that they use a densely packed unit cell and periodic boundary conditions to generate the unique molecular structure of a collagen fibril.

RESULTS: These novel MD simulations ran successfully to generate a 60 ns molecular dynamics trajectory. The proteins and water molecules were mobile, and they gyrated and flexed within their fibrillar positions.

Hydrophillic attractions were observed to form

between neighbouring tropocollagens within the fibril, such as hydrogen bonds and water-mediated hydrogen bonds. These hydrophillic interactions were more prevalent in bands of the fibril that contain lots of charged amino acids.

Compared to the gap region, the overlap region of the fibril had a lower “concentration” of water, and a greater fraction of water molecules closely bound to the proteins. The water “concentration” went through a minimum in the region of the telopeptides.

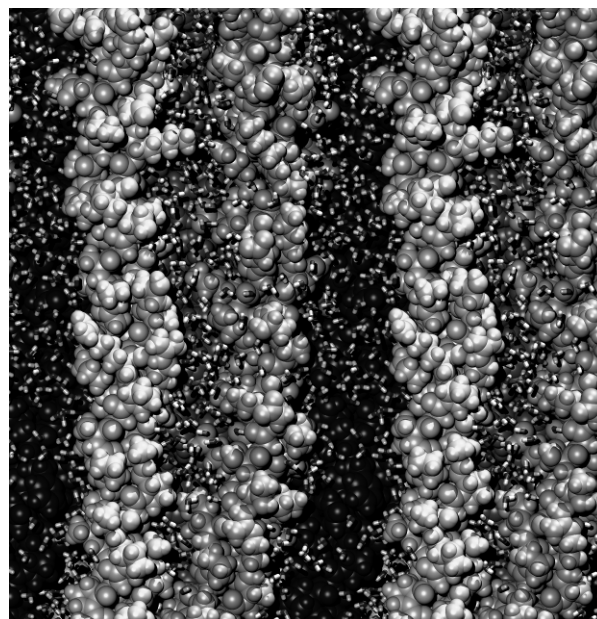


Fig. 1: Atomistic model of a collagen fibril.

DISCUSSION & CONCLUSIONS: The most important conclusion of this work is that it is now possible to simulate an entire collagen fibril whilst retaining atomistic resolution. This contrasts with previous MD simulations which generally only focused on single collagen molecules. This new simulation method allows a study of how the proteins and water interact to determine and control the fibril's characteristic properties.

Understanding the nature of hydrophillic interactions between neighbouring proteins within the fibril will help us to understand the process of fibrillogenesis, and the nature of the forces that hold the fibril together.

Understanding the behaviour of water molecules within a fibril has implications for understanding hydroxyapatite crystallisation. The ability of the fibril to withstand stress is also likely to depend crucially on the nature of intrafibrillar water molecules and their interactions with the collagen proteins at atomistic length scales.

REFERENCES: ¹ J. Orgel, T. Irving, A. Miller, et al (2006) *Proc Natl Acad Sci USA* **103**:9001-9005. ² D. Case, T. Cheatham, et al (2005) *J Comput Chem* **26**:1668-1688.

Developing Self-Assembled Peptide Hydrogels with Biological Function for the Culture of Stem Cells

K.Thornton¹, C. L. R. Merry¹ & R. Ulijn²

¹ *Material Science Centre, University of Manchester, Grosvenor Street, Manchester, M1 7HS*

² *WestCHEM, University of Strathclyde, Cathedral Street, Glasgow, G1 1XL*

INTRODUCTION: Self-assembled peptide hydrogels have been shown to be a suitable substratum for a range of cell types [1]. We are investigating the suitability of these systems for the culture of stem cells. Stem cells are sensitive cells with particular requirements of their environment and culture media for growth and differentiation [2]. We have developed the peptide, Fmoc-Phenylalanine-Tyrosine(phosphate)-OH, (Fmoc-FY(p)-OH) with the aim of being a suitable material for the growth and guided differentiation of the cells. We aim to guide the differentiation through incorporation of short saccharide chains suitable for the cells at their specific stages of development.

METHODS: Fmoc-FY(p)-OH was prepared in two ways. The first was in an alkaline phosphate buffer, pH adjusted to neutral, to give a final salt concentration of 0.15M. The second was in Knockout Dulbecco's Modified Eagles Medium (DMEM), the pH was raised to fully dissolve the peptide and adjusted back to neutral by addition of hydrochloric acid. A stable-self-supporting hydrogel formed on addition of alkaline phosphatase (0.039 – 3.9 DEA μl^{-1} , where one DEA will hydrolyse 1 μmole 4-nitrophenyl phosphate per minute at 37 °C and pH 9.8). Biological functionality was added to the hydrogel in the form of the sulphated saccharide, heparin, and the non-sulphated saccharide, K5 polysaccharide prior to enzyme addition. The hydrogel produced was characterised by High Pressure Liquid Chromatography, Atomic Force Microscopy (AFM), rheology, Circular Dichroism, fluorescence spectroscopy and Wide Angle X-ray Scattering.

RESULTS: A range of environments for the self-assembly of the peptide were assessed in order to provide the best conditions for the stem cells. The alkaline phosphatase dephosphorylates the Fmoc-Phenylalanine-Tyrosine(phosphate)-OH forming the self-assembling peptide, Fmoc-Phenylalanine-Tyrosine-OH (Fmoc-FY-OH). The gelation times were found to be dependant on the environmental conditions and enzyme concentrations. The

mechanical properties were found to be dependant only on the environmental conditions. The molecules self-assembled into a β -sheet structure within nanofibres (average width 51.10 ± 14.81 nm, height 12.36 ± 5.76 nm) in an interconnecting network, Figure 1.

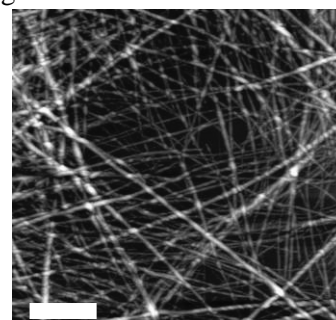


Fig. 1: Fibres formed from the self-assembling peptide, Fmoc-FY(p)-OH in buffer on addition of alkaline phosphatase at 1.1 DEA μl^{-1} by AFM. Scale Bar 1 μm .

The incorporation of soluble saccharides (at 1 $\mu\text{g/ml}$, a suitable level for cell culture) was found to have no significant effect on the gelation times, structure or mechanical properties of the hydrogels formed.

DISCUSSION & CONCLUSIONS: We have been able to produce two different hydrogels from the same peptide by altering the environmental conditions where gelation occurs. To date, the work has focused on the characterisation of the hydrogels produced. These hydrogels, with and without the addition of saccharide chains, will now be assessed to determine their suitability as a substrata for the culture of stem cells.

REFERENCES: [1] Jayawarna, V et al, *Advanced Materials* (2006), 18. [2] Amit, M. and Itskovitz-Eldor J., *Methods in Enzymology*,(2006) 420.

ACKNOWLEDGEMENTS: Dr. Nigel Hodson for his help and advice with the AFM.

Pulp capping agents release hepatocyte growth factor from dentine which may contribute to mineralised tissue repair in the dentine-pulp complex

P.L. Tomson¹, P.J. Lumley¹, J. Yan², M.Y. Alexander², A.J. Smith¹, and P.R. Cooper¹

¹Oral Biology, University of Birmingham School of Dentistry. ²Cardiovascular Research Group, Biomedicine, University of Manchester

INTRODUCTION: Maintaining a healthy dental pulp can prevent odontogenic pain, the need for complex root canal treatment or tooth extraction. The dentine matrix is a known reservoir of potent signalling molecules, which can regulate regenerative events following their mobilisation by bacterial acids during caries or by therapeutic materials such as Mineral Trioxide Aggregate (MTA)¹. Hepatocyte growth factor (HGF) is recognized as a multifunctional growth factor, which regulates a range of processes including tissue development and regeneration. The presence of HGF within dentine has not previously been reported. The aim of this work was to determine if HGF is i) present within dentine, ii) is released by therapeutic pulp capping agents, and iii) can stimulate mineralisation in dental pulp cell cultures.

METHODS: Powdered human dentine was exposed to solutions of 0.02M calcium hydroxide and the soluble products of white/gray MTA (Dentsply, USA) over 14 days. Solubilised dentine matrix proteins (DMPs) were exhaustively dialyzed and lyophilised. Human Cytokine Antibody Arrays (Raybio, USA) were used to determine relative amounts of HGF in DMP extracts. Relative expression of HGF and its receptor, c-Met, were analysed by RT-PCR in rat pulp tissue and primary dental pulp cultures (DPCs). Alizarin red staining was used to determine mineralisation in DPCs up to 15-days following single adenoviral infection of HGF and its antagonist NK4 as well as addition of a range of concentrations of recombinant HGF.

RESULTS: HGF was solubilised from human dentine by calcium hydroxide and MTA (Fig 1). HGF and cMet were relatively abundantly expressed in rat dental pulp and DPCs. Compared with control and adenoviral NK4 transfected DPCs, mineralisation was significantly accelerated ($P < 0.001$) in DPCs exposed to recombinant and adenoviral delivered HGF (Fig 2).

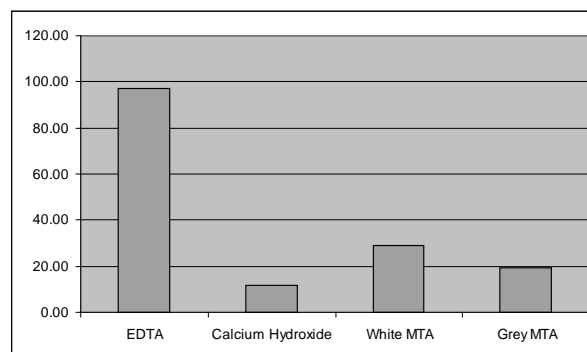


Fig. 1: Relative levels of HGF in DMPs extracted by EDTA, Calcium Hydroxide, White MTA and Grey MTA

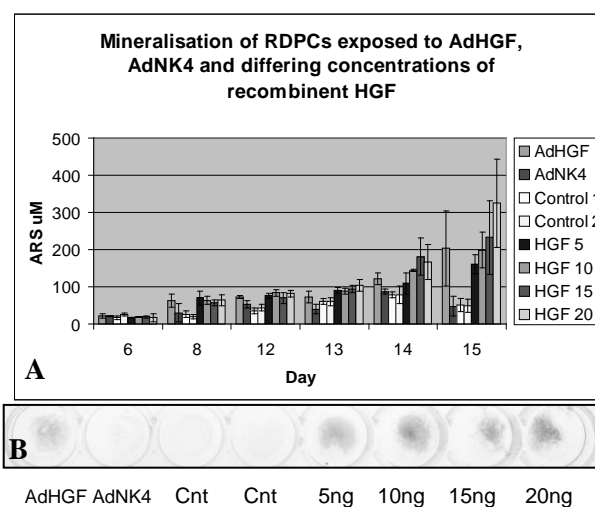


Fig 2: Alizarin red staining (ARS) of rat dental pulp cells A) summary of total ARS from between 6 to 15 days. B) Image of ARS profile at day 15.

DISCUSSION & CONCLUSIONS: These data suggest that *in vivo* HGF may be released from the dentine matrix by Calcium Hydroxide and MTA and that it may subsequently act in synergy with other signalling molecules to promote dental tissue regeneration.

REFERENCE: ¹PL Tomson, LM Grover, PJ Lumley et al (2007) *J Dent* **35**:636-42.

ACKNOWLEDGEMENTS: This research was supported by a grant from the Faculty of Dental Surgery Royal College of Surgeons of England.

Biodegradable Scaffolds For Human RPE Implantation

L.A. Turner¹, Z. Drymoussi¹, S. Downes¹ & P.N. Bishop²

¹ *Materials Science Centre, University of Manchester, Grosvenor Street, Manchester M1 7HS.*

² *Clinical and Laboratory Sciences, AV Hill Building, Oxford Road, Manchester, M13 9PT.*

INTRODUCTION: Age-related macular degeneration (AMD) is the leading cause of blindness in industrialized countries and the third leading cause of blindness worldwide¹. Three million people worldwide are legally blind with AMD and this number is expected to double by 2020¹. Dry AMD is more common than wet AMD; however no treatment is currently available for dry AMD, which is characterised by loss of or damage to the retinal pigment epithelium (RPE). In animal models, transplantation of RPE cells has shown some success, but in humans experimental transplantation has not been successful, and one of the problems has been to the lack of a suitable substrate for the RPE cells. In this study, we addressed the lack of a suitable membrane for RPE cell culture and transplantation by evaluating RPE attachment, viability, proliferation and morphology on thin biodegradable polymer films. A range of film topographies and polymer blends were assessed to determine optimal film topography and polymer composition. In addition, the effects of laminin coatings were evaluated.

METHODS: Scaffolds were solvent cast from 3% poly (ϵ -caprolactone) (PCL), polylactic acid (PLA) and 1:1 (PCL:PLA) blend solutions onto borosilicate glass slides and left overnight to enable solvent evaporation. Glass-exposed and air-exposed surfaces were used for culture of the human RPE cell line, ARPE-19, cells *in vitro*. In addition, prior to cell seeding, half the scaffolds were coated with laminin. Cell viability was determined using live/dead assays. In order to determine adherent cell numbers, samples were washed to remove non-adhered cells and fluorescently stained using DAPI, before imaging and subsequent nuclei counting using ImageJ. Counts were taken at days 1, 3 and 5 to determine proliferation rates on each substrate. In order to assess cell morphology, which is a crucial indicator of RPE function, nuclei, actin and vinculin were highlighted using immunostaining. In addition, immunostaining was carried out on Ezrin and ZO-1 proteins in order to assess the presence of “tight junctions” (another morphological feature important for correct RPE functioning).

RESULTS: Film characterisation revealed a decrease in roughness and pit formation with increasing PLA content. RPE cells were viable,

attached well and proliferated on all substrates. Alterations in substrate topography and chemistry induced differences in initial RPE morphology and rates of proliferation. Smoother topographies and laminin coatings induced more rounded morphologies, and laminin coatings significantly increased rates of RPE cell proliferation. However, after five days in culture, RPE cells formed the desired morphology on all film types, regardless of topography and laminin coatings.

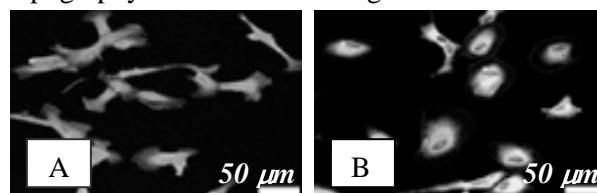


Fig. 1: Confocal microscopy images of RPE cells A) elongated morphology on rough PCL scaffolds. B) rounded ‘cobblestone’ morphology on smooth PLA scaffolds (day 1). Green:actin, red:vinculin.

DISCUSSION & CONCLUSIONS: Thin films fabricated from PLA and PCL, and their blends, constitute suitable substrates for RPE cell culture. Alterations in substrate topography and chemistry induce differences in initial RPE morphology and rates of proliferation. However, neither changes in topography nor laminin coatings altered the final cobblestone morphology, which was produced on all film types. Although laminin coatings increased initial rates of cell proliferation on all film types, it is unclear whether the rate of proliferation is necessary for cell function. These scaffolds provide suitable substrates for RPE cell attachment, survival and proliferation - in addition to inducing the desired cell morphology, which is necessary for RPE function *in vivo* and thus physiological vision. Accordingly, PCL, PLA and blend scaffolds warrant further investigation for *in vivo* use.

REFERENCES: ¹World Health Organisation (2007). Global Initiative for the Elimination of Avoidable Blindness: action plan 2006-2011. WHO, ISBN: 9789241595889

ACKNOWLEDGEMENTS: Thanks go to Ms Caroline Ridley (UoM) for the ARPE-19 cells.

Chondrocyte morphology on electrospun nanomats

I. Wimpenny¹, N. Ashammakhi^{1,2}, Y. Yang¹

¹Institute of Science and Technology in Medicine, Keele University, UK.

²Institute of Biomaterials, Tampere University of Technology, Tampere, Finland

INTRODUCTION: Extracellular matrix (ECM) comprises nano to micro-scale fibres arranged in a specific architecture to provide form and function to the tissue. ECM is maintained by cells, thus by seeding cells to synthetic nanofibrous environments, and it is possible to generate a suitable biomimetic scaffold for tissue regeneration. In this study the ability for nanofibrous materials to promote typical chondrocytes morphology is examined.

METHODS:

Polymer processing:

Poly L,D lactic acid (PLDLA; 96%L, 4%D) was dissolved in chloroform and cast to form films., PLDLA was dissolved in a mixture of chloroform and dimethylformamide (Sigma, UK) at a ratio of 7:3. The solutions were then electrospun to cast films at 15cm, 6kV, 0.025ml/min.

Cell culture:

Bovine chondrocytes were isolated by enzymatic digestion and seeded onto surfaces at either zero passage (P0) or second passage (P2). Cell were cultured in DMEM/F12, 10%FBS and 1%A&A and were allowed adhere and proliferate on surfaces before examination (7 days for P0, or 24h and 3 days for P2)

Cell morphology analysis:

Light microscopy was used to examine cell morphology. Images were recorded as assessed using generic Image J software to determine cell area and circularity, determined using a modified method from Bashur *et al.* (2006)¹.

RESULTS:

Cells demonstrated a more polygonal morphology after a short period on cast films, compared to nanofibrous surfaces. Furthermore, the area covered by flattened cells was far greater on cast films than on nanofibres, regardless of the number of cell passages. P0 cells maintain a smaller area than P2 cells in all cases. Cell area appears to increase over time, which corresponds with a decrease in cell circularity.

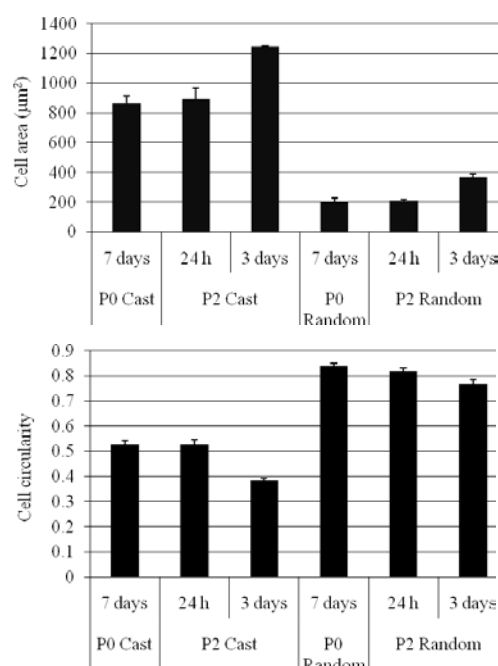


Figure 1. Charts comparing cell areas (top) and cell circularity (bottom) of P0 and P2 bovine chondrocytes on PLDLA films and nanofibres at different timepoints.

DISCUSSION & CONCLUSIONS: Previously, it has been demonstrated that nanofibres can result in decreasing the wettability of surfaces², which may promote more rounded cell morphology. This does not inhibit proliferation and is associated with chondrogenic behaviour, demonstrated by positive staining for sulphated mucins, e.g. aggrecan and also greater expression of chondrogenic markers on nanofibres (data not shown). The use of

REFERENCES:

- ¹Bashur CA, Dahlgren LA, Goldstein AS. Effect of fiber diameter and orientation on fibroblast morphology and proliferation on electrospun poly(d,l-lactic-co-glycolic acid) meshes. *Biomaterials* 2006;27(33):5681-5688.
- ²Wimpenny I, Ashammakhi N, Yang Y. Study of the surface properties of electrospun nanomats. *European Cells & Materials* 2009;18 (Supplement 2):111.

ACKNOWLEDGEMENTS: Funding by BBSRC CASE Studentship award.